

University of Nebraska - Lincoln

DigitalCommons@University of Nebraska - Lincoln

Civil Engineering Theses, Dissertations, and
Student Research

Civil Engineering


Winter 12-1-2016

Condition Factor Calibration for Load and Resistance Factor Rating of Steel Girder Bridges

Pranav M. Shakya

University of Nebraska - Lincoln, pranav.shakya@huskers.unl.edu

Follow this and additional works at: <http://digitalcommons.unl.edu/civilengdiss>

 Part of the [Structural Engineering Commons](#), and the [Transportation Engineering Commons](#)

Shakya, Pranav M., "Condition Factor Calibration for Load and Resistance Factor Rating of Steel Girder Bridges" (2016). *Civil Engineering Theses, Dissertations, and Student Research*. 98.

<http://digitalcommons.unl.edu/civilengdiss/98>

This Article is brought to you for free and open access by the Civil Engineering at DigitalCommons@University of Nebraska - Lincoln. It has been accepted for inclusion in Civil Engineering Theses, Dissertations, and Student Research by an authorized administrator of DigitalCommons@University of Nebraska - Lincoln.

CONDITION FACTOR CALIBRATION FOR
LOAD AND RESISTANCE FACTOR RATING OF STEEL GIRDER BRIDGES

by

Pranav Shakya

A THESIS

Presented to the faculty of
The Graduate College at the University of Nebraska
In Partial Fulfillment of Requirements
For the Degree of Master of Science

Major: Civil Engineering

Under the Supervision of Professor Joshua Steelman

Lincoln, Nebraska

December, 2016

Condition Factor Calibration for Load and Resistance Factor Rating

of Steel Girder Bridges

Pranav Shakya, M.S.

University of Nebraska, 2016

Advisor: Joshua Steelman

The Load and Resistance Factor Rating (LRFR) is a reliability-based rating procedure complementary to the Load and Resistance Factor Design (LRFD). The intent of LRFR is to provide consistent reliability for all bridges regardless of in-situ condition. The primary difference between design and rating is the uncertain severity and location of deterioration, including the potential future loss of strength for an element already evidencing deterioration. Ostensibly, these uncertainties are accounted for by applying an additional strength reduction factor: the condition factor, ϕ_c . Currently, condition factors are nominally correlated to the condition of the member, which can be Good, Fair, or Poor. However, definitions of these condition categories are deferred to inspection documents, which themselves lack clear, objective definitions. Furthermore, lack of guidance to account for the location and extent of deterioration exacerbates confusion in the methodology to appropriately assign condition factors. These ambiguities cause incoherence between inspection and rating processes by introducing additional uncertainty. The additional uncertainty skews load ratings, sometimes producing ratings with unintended conservatism, and sometimes overestimating the safe load-carrying capacity of a bridge. This study presents a calibration of ϕ_c to be used with steel girder

bridges, accounting for uncertainty due to non-uniform deterioration throughout transverse sections, lack of knowledge of the longitudinal location(s) of the deterioration, and the likelihood of further deterioration over the next inspection cycle for ranges of section loss for each condition. Section loss ranges are proposed to define each condition state for potential implementation by inspectors. The proposed condition state definitions and implementation methodology can improve uniformity in the inspection process and produce bridge load ratings that are more consistent with the target reliability intended by the LRFR rating procedure.

Acknowledgement

I would first like to thank my advisor Dr. Joshua Steelman. It has been an honor to be his student. He has taught me, both consciously and unconsciously, how good engineering and research is done. The door to Professor Steelman's office was always open whenever I had a question about my research or writing. He consistently allowed this paper to be my own work: steering me in the right direction only when he thought I really needed it. I appreciate all his contributions of time, ideas, and funding to make my master's experience productive and stimulating.

I would also like to thank my committee members, Dr. Maria Szerszen and Dr. Daniel Linzell, for their helpful feedback, which has helped improve my thesis immensely.

Other students have contributed immensely to my personal and professional time at the University of Nebraska- Lincoln. Fayaz Sofi, Hai Do and Steven Stauffer have been a source of friendship as well as a source of good advice.

I would also like to acknowledge Rosemary McLaughlin and Neha Dixit for reviewing and critiquing my thesis. They have been a tremendous help and I am gratefully indebted to them for their very valuable comments on this thesis.

Lastly, I would like to express my very profound gratitude to my family for their love, unfailing support and continuous encouragement throughout my years of study and throughout the process of researching and writing this thesis. This accomplishment would not have been possible without them. Thank you

Pranav Shakya

Table of Contents

Acknowledgement	iv
Table of Contents	v
List of Figures	vii
List of Tables	ix
Chapter 1: Introduction	1
1.1 Load Rating and Condition Factor.....	2
Chapter 2: Literature Review	7
2.1 Overview of Bridge Inspection and Evaluation.....	7
2.2 Deterioration Mechanisms and Documentation.....	11
2.3 Development of LRFR Methodology	20
2.4 Steel Bridge Reliability.....	27
2.5 Conclusion of Literature Review	32
Chapter 3: Objectives and Scope	34
Chapter 4: Overview of Methodology	36
4.1 Condition States and ϕ_c	36
4.2 Bridge Surveying and Describing and Profiling the Deterioration.....	40
4.3 Conclusion	44
Chapter 5: Reliability Analysis	46
5.1 Rackwitz-Fiessler Reliability Analysis.....	46
Chapter 6: Uncertainty Contributions to Condition Factors	53
6.1 Uncertainties in Section Deterioration.....	53

6.2 Future Corrosion	62
6.3 Uncertainty due to Range of Section Loss in each Condition State	66
6.4 Uncertainty in the Location of the Deterioration	76
6.5 Conclusion	86
Chapter 7: Condition Factor Calculation and Implementation	87
7.1 Approach 1	87
7.2 Approach 2	96
7.3 Approach 3	108
7.4 Special Approach	112
7.5 Selection of ϕ_c for Load Rating	113
7.6 Conclusion	120
Chapter 8: Summary and Conclusion	123
References	127
APPENDIX A: PLASTIC MOMENT CAPACITY USING LRFD	130
APPENDIX B: USING MEAN SECTION FOR MOMENT CALCULATION	134
APPENDIX C: ALTERNATIVE FUTURE CORROSION CALCULATION	136
APPENDIX D: CATEGORIZING THE ENVIRONMENT	138

List of Figures

Figure 1.1 PDF curve explaining ϕ_c	3
Figure 2.1 Average corrosion of carbon steel using Komp's model	14
Figure 2.2 Average corrosion of weathering steel using Komp's model	14
Figure 2.3 Corrosion of a steel girder bridge	19
Figure 2.4 Typical corrosion pattern in a steel girder	20
Figure 2.5 Flowchart for selecting resistance factor according to NCHRP 301	26
Figure 4.1 Deterioration pattern at girder ends	41
Figure 4.2 Bottom flange deterioration along the girder	41
Figure 4.3 Deterioration pattern where entire section of girder is deteriorated	42
Figure 4.4 Entire girder section deteriorated below the cracked slab	42
Figure 4.5 Deterioration profile "GP1"	43
Figure 4.6 Section deterioration "GP 1"	44
Figure 4.7 Entire web deteriorated along the span "GP 2"	44
Figure 6.1 Section deterioration	54
Figure 6.2 Variation of the flange thickness along the section	54
Figure 6.3 Sample location of measurement taken along the bottom flange	56
Figure 6.4 Wide mouth caliper used for measurement of the flange	57
Figure 6.5 Example field measurement sheet along with the calculated loss and COV ...	59
Figure 6.6 Percentage loss VS COV	60
Figure 6.7 Prediction of future corrosion	63
Figure 6.8 Bridge with multiple condition states	68

Figure 6.9 Example section loss profile along the span.....	77
Figure 6.10 Load rating along the span for the section loss shown in Figure 6.9	78
Figure 6.11 Example scenarios for various levels of section loss along the span	81
Figure 6.12 Flowchart to categorize CS's.....	82
Figure 6.13 Possible distribution of condition state 2 within scenario 2	83
Figure 7.1 Sample of possible distribution for one of the scenarios.....	96
Figure 7.2 Moment capacity VS ϕ_c for the 231 combinations	100
Figure 7.3 ANN's neural networks layers	104
Figure 7.4 ϕ_c predicted using ANN VS actual ϕ_c for girder with GP1	105
Figure 7.5 ϕ_c predicted using ANN VS actual ϕ_c for girder with GP2	105
Figure 7.6 ϕ_c predicted using ANN VS actual ϕ_c with GP1 and NDOR's Range.....	107
Figure 7.7 ϕ_c predicted using ANN VS actual ϕ_c with GP2 and NDOR's Range.....	107
Figure 7.8 Modeled condition state in a girder	108
Figure 7.9 Flowchart to start the rating procedure.....	114
Figure 7.11 Flowchart to determine the ϕ_c for Approach 1.....	117
Figure 7.12 Flowchart to determine the ϕ_c for Approach 2.....	118
Figure 7.13 Flowchart to determine the ϕ_c for Approach 3.....	119
Figure 7.14 Flowchart to determine the ϕ_c for Special Approach.....	120

List of Tables

Table 2.1 Corrosion parameters in Komp's corrosion model	13
Table 2.2 Corrosion penetration of sheltered VS exposed conditions.....	17
Table 2.3 Uniform corrosion rate for a 4" X 6" steel plate specimen, [ASTM,1968].....	18
Table 2.4 Bias and COV for the loads	22
Table 2.5 Condition rating and the penalization as suggested by NCHRP 301	23
Table 2.6 Corrosion rate for carbon steel for different corrosion of section	24
Table 2.7 Calculation of average thickness loss for difference corrosion of section	24
Table 2.8 Summary of % reduction in section modulus (2 years).....	24
Table 2.9 Summary of bias and COV for different section condition.....	25
Table 2.10 Bridge components affected by different forms of corrosion.....	27
Table 2.11 Parameters associated with mode of resistance.	29
Table 2.12 Proposed condition factors by Wang and Ellingwood.....	32
Table 4.1 MBE structural condition of member and corresponding ϕ_c values	36
Table 4.2 MBE condition state rating Table 6A.4.2.3-1.....	37
Table 6.1 List of bridges visited, their condition state and max % loss summary.....	55
Table 6.2 Summary of % loss and COV of bridges after being grinded	61
Table 6.3 Summary of max COV for all percentage loss	62
Table 6.4 Element #107 condition state definitions.....	69
Table 6.5 Table C6A.4.2.3-1- from MBE: description of member condition	70
Table 6.6 Condition state and its equivalent condition rating and its description	71
Table 6.7 Condition state and a range of section loss in each condition state.....	72

Table 6.8 Range of condition state consistent with Element Inspection	73
Table 6.9 ϕ_c for two deterioration profiles using the range consistent with NDOR	74
Table 6.10 Range of section loss for condition state and their corresponding ϕ_c	75
Table 6.11 Range of section loss for condition states.....	76
Table 6.12 Categorization of possible condition state into CS's.....	84
Table 6.13 Sample scenarios of condition states distribution in percentage	86
Table 7.1 Summary of values of m, n and o used in Eq. (24) through (32)	92
Table 7.2 Summary of values of COV_{max} used in Eq. (34), (37) and (40)	92
Table 7.3 Sample mean and standard deviation for CS's with GP1 and GP2.....	93
Table 7.4 ϕ_c for carbon steel when the worst CS is known in a rural environment	95
Table 7.5 Multiplier for ϕ_c for carbon steel in urban and marine environment	95
Table 7.6 Multiplier for ϕ_c for weathering steel in the three environments	95
Table 7.7 Percentage loss for condition states in Approach 1	95
Table 7.8 ϕ_c and distribution variable for combinations shown in Table 7.3.....	99
Table 7.9 Percentage loss for each condition state for Approach 2.....	102
Table 7.10 ANN multiplier for GP1 deterioration profile	102
Table 7.11 ANN multiplier for GP2 deterioration profile	102
Table 7.12 ANN multiplier for GP 1 deterioration profile with NDOR Range	103
Table 7.13 ANN multiplier for GP2 deterioration profile with NDOR Range	103
Table 7.14 Percentage loss for each condition state in Approach 3	111
Table 7.15 ϕ_c for each condition state and the range of percentage loss.....	111
Table 7.16 Multiplier for ϕ_c for carbon steel in urban and marine environment	111

Table 7.17 Multiplier for ϕ_c for weathering steel in the three environments	112
Table 7.18 ϕ_c and multiplier for different range of deterioration	113
Appendix Figure A Flowchart for LRFD Article 6.10.6- strength limit state	131
Appendix Figure B Flowchart for Article 6.10.7- composite sections in positive flexure	132
Appendix Figure C Location of Ybar and PNA to calculate moment capacity.....	133
Appendix Figure D Different pattern of bottom flange corrosion.....	134
Appendix Figure F Loss of thickness predicted using Komp's corrosion model.....	137

Chapter 1: Introduction

Bridge inspections and evaluations ensure that new and ongoing deterioration does not compromise the load-carrying capacity of the bridge. AASHTO's LRFD has set an acceptable level of reliability for bridges and their components at the design stage to ensure sufficient safety. Reliability is defined by the probability of failure, which requires the quantification of demand and capacity means and dispersions. Corrosion both decreases the expected value and increases the uncertainty in capacity. Capacity is assessed using the remaining sound section of the bridge found through inspection.

Bridge collapses in the past have resulted in government agencies establishing regular intervals for the bridge inspections and evaluations. In the United States, the collapse of the 2,235 ft. Silver Bridge at Point Pleasant, West Virginia on December 15, 1967, claimed the lives of 46 people and led to the establishment of the National Bridge Inspection Standards (NBIS) (Federal Highway Administration, 2012). The NBIS established the national policy regarding inspection procedures, frequency of inspections, qualifications of personnel, inspection reports, and maintenance of state bridge inventory. The NBIS has been modified multiple times to obtain a comprehensive database of pertinent data for all bridges in the United States.

The National Bridge Inventory (NBI) maintains records for the condition of multiple bridge components for each bridge in the United States. Data available in the NBI is also used to assess the structural deficiency of bridges. For example, a superstructure condition rating less than or equal to 4, categorizes the bridge as structurally deficient. Out of 611,845 highway bridges in the United States, 58,795 bridges are structurally deficient. Corrosion of steel and steel reinforcement are the

primary cause of structurally deficient bridges (Yunovich, Thompson, Balvanyos, & Lave, 2001). The projected annual direct cost of corrosion for highway bridges is estimated at \$8.3 billion, of which \$3.8 billion is needed to replace structurally deficient bridges over the next 10 years. (Vermani, 2002) Although bridges with one or more majorly deteriorated components are classified as structurally deficient, the existence of deterioration does not necessarily compromise structural safety. Load rating is a direct method that can be used to assess the safe load carrying capacity of a bridge.

1.1 Load Rating and Condition Factor

The American Association of State Highway and Transportation Officials (AASHTO) Manual for Bridge Evaluation (MBE) requires load rating to be performed using the Allowable Stress Rating (ASR), Load Factor Rating (LFR) or Load and Resistance Rating Factor (LRFR) (AASHTO, 2014). These three rating methods parallel the design philosophy of the Allowable Stress Design (ASD), Load Factor Design (LFD) and, Load and Resistance Factor Design (LRFD), respectively. Although LRFR is a parallel rating procedure to LRFD (the preferred method for design of AASHTO), the MBE does not have a preference among the three rating methods.

All three methods have been shown to give different rating results. Nowak did a comparison of these methods and concluded that the LRFR is very conservative compared to the other two and suggested a lower target reliability index to make it comparable to the other method. Christopher D. Moen in “A comparison of AASHTO Bridge load rating methods,” saw load rating factors up to 40% lower than the LFR for an interior steel composite girder in flexural. Although there might be an inconsistency as to which load rating procedure delivers a better load rating, it is generally agreed upon that

the LRFR produces a uniform reliability across all existing bridges. On this basis, it can be understood that the LRFR is a more rational method for rating.

The LRFR, a reliability based rating procedure, seeks to maintain a consistent reliability across all bridges. Increased deterioration in the bridge increases the uncertainty in capacity. Section 6A.4.2.3 of the MBE introduces the condition factor ϕ_c to account for the increased uncertainty in the resistance of the deteriorated member. The MBE has categorized the ϕ_c into three condition states: “Good or Satisfactory”, “Fair” and “Poor”. The severity of penalization increases with the decreasing condition of the girder.

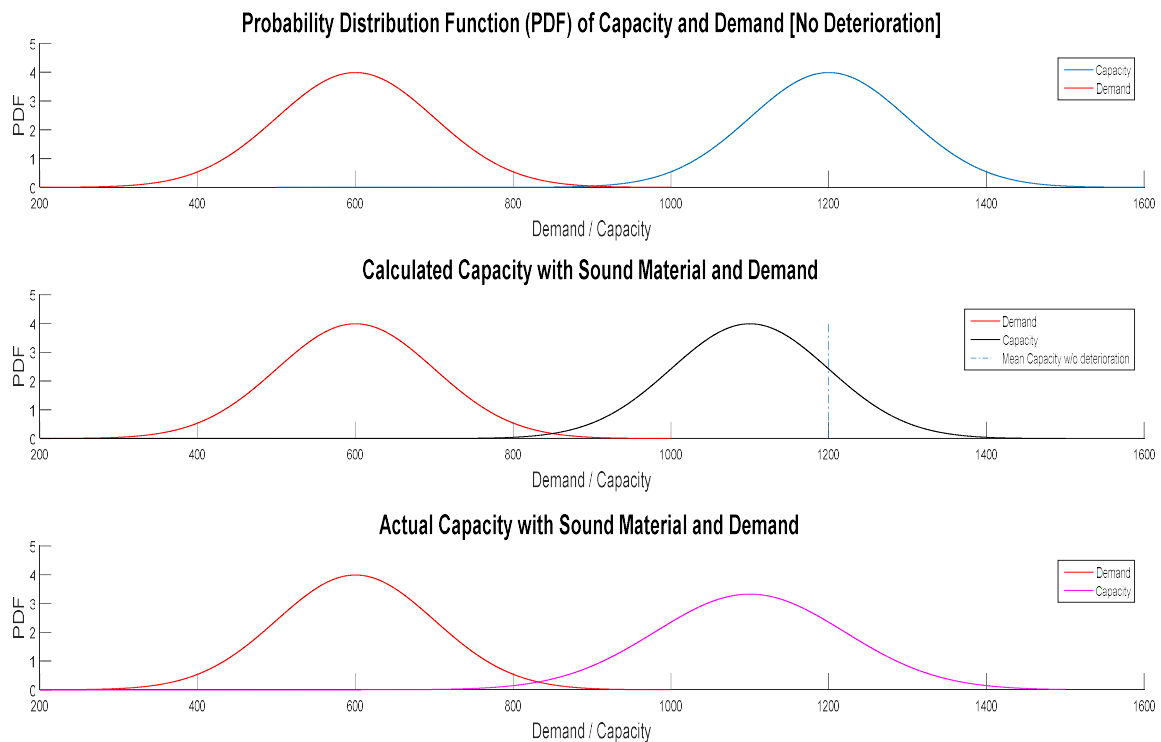


Figure 1.1 PDF curve explaining ϕ_c

Figure 1.1 contains multiple graphs that illustrate the concept of ϕ_c . The first graph in the figure shows the variable demand and capacity of a new girder. The area underneath the capacity (blue/ right) and demand (red/ left) curve is where failure occurs.

As the girder deteriorates, its capacity decreases, resulting in a shift of the capacity curve to the left, as seen in the second graph. In the second graph, the remaining section is used to calculate the capacity, but it does not capture the increased uncertainty in the capacity due to deterioration. The third graph has a higher spread in the capacity and a higher standard deviation, which captures the increased uncertainty. The shift to the left by the ϕ_c , bringing the capacity down to the design point to capture the actual probability of failure present and to provide a consistent reliability in the load rating.

Some of the reasons behind the increased uncertainty in the capacity of deteriorated girders are due to non-uniform deterioration in the girder that increased variability in the remaining section, the likelihood of future deterioration and human error during the inspection. The penalization by the ϕ_c increases to account for the increased uncertainty as the condition of the girder decreases. The ϕ_c allows the load rating to provide consistent reliability among all bridges that have been rated using the LRFR.

Uneven deterioration causes variation in the remaining section of the girder, which increases the uncertainty in the capacity of the member. The cross-section of the girder directly affects its flexure, shear and bearing capacity. The variability in the capacity increases with increasing variability in the cross-section. Therefore, an increase in deterioration in the girder increases the uncertainty in the capacity of the member.

NCHRP 301, the first documentation of the condition factor, by Moses and Verma, introduced the condition factor to keep the reliability among all bridges consistent. The condition factor was introduced to account for the increased likelihood of possible future corrosion in a girder with a decreasing condition.

Inspection detail varies with the type of inspection performed in the field. Varying levels of inspection detail translate to varying degrees of uncertainty. Pertinent inspection details for the characterization of the ϕ_c include the spatial dispersion and severity of deterioration. Section loss is generally noted by the inspector during the inspection, but the location of the deterioration is not always noted. Higher deterioration results in a higher variability in measurement, which increases the uncertainty in the capacity.

In a new bridge, the critical location for all the modes of failures (Flexure, Shear, Bearing, and Buckling) are known. For example, the location of the minimum load to capacity ratio is near the mid-span because the uniform cross-section of a new girder provides uniform load capacity along the span. The same girder after deterioration would have non-uniform load carrying capacity, which could move the critical location away from the mid-span. If the cross-section along the span is unknown, there will be uncertainty in the location of the critical section.

The load rating using LRFR defined in the Manual for Bridge Evaluation (MBE) uses ϕ_c to account for the increased uncertainty in the resistance of deteriorated member. Currently, condition factors are nominally correlated to the condition of the member, which can be Good, Fair, or Poor, with corresponding ϕ_c values to account for “increased uncertainty in the resistance of deteriorated members and the likely increased future deterioration of these members during the period between inspection cycles.” (AASHTO, 2014)

The MBE defers the task of providing member condition definitions to the MBEI. However, the MBEI also lacks clarity and objective definitions. Furthermore, lack of guidance to account for the location and the extent of deterioration exacerbates confusion

when classifying the member into one of the three general conditions. In practical terms, **the problem is that load ratings produced based on existing guidance in MBE and MBEI do not consistently provide the target level of reliability, as intended by the LRFR procedure.** The problem is complex, and it is not even possible to say that the current guidance for load ratings typically produces either conservative or unconservative estimates of load ratings, because the outcome will vary from bridge to bridge. The objective of this research is to provide a procedure to select a calibrated ϕ appropriate to field conditions, accounting for the uncertainty due to non-uniform deterioration in the girder across a section, the lack of knowledge of the location of the deterioration, and the likelihood of further deterioration over the next inspection cycle.

Chapter 2: Literature Review

Calibration of the ϕ_c required an understanding of the bridge inspection and evaluation process, the effects of corrosion and the use of the ϕ_c in the LRFR to provide a reliable load rating. The details of bridge inspection and evaluation, including the needs for, are discussed in section 2.1 Overview of Bridge Inspection and Evaluation. The effects of corrosion in the steel bridges, the rate of corrosion in carbon and weathering steel, and the patterns of corrosion seen in the field are discussed in section 2.2 Deterioration Mechanisms and Documentation. A summary of the LRFR procedure along with the history of the ϕ_c is shown in section 2.3 Development of LRFR . Finally, previous studies on the effects of corrosion on the steel bridge reliability are shown in section 2.4 Steel Bridge Reliability.

2.1 Overview of Bridge Inspection and Evaluation

The U.S. Congress added a section to the Federal Highway Act of 1968, which required the Secretary of Transportation to establish a National Bridge Inspection Standard (NBIS) in 1971. The NBIS established a national policy regarding inspection procedures, the frequency of inspections, qualifications of personnel, inspection reports, and maintenance of state bridge inventory (Federal Highway Administration, 2012).

Over the years, the Federal Highway Administration (FHWA) has added reference manuals, including the Bridge Inspector's Training Manual 70, Manual for Maintenance of Bridges, Recording and Coding Guide for the Structure Inventory and Appraisal of the Nation's Bridges, The Bridge Inspector's Manual for Movable Bridges, Culvert Inspection Manual, Inspection of Fracture Critical Bridge Members, etc. These manuals have evolved in time and are currently being used by local, state and federal

agencies for bridge inspection and evaluation. Some of the current FHWA reference materials are discussed below: (Federal Highway Administration, 2012)

- Bridge Inspector's Reference Manual (BRIM)

A manual for inspectors that include: a bridge inspection program; safety fundamentals for bridge inspectors; bridge terminology; bridge inspection reporting; bridge mechanics; bridge materials, inspection and evaluation of bridges decks and areas adjacent to bridge decks; inspection and evaluation of superstructures, bridge bearing, substructures; characteristics, inspection and evaluation of culverts; and advanced inspection methods for complex bridges.

- Manual for Bridge Element Inspection (MBEI):

The MBEI defines a comprehensive set of elements that are designed to be flexible in nature to satisfy the needs of all agencies, and are characterized into general condition assessments. The four condition states that are Good, Fair, Poor and Severe. These condition states are defined differently for each element.

- Manual for Bridge Evaluation (MBE):

The MBE is a standard for providing uniformity in the procedures and policies used to determine the physical condition, maintenance needs, and load capacity of the nation's highway bridge. It assists bridge owners by establishing inspection procedures and evaluation practices that meet the NBIS.

- Recording and Coding Guide for the Structure Inventory and Appraisal (SI&A) of the Nation's Bridges;

This guide has been prepared for state, federal and other agencies to use for recording and coding the data elements that will comprise the NBI database. This guide is

used to formulate an accurate report that can be made to the Congress on the number and the state of the nation's bridges, and also to provide a complete and thorough inventory by FHWA and the military to identify and classify the strategic highway corridor network and its connectors for defense purposes. The coded items in this guide are considered an integral part of the database that can be used to meet several federal reporting requirements, as well as part of the states' needs. This guide is used to generate reports to be submitted to the Highway Bridge Replacement and Rehabilitation Program and the National Bridge Inspection Program (Weseman, 1995). The broad NBI condition ratings (superstructure, substructure, and deck) have been collected for all bridges, both on and off the National Highway System (NHS) since the NBIS was established in 1971. condition ratings and other functional and geometric data for bridges allowed FHWA to use the Sufficiency Rating for funding prioritization (Bridge Inspection Manual NDOR).

Although the use of the code and instructions in this guide is not required for the the state, federal and other agencies, each agency needs to submit data to FHWA in a format that will be consistent with the guide (Weseman, 1995).

- Code of Federal Regulation

The purpose of the regulations in this part is to implement and carry out the provisions of federal law relating to the administration of federal aid for highways. This federal aid policy guide has the process that FHWA needs to follow for distributing federal funding to the states for transportation. It also has the requirements that the state governments need to fulfill for the federal funding (Federal Highway Administration, 2010).

2.1.1 Bridge Inspection Types and Report

The MBE requires bridges to be inspected at regular intervals and not to exceed 24 months without prior approval from FHWA and justification by past reports and performance history and analysis. There is a maximum inspection cycle of 48 months that cannot be exceeded. There are many types of inspections listed in the MBE, including initial inspection, routine inspection, damage inspection, in-depth inspection, fracture-critical inspection, underwater inspection, and special inspections.

The reports from an inspection have varying level of details about the bridge and its element depending on the type of inspection performed. There are two major types of inspections: Structure Inventory and Appraisal (SI&A) and Element Level Inspection. These inspections have fundamentally different inspection reporting techniques. SI&A reports the overall condition of bridge parts like the superstructure, the substructure, or the deck. Whereas Element Level Inspection reports the condition of all elements of the bridge like girders, abutments, piers etc.

NDOR's inspector include the SI&A condition of the bridge in their report because it is reported to the NBI. The load rating is done through the use of the Element Inspection data.

NDOR has moved to a more detailed inspection technique, the Element Level Inspection, which allow NDOR to manage their bridge inventory more effectively, allowing them to:

- quantify and describe element condition observed during the inspection and the extent of deterioration;

- identify candidates for preservation, maintenance, rehabilitation, improvement (i.e. widening, raising, strengthening) and replacement practices/strategies;
- predict future deterioration of bridge elements for scheduling purposes; and
- manage their budgets for bridge preservation.

(Nebraska Department of Roads: Bridge Division, 2015)

2.2 Deterioration Mechanisms and Documentation

The MBEI requires inspection of all the elements for various defects including corrosion, cracking, connection defects, delamination/spall/patched area, efflorescence/rust staining, cracking, deterioration, distortion, and damage. The most common form of deterioration identified in inspections of steel girders is corrosion, which is the oxidization of metal through a reaction involving oxygen, water, or other agents. It is an electrochemical process between two metals: the metal areas having higher tendency to corrode (anode) and the metal areas having a lower tendency to corrode (cathode); when an electrolyte is present between them, which allows the current flow to occur. On bridges, this electrolyte is usually water (Kulicki, Prucz, Sorgenfrei, Mertz, & Young, 1990).

There are different types of corrosion in metal: galvanic corrosion, crevice corrosion, pitting, intergranular corrosion, selective leaching, erosion corrosion, stress corrosion, and hydrogen damage are the most common ones. As all of the corrosion causes loss in a section, it is not necessary to study them individually, only their effect in the cross-section of the girder.

2.2.1 Corrosion Effects

It is crucial to consider corrosion during the design of steel bridges. The effects of corrosion vary from non-structural maintenance problems to a local failure or an overall collapse. In the NCHRP report 333, there are four major corrosion effects: loss of section, creation of stress concentration, introduction of unintended fixity, and introduction of unintended movement (Kulicki et al., 1990).

The loss of section reduces the geometric properties, such as the moment of inertia, radius of gyration, slenderness ratio of the web and flanges (Kayser & Nowak, 1989a). This reduction lowers the bending, axial and shear capacity of the member, and it can also affect the fatigue life of the member because of the increased stress range (Czarnecki & Nowak, 2008). Creation of stress raisers results from the formation of holes and notches which creates stress concentrations and can initiate cracks (Kulicki et al., 1990). The introduction of unintentional fixity is the freezing of moving parts of the bridge, such as expansion devices or hangers. Unintentional fixity can cause the structure to behave differently than designed and to experience unexpected high stresses up to 10,000 psi. Out of the four effects of corrosion, the focus of this study was the loss of section due to corrosion.

2.2.2 Rate of Corrosion

A large amount of energy consumed during the manufacturing process is stored in the metal. The natural tendency of the metal to return to its lower energy state results in corrosion. The rate of corrosion depends on the presence of electrolytes like water, oxygen, and salt. The presence of these electrolytes can vary depending on the

environment such as marine environment which has a higher abundance of water and salt increasing the rate of corrosion significantly (Kayser & Nowak, 1989a).

Komp studied the rate of corrosion for various metals in different environments. The types of steel included carbon steel and weathering steel, and the different environments are rural, urban and marine environments. This equation follows an asymptotic function to predict the corrosion in metal, so the rate of corrosion decreases in time. The parameters A and B are specific to the type of steel and environment; therefore, the prediction varies for the steel in each environment (Komp, 1987). The various parameters are shown in Table 2.1.

$$C = At^B \quad (1)$$

Where C is the average corrosion penetration in microns

t is the number of years

A and B are the parameters

Table 2.1 Corrosion parameters in Komp's corrosion model

Environment	Carbon Steel		Weathering Steel	
	A	B	A	B
Rural	34.0	0.65	33.3	0.50
Urban	80.2	0.59	50.7	0.57
Marine	70.6	0.79	40.2	0.56

Although there are multiple models for predicting the rate of corrosion, Komp's model has been adopted by many researchers. A model by R.J. McCrum suggests a linear increase in corrosion penetration contrary to the logarithmic corrosion penetration suggested by Komp (see Figure 2.1 and Figure 2.2). The model by Komp seems to have a better prediction of corrosion. It followed the standard ASTM procedure for corrosion

test and measurement after corrosion. Komp's corrosion model has been repeatedly used by many researchers including Nowak and Moses (McCrum, Arnold, & Dexter, 1985).

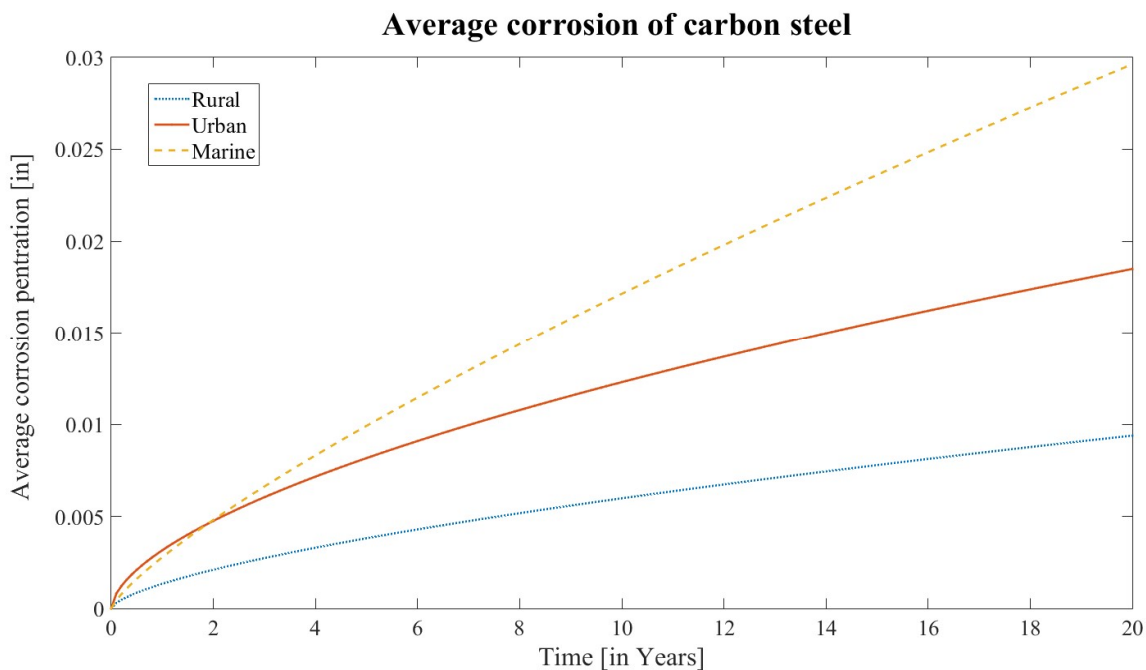


Figure 2.1 Average corrosion of carbon steel using Komp's model

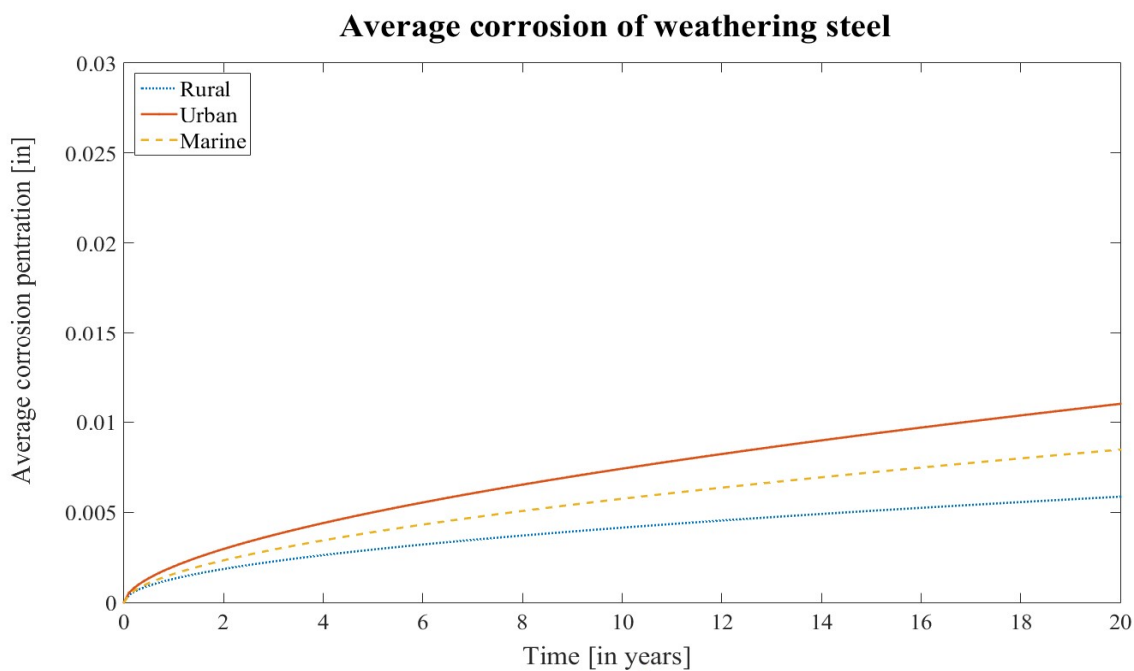


Figure 2.2 Average corrosion of weathering steel using Komp's model

The ASTM G 50-10 “Standard Practice for Conducting Atmospheric Corrosion Tests on Metals” was followed by Komp to evaluate the corrosion resistance of metals when exposed to weather, as well as to evaluate the relative corrosivity of the atmosphere at a specific location. The test sites – described typically as rural, industrial (urban) and marine atmospheres are characterized in accordance with practice G92 “Practice for Characterization of Atmospheric Test Sites.” The ASTM G 50-10 provides a suggestion for the locations to place the test specimens. The specimen has to be preferably larger than 4 by 6 inches, with a minimum thickness of 0.030 inches and a maximum thickness of 0.25 inches. Specimens should be weighed at least to 0.01g before exposure. Multiple specimens’ need to be sampled at a suitable rate suggested at 1, 2, 4, 8, and 16 years, and there should be an appropriate number of control specimens. Records of the weight, dimensions, and appearances of each specimen at the beginning of the test should be kept (ASTM International, 2015).

At the time of evaluation, the specimens should be cleaned according to the practice described in G1 “Practice for Preparing, Cleaning, and Evaluating Corrosion Test Specimens.” Practice G1 designates careful removal of corrosion products without the extraction of a significant amount of base metal. It is recommended to repeat the cleaning procedure and weigh the specimens after each cleaning. The mass loss should be graphed; the location where the rate of mass loss per cleaning decreases is the location that is considered to be the mass loss for the specimen. A low powered microscope can be used to confirm the removal of all corrosion products (ASTM International, 2011).

Corrosion product removal is divided into three general categories: mechanical, chemical, and electrolytic. Chemical procedures can involve the immersion of the

corrosion test specimen, brushing or ultrasonic cleaning; but should be done before and after electrolytic cleaning. Mechanical procedures can include scraping, scrubbing, brushing, ultrasonic cleaning, mechanical shocking, and impact blasting. Vigorous mechanical cleaning may result in the removal of base metal; therefore, this is only recommended when other methods fail (ASTM International, 2011).

The average corrosion rate may be obtained by using the following equation:

$$\text{Corrosion rate} = \frac{K * W}{A * T * D} \quad (2)$$

Where:

K = a constant depending on the desired unit

T = time of exposure in hours

A = area of cm^2

W = mass loss in grams, and

D = density in g/cm^3

Precision of the prediction of the corrosion rate depends on the corrosion product removal and the determination of the area. The precision can be improved by increasing the frequency of the cleaning of the specimen. Bias can also result from inadequate or over cleaning and minimized by increasing the frequency of measurement between cleaning (ASTM International, 2011).

The data collected for the exposed specimens include dimensions, chemical composition, metallurgical history, surface preparation, and post-corrosion cleaning methods. The detail of exposure condition which includes its location, dates and periods of exposure, and a description of the atmospheric conditions prevailing during the

exposure period should also be noted along with any change in the physical appearance of the specimen (ASTM International, 2015).

The corrosion rate needs to be expressed in terms of penetration per year or loss in thickness over the exposure period. This corrosion rate is the average of the top and bottom surface loss (ASTM International, 2015).

Table 2.2 Corrosion penetration of sheltered VS exposed conditions

Environment	Corrosion for sheltered conditions Corrosion for exposed conditions
Rural	1.0
Industrial	1.7
Marine	2.0

The Initial climate condition, the shelter and orientation, the angle of exposure, a continuously moist condition, and deicing salts affect the rate of corrosion. Out of these factors, shelter and orientation and deicing salt significantly affect the rate of corrosion. McKenzie suggested multipliers for the amount of corrosion for the sheltered corrosion condition. In Table 2.2, a ratio of the average corrosion of the sheltered condition and the corrosion of the exposed condition is shown. Similarly, tests by Larrabee have shown that the corrosion under the sheltered conditions (continuously wet conditions) is about three times compared to the exposed condition (dry atmosphere). Sereda showed that the percentage of time over certain critical humidity levels called the “time of wetness”, it is a significant factor promoting the atmospheric corrosion of metals. Due to the lack of a reliable method of estimating the time of wetness, it’s more reliable to use the biannual inspection. Finally, deicing salts causes approximately 2.75 times more corrosion the absence of salt, as noted by Albrecht and Naeemi (Albrecht & Naeemi, 1984; Moses & Verma, 1987).

Table 2.3 Uniform corrosion rate for a 4" X 6" steel plate specimen, [ASTM,1968].

Mean loss gram	Standard deviation grams	C.O.V.	Environment and location
2.2	0.1	0.05	Arid, Phoenix, AZ
7.0	0.68	0.10	Industrial, Detroit, MI
14.0	1.87	0.13	Heavy Industrial, Pittsburgh, PA
41.1	1.20	0.03	Severe Industrial, East Chicago, IN

Nowak and Kayser found that the rate or predictability of corrosion is variable.

Several forms of corrosion that take place on a metal surface depend upon the local chemistry and configuration of the materials. Nowak and Kayser used the reliability methods to predict structural deterioration on a structural basis by formulating the variability as a statistical distribution. Several rates of general corrosion for carbon steel in different environments from ASTM 1968 are listed in Table 2.3. A large variation in both the mean rate of corrosion and the corresponding Coefficient of variation (COV) can be seen in the table (Kayser & Nowak, 1989b).

2.2.3 Corrosion Pattern in Steel Girder

Corrosion in steel girders occurs at a faster rate at the location where a higher amount of electrolytes (water and contaminants) accumulates. On a simple-span bridge, this accumulation occurs at the deck joints and on flat undrained surfaces. Nowak suggested corrosion would occur at the bottom flanges and the bottom portion of the web along the span in a simple span bridge. This pattern for a simple span steel girder bridges is seen commonly in the field. The corrosion is most likely to occur along the top surface of the bottom flange and bottom portion of the web, due to traffic spray accumulation. The corrosion would occur over the entire web near the support due to deck leakage (Kayser & Nowak, 1989a). At the mid-span, corrosion of the web usually reaches $\frac{1}{4}$ of

the web height. Figure 2.3 shows the corrosion pattern along the section as developed by Czarnecki and Nowak (Czarnecki & Nowak, 2008).

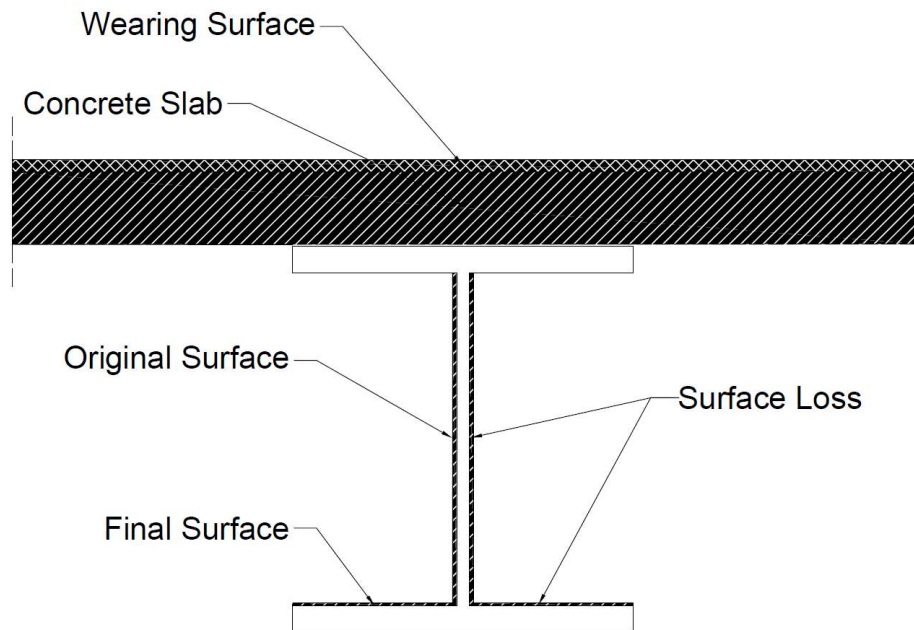


Figure 2.3 Corrosion of a steel girder bridge

(Recreated from A. A. Czarnecki, A.S. Nowak / Structural Safety 30 (2008) 49-64)

Factors, including the presence of electrolytes, deck leakage, and the accumulation of water on the superstructure increase the rate of corrosion. An estimate of the location of deterioration can be made on the basis of the bridge design by knowing the common location for corrosion on the superstructure which is in the vicinity of the deck joints and along horizontal surfaces, where dust, road spray, and water accumulate. A typical corrosion pattern in the steel girder bridge is deduced and shown in Figure 2.4.

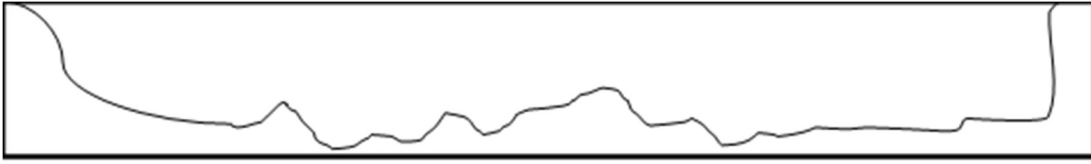


Figure 2.4 Typical corrosion pattern in a steel girder

2.3 Development of LRFR Methodology

Load rating is a measure of the live-load capacity of a bridge. The process of load rating is defined extensively in the MBE. The MBE has three different load rating procedures. This research focuses on the LRFR which goes parallel to the LRFD.

2.3.1 LRFR Procedure

The LRFR calculates the remaining live-load capacity of the bridge with consistent reliability. In Eq. (3), the dead and permanent loads are subtracted from the capacity and the remainder is then divided by the live-load to calculate the load rating. A load rating value greater than 1 means that the bridge can reliably carry the design live-load. A load rating value less than 1 means that the bridge cannot reliably carry the traffic load it encounters and needs to be posted for a lower load to avoid failure.

$$\text{Load Rating} = \frac{C - \gamma_{DC}(DC) - \gamma_{DW}(DW) \pm \gamma_P(P)}{\gamma_{LL}(LL + IM)} \quad (3)$$

$$C = \phi * \phi_S * \phi_c \quad (4)$$

Where,

C = Capacity

ϕ = Resistance factor

ϕ_S = System or Redundancy factor

ϕ_c = Condition factor

γ_{DC} & γ_{DW} = Dead Load factor for component and wearing surface

DC & DW = Load effects due to Components and Wearing Surface

γ_P = Load factor for permanent loads

P = Load due to Permanent Loads

γ_{LL} = Live Load factor

LL = Live load effect

IM = Impact factor

Multiple factors included with the capacity are the ϕ , ϕ_s , and ϕ_c . The ϕ is resistance factor which is associated with fabrication, material, and professional uncertainties. These uncertainties are the result of the tolerances in the manufacturing process, the variability in the yield strength of the material, the estimation done during calculation of the capacity, etc. The system or redundancy factor is ϕ_s . In most cases, ϕ_s is a penalty for the lack of redundancy in the structure for the element that is load rated. There are some cases where ϕ_s can be greater than 1 but these instances are rare and very difficult to justify. The condition factor of the girder is the ϕ_c , which is present to account for the increased uncertainty associated with the current condition of the girder.

The LRFR permits two levels of target reliability index. The reliability index is a measure of the probability of failure. The probability of failure is set to avoid failure of a structure in its design life. Load rating at the reliability index of 3.5 is called the inventory rating, and load rating at reliability index of 2.5 is called the operating rating. The reliability rating at the inventory level targets the same level of reliability as the LRFD. As the condition of the bridge decreases, AASHTO allows the bridges to be rated at a lower target reliability level because achieving the inventory level is not always

practical and can be justified with a biannual inspection. The two target levels in the MBE are achieved in the LRFR by the use of different live-load factors. The inventory level rating has higher live-load factors of 1.75 in the strength I load combination to achieve the higher reliability index of 3.5 and similarly the operating level rating has lower live-load factors of 1.35 in the strength I load combination to achieve the lower reliability index of 2.5. The resistance factor and other load factors do not change for the two rating levels.(AASHTO, 2014)

The bridge loads and the capacity are random variables and their distribution is modeled to generate the load and resistance factors in the LRFD and LRFR to achieve the target reliability index.

$$Q = D + L + I + E + S \quad (5)$$

The model of bridge load (Q) is the sum of dead-load (D), live-load (L), Dynamic load (I), Environmental loads (wind, earthquake, temperature, etc.) (E), and other loads (collision, emergency braking, etc.) (S). The bias and COV for the dead-load are shown in Table 2.4 (Kayser & Nowak, 1989b).

Table 2.4 Bias and COV for the loads

Member	Bias	COV
Factory made	1.03	0.04
Cast in place	1.05	0.08
Asphalt	1.10	0.25

Ghosn and Moses modeled the live-load by combining the static and dynamic live-load into a lognormally distributed random variable as shown in Eq. (6).

$$L + I = amW * HgiGr \quad (6)$$

Where,

$L + I =$ mean 50 year moment in the girder due to static and dynamic load,

$a =$ deterministic value depending on truck configuration and span length,

$m =$ random value based on the variation of load effect,

$W =$ 95th percentile of weight for the dominant truck type at the bridge site,

$H =$ value related to the probability of closely spaced vehicles on a bridge,

$g =$ girder distribution factor,

$i =$ dynamic amplification factor, and

Gr is the future growth factor. (Kayser & Nowak, 1989b)

2.3.2 Introduction of ϕ_c

The condition factor in the LRFR accounts for the increased uncertainty in the capacity due to deterioration. Moses and Verma in the NCHRP 301 introduced the condition factor to account for the increased likelihood of future corrosion with an increasing level of corrosion (decrease in condition). The NCHRP 301 had three conditions for the girder; “Good”, “Slight” corrosion and “Severe” corrosion along with their capacity reduction factor, ϕ . (see Table 2.5).

Table 2.5 Condition rating and the penalization as suggested by NCHRP 301

Condition	Capacity Reduction Factor, ϕ
Good condition	0.95
Slight corrosion, some section loss	0.85
Severe corrosion, considerable section loss	0.75

The NCHRP 301 uses Komp’s corrosion model in different environments to predict the corrosion in time. Komp’s model has been described earlier in section 2.2.2 Rate of Corrosion on page 12. Moses and Verma linked different environments to the condition of the girder; the “Good” condition girder is considered to corrode in a rural environment, “Slight” corrosion in a girder suggests corrosion in an urban environment,

and the similarly “Severe” corrosion condition is linked with the marine environment. For their study, the Komp’s model along with multipliers to account for the increased rate of corrosion due to the presence of deicing salt and the sheltered condition (Table 2.8), is used to predict the section loss. The amount of loss per side for each condition state in 2 years is summarized in Table 2.7. The section modulus of the remaining section is used to calculate the remaining capacity and adjusted to the bias. A mean reduction in the section modulus for a W 27X 94 is summarized in Table 2.8 (Moses & Verma, 1987).

Table 2.6 Corrosion rate for carbon steel for different corrosion of section

Corrosion of Section	Type of Environment	Eq. H-1
Normal, Good Condition	Rural	$C = 34 \text{ t}0.65$
Medium, Slight Corrosion	Industrial	$C = 65 \text{ t}0.5$
Severe Corrosion	Marine	$C = 80 \text{ t}0.8$

Table 2.7 Calculation of average thickness loss for difference corrosion of section

Condition of Section	Eq. H-1 (2 years)	Multipliers* Eq. H-1	Amount of Thickness loss per side, mils
Good condition	$34*20.65=53.35/25.4$	$1.0*2.10*2.75$	$5.77 = 6$
Slight corrosion	$65*20.5=91.92/25.4$	$1.7*3.625*2.75$	$16.9 = 17$
Heavy corrosion	$80*20.8= 139.29/25.4$	$2.0*5.48*2.75$	$30.16= 30$

Table 2.8 Summary of % reduction in section modulus (2 years)

Condition of Section	% reduction in Section modulus (mean, 2-year period)
Good condition	1.8
Slight corrosion	5.0
Heavy corrosion	9.0

In the NCHRP 301, Moses and Verma directly correlated the percentage reduction in the section modulus to the percentage reduction in the moment capacity. The moment capacity was taken as the yield strength of the steel times the section modulus, therefore reduction in section modulus was equal to the reduction in moment capacity. Local buckling was ignored because the girders were assumed to be fully composite with the deck and the compression (top) flange continuously braced throughout the span. The

bracing allowed the girder to reach its moment capacity without local or torsional buckling.

Moses and Verma updated the bias to reflect the loss in moment capacity and increased the coefficient of variation for the different condition of the girder. A bias of a new girder was taken as 1.1 during the LRFD code calibration, which was adopted by the Good condition girder. The biases for the other conditions were determined by multiplying the remaining percentage of the section to the original bias. McCrum's suggestion for the increased COV for each condition state was used for this study. This COV had been made with some subjective estimates. The NCHRP 301 suggested the use of the following data for the bias and COV for different condition of girder which is summarized in Table 2.9

$$1.1 * (1 - 0.05) = 1.05 \text{ for slight corrosion}$$

$$1.1 * (1 - 0.09) = 1.0 \text{ for severe corrosion}$$

Table 2.9 Summary of bias and COV for different section condition

	Bias	COV
New condition, steel member	1.10	12%
Partially corroded with some section loss	1.05	16%
Severe corrosion with considerable loss of section	1.00	20%

For the effect of the influence of deterioration NCHRP 301 suggested using the following flow chart in Figure 2.5. Lack of guidance for “None”, “Slight”, or “Heavy” corrosion level in Figure 2.5 is apparent as only qualitative description are given for the three categories. This leaves practitioners to make independent decisions to determinate the category for the corrosion level in the girder.

Moses in the NCHRP 454, revisited the condition factor with recommendations to use the condition factor to account for the increased uncertainty in the girder only. This

report cleared any confusion, if present, that the use of the condition factor does not replace adequate inspection data to estimate the nominal resistance, R_n – the best estimate of the capacity. The NCHRP 454 discourages imposing a double penalty to the deteriorated sections such that a conservative estimate of section loss and a member condition factor both reduce the factored strength in the rating check. The condition rating is meant to recognize the greater uncertainty in estimating the true strength of the member. The condition factor values were revisited to the current ϕ_c used in the MBE (Moses, 2001).

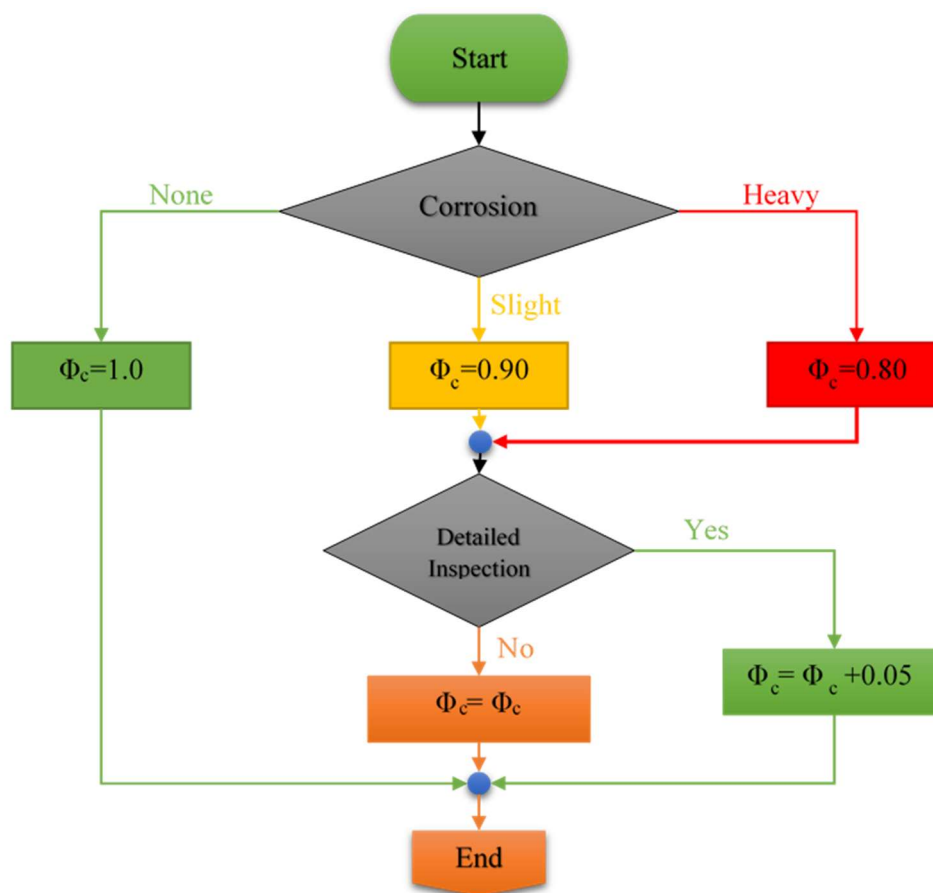


Figure 2.5 Flowchart for selecting resistance factor according to NCHRP 301

2.4 Steel Bridge Reliability

In their “Evaluation of corroded steel girder bridges”, Kayser and Nowak created a general framework to evaluate bridges using the probabilistic method along with the Bayesian approach. The Bayesian approach allows updates to the corrosion estimates with new information. This approach examined the problems associated with corrosion and presented a methodology for evaluating the strength and reliability of corroded steel bridges. The reliability analysis was used to determine bridge safety and update the Bayesian approach to include corrosion loss estimates with new data. Sensitivity analysis was performed to identify the critical bridge components that affect capacity due to an increasing level of corrosion (Kayser & Nowak, 1989b).

Various types of corrosion and their influence on metal bridge components are summarized in Table 2.10. This table serves as a guide relating steel bridge components to the typical forms of corrosion damage.

Table 2.10 Bridge components affected by different forms of corrosion

Bridge Component	Form of Corrosion				
	Uniform	Galvanic	Pitting	Crevice	Stress
Web	S, I		S, I, F		
Flange	S, I		S, I, F		
Stiffener	S, I		S, I, F		
Splice	S	S	F	W	F
Connection		S	F	W	F
Weld		S, F	S, F	W	F
Bolt		S	F	W	F
Hanger	S	S	S, F	W	F
Pin		S	S, F	W	F
Bearing		W		W	

Type of Deterioration:

F- Fatigue and Cracking
I - Reduction in Stiffness
S – Reduction in Strength
W – Oxide Wedging

The data from the periodic inspection were used for the evaluation of bridge reliability. Eq. (7), in which β is the reliability index, can be used to measure the structural performance. Statistical parameters R and Q , required for the calculation of β are estimated using the available data.

$$\beta = \frac{\bar{R} - \bar{Q}}{\sqrt{S_R^2 + S_Q^2}} \quad (7)$$

Where,

\bar{R} , S_R = mean and standard deviation of R ,

\bar{Q} , S_Q = mean and standard deviation of Q .

A sensitivity analysis was performed to determine the parameters that affect the safety of a bridge. The sensitivity function can identify the parameters that affect the reliability of the bridge by changing the values of the parameters and by seeing the corresponding change to the reliability. The parameters studied for the sensitivity analysis were yield strength of steel, concrete, and reinforcement; flange and web thickness; shear plate coefficient; Poisson's ratio; bearing plate coefficient; corrosion coefficient; corrosion exponent; bearing plate coefficient; and shear distribution factor. These parameters and their association to the three modes of resistance (bending, shear and bearing) are shown in Table 2.11. Among the parameters, Kayser and Nowak found that the corrosion rate had a large influence on the structural reliability of a bridge. Shear factor was the second most influential parameter on the structural reliability. The corrosion coefficient had a minor linear effect, whereas the bearing coefficient did not influence the safety until it was reduced by more than 30% (Kayser & Nowak, 1987).

A 12 m and an 18 m bridge were analyzed for all three modes of resistance. The reliability index for a moment did not change much with time. Shear and bearing were the critical modes that controlled the reliability index because the loss of girder material due to corrosion had more effect on the web compared to the flange. This study analyzed the reliability index in bearing capacity of both a stiffened and unstiffened girder, researchers found out reliability index of the unstiffened girder would drop to 0 in about 25 years of exposure for a 12 m girder, but the stiffened girder would have the reliability of the system about the same as the reliability corresponding to the shear mode (Kayser & Nowak, 1989b).

Table 2.11 Parameters associated with mode of resistance.

Parameter	Mode of Resistance		
	Bending	Shear	Bearing
Fy steel compression	*		*
Fy Steel Shear		*	*
E Steel	*	*	*
Fy Steel reinforcement	*		
F'c Concrete	*		
Uncorded web thickness	*		
Uncorded flange thickness	*		
Corroded web thickness	*		
Corroded Flange thickness	*		
Shear Plate Coefficient		*	*
Poisson's ratio		*	*
Bearing plate coefficient			*

2.4.1 Recent Study of ϕ_c

In "Reliability-based condition assessment of existing highway bridges," Wang (2010) presented a general framework for bridge safety evaluation that directly addresses

the deficiencies in current practice. The framework had three levels of assessment for increasing complexity.

In the first level, the deterministic member-based format of the AASHTO LRFR method was kept, and the correlation between the visual condition rating and the capacity evaluation was established (Wang, 2010). The level-one assessment consistent with the current AASHTO LRFR method had one significant adjustment: a new method was introduced to correlate visually-based bridge condition ratings from the routine periodic inspections with structural capacity. A revised set of values of the ϕ_c tied to the AASHTO LRFR rating equations was developed to be consistent with the structural reliability-based philosophy. This study incorporated recent developments in bridge resistance degradation modeling and comprehensive databases of bridge condition rating history. The bridge condition rating history was linked to the statistical models of bridge resistance by mapping the condition rating history model onto the bridge degradation model to develop a reliability-based optimization technique that can identify a set of ϕ_c values. The ϕ_c values satisfy the reliability requirement embodied in the AASHTO LRFR.

The time-dependent structural resistance model by Mori and Ellingwood (1993) as shown in Eq. (8), was used by McCrum to determine the loss in surface area of the reinforcements. Using Thoft- Christensen et. (1977) and Mori and Ellingwood (1994) the equation to calculate the diameter of the rebar at any given time was found, as shown in Eq. (9). Moment capacity of a reinforced concrete beam was found using the remaining diameter in the LRFD moment equation.

$$R(t) = R_0 g(t) \quad (8)$$

$$D_j(t) = \begin{cases} D_{j0} & \text{for } t \leq T_{1j} \\ D_{j0} - r_{corr}(t - T_{1j}) & \text{for } T_{1j} \leq t \leq T_{1j} + D_{j0}/r_{corr} \\ 0 & \text{for } t \geq T_{1j} + D_{j0}/r_{corr} \end{cases} \quad (9)$$

Where

R_o = resistance,

$g(t)$ = the degradation rate,

$D_j(t)$ = diameter of bar j at time t ,

n = number of bars,

D_{j0} = initial diameter of bar j ,

r_{corr} = corrosion rate,

t = elapsed time, and

T_{1j} = corrosion initiation time for bar j .

Variable $g(t)$, the degradation rate, resulted in a variable resistance. A Monte Carlo simulations for resistance, the corrosion initiation time for the bar, and the remaining diameter of the bar were performed (Wang, 2010).

Wang used the bridge degradation modeled by Bolukbasi as a third order polynomial, which is shown in Eq. (10). It was adopted in this study to predict the average condition rating history. The correlation between the condition rating $C(T)$ and the statistical descriptors of degradation $g(t)$ are developed by mapping the average condition rating history of concrete bridges onto the stochastic resistance degradation model with a medium degradation rate. The proposed statistical descriptions of resistance as a function of the condition rating are independent of corrosion rate.

$$C(T) = 8.662 - 0.146T + 0.003T^2 - 3.09E5T^3 \quad (10)$$

Where

$C(T)$ = condition rating of the bridge at age, and

T = time, in years.

The time-dependent mean and COV of the bridge flexural capacity along with the load models used in the AASHTO LRFD (Nowak, 1999) and the bridge condition rating values, were used in the estimation of the time-dependent failure probability and the reliability index of a given bridge. A set of ϕ_c values necessary to achieve the target reliability requirements consistent with the AASHTO LRFR method were obtained by minimizing the mean-square error between the target β_T and the reliability achieved by the use of the specific values of the ϕ_c . Live load factors account for the difference in target reliability (β_T): 3.5 at the inventory level versus 2.5 at the operating level. Therefore, it does not affect the calibration of the ϕ_c . The suggest values are shown below in Table 2.12.

Table 2.12 Proposed condition factors by Wang and Ellingwood

Structural Condition Rating (SI&A)	ϕ_c
≥ 8	1.0
7	0.95
6	0.85
5	0.75
≤ 4	0.70

2.5 Conclusion of Literature Review

This research focuses on providing consistent reliability across all steel bridges using the condition factor ϕ_c . According to the 2013 NBI database, steel bridges constitute over 48% of 15370 bridges in Nebraska, and over 23% of the steel bridges are structurally deficient. The condition factor is determined by the inspection and current condition of the bridge. The only recent similar investigation was by Wang for concrete

bridges. As severity of deterioration of reinforcement is not easily characterized for concrete, Wang used a model to estimate and determine the remaining section area of the reinforcement in time. As this research is for steel girder bridges is conducted in which the severity of research can be categorized. This research addresses a broad range of scenarios for which steel deterioration is documented with varying degrees of detail.

This research focuses on the change in reliability due to corrosion in the flexural capacity of steel girder bridges. Although Czarnecki and Nowak have shown that shear and bearing can be a critical influence on the reliability of the bridge, and they could control over extended periods of time with severe deterioration, researchers focused on flexural capacity because there is a large reserve of shear and bearing capacity for light to moderate deterioration. Additionally, Czarnecki employed simplified uniform deterioration along the span which is not typical of actual field conditions (Czarnecki & Nowak, 2008). NDOR's engineers have also found that flexure generally controls steel girder bridge capacity (Patras, 2016). Finally, Zmerta, Zaghi and Wille have developed a retrofit that can double the bearing and shear capacities of the girder (Zmerta, Zaghi, & Wille, 2015).

Previous research has been able to capture some of the uncertainties that increase with the decreasing condition of the girder. Future possible corrosion and the increase of the variability in section properties are among the few that that been addressed. An objective description of the condition of the girder that would help inspectors identify the bridges consistently and reliably is addressed by this research.

Chapter 3: Objectives and Scope

The ϕ_c in MBE accounts for the increased uncertainty in the resistance of deteriorated member, which is nominally correlated to the condition of the member: Good, Fair, or Poor. Criteria to define the condition state is deferred to MBEI, which itself lacks clarity and an objective basis for categorization. Furthermore, lack of guidance to account for the location and the extent of deterioration exacerbates confusion when classifying the member into one of the three general conditions. In practical terms, the problem is that load ratings produced based on existing guidance in MBE and MBEI do not consistently provide the target level of reliability, as intended by the LRFR procedure. This research seeks to provide a procedure to assign a calibrated ϕ_c appropriate to field conditions, accounting for the uncertainty due to non-uniform deterioration in the girder across a section, the lack of knowledge of the location of the deterioration, and the likelihood of further deterioration over the next inspection cycle. To address these challenges, the following four objectives were identified:

1. survey, describe, and categorize inspection methods, policies, and procedures used by NDOR,
2. identify and categorize types of corrosion commonly observed for steel girder bridges,
3. formulate and assess the relationship between deterioration, loss of capacity, and increase in uncertainty,
4. develop a procedure to map knowledge available from inspections to corresponding condition factors, ϕ_c , and the reduction in nominal capacity.

The scope of this Master's thesis is constrained to:

- simple span girder bridges,
- rolled steel girders of mild steel with yield strengths of 36 ksi,
- carbon and weathering steel,
- projected future deterioration within a 2-year inspection cycle,
- composite girders with concrete slabs having depths of 8 inches and specified compressive strengths of 4 ksi,
- compact cross-sections in flexure,
- consideration of flexural limit states, and
- urban, rural and marine environments

Chapter 4: Overview of Methodology

The condition factors (ϕ_c) in the LRFR accounts for the increased uncertainty in capacity due to deterioration. Procedures in the MBE along with supporting documents in the MBEI, help with the inspection process as well as the rating procedure. This study includes the uncertainties in capacity due to the lack of knowledge of the level and location of a deterioration along the girder; these uncertainties vary depending on the level of detail provided to the load rating.

4.1 Condition States and ϕ_c

The MBE has three conditions of the member to classify the condition of a deteriorated girder. Table 4.1 lists the three structural conditions of the member and their corresponding ϕ_c reduction. The MBE doesn't describe these structural conditions of the member in any detail. The MBEI has some descriptions for the "Good", "Fair", or "Poor" conditions to help inspectors classify the defects present in the field.

Table 4.1 MBE structural condition of member and corresponding ϕ_c values

Structural Condition of Member	ϕ_c
Good or Satisfactory	1.00
Fair	0.95
Poor	0.85

Inspectors follow the MBEI to inspect and report on the present condition of the bridge. There are four condition states to define the level of defect present in the girder. These condition states 1, 2, 3 and 4 are described as Good, Fair, Poor and Severe respectively. There are hundreds of elements described in the MBE, which can be present in bridges. Each element has multiple defects that are further categorized into one of four condition states depending on the level of severity.

This research focuses on steel girders, element #107 in the MBEI, for which corrosion is one of the recognized defects being inspected. The condition states within corrosion defined in the MBEI are provided in Table 6.4. The description of the defect condition state criteria is ambiguous and subjective. For example, condition state 4 is defined as, “The condition warrants a structural review,” which can be interpreted by inspectors inconsistently.

The value for ϕ_c in the MBE can be determined using information from either SI&A or Element Level Inspection reports. There is an equivalent member condition from the element inspection that corresponds to the SI&A superstructure condition ratings. This approximate equivalency is shown below in Table 4.2.

Table 4.2 MBE condition state rating Table 6A.4.2.3-1

Superstructure Condition Rating (SI & A Item 59)	Equivalent Member Structural Condition
6 or higher	Good or Satisfactory
5	Fair
4 or lower	Poor

An objective description of each condition state would bring a uniformity to the inspection process that is currently subjective. Neither the MBEI nor NDOR’s BRIM has an objective range or detail for these condition states for corrosion. NDOR’s Bridge Inspection Program (BIP) manual has descriptions for the SI&A inspection code with percentage ranges for section loss in the superstructure (see Table 6.5). A similar percentage range of section loss for each condition state would be an objective way to define each condition state because the loss of section in the girder can be measured and has an inverse relationship between percentage loss and the moment capacity since moment capacity is directly proportional to the section properties including the area. The

percentage loss range will bring consistency among all bridges because percentage loss is independent of the size of the section. Also categorizing a range of section loss within each condition state can help quantify the uncertainty that can be measured and accounted for by the ϕ_c .

The bridge inspection reports were studied to find the details provided to quantify the uncertainty in the inspection. There are different types of inspection reports provided to the load-rating engineers. Inspections report of county bridges had fewer details compared to the report by NDOR's inspectors. Due to the varying level of details provided to the load-rating engineer, multiple approaches for selecting a ϕ_c are suggested in this study. These approaches account for the uncertainty associated with the details provided from the inspection. The approaches, along with the information provided to the load-rating engineers, are detailed below.

- Approach 1: Only the worst condition state in the girder is known.
- Approach 2: All condition states present in the girder and the corresponding total length of girder segments classified in each condition state are known.
- Approach 3: All condition states present in the girder and the corresponding length of girder segments classified in each condition state along with the location, are known.
- Special Approach: Deterioration profile along the span is known.

4.1.1 Inspection Methods, Policies, and Procedures in use by NDOR

The amount of information reported to the load-rating engineer varies. Depending on the level of the detail there can be shortcomings. These shortcomings are accounted

for by the ϕ c. NDOR's Bridge Inspection Program (BIP) Manual has all their policies and procedures needed for their bridge inspection.

NDOR's BIP manual includes the policies, procedures, required forms, reference documents, supplemental guidance and memos to help inspectors with their duties. This document has detailed instructions on bridge inspection procedures and the qualifications as well as the certifications of the inspectors to perform the inspections. The manual also includes instructions for the structure of the bridge inspection team in Nebraska, quality assurance procedure for inspection, and bridge data to be submitted and reported to FHWA and NDOR. Since 2014, NDOR has moved to the Element Inspection method for rating their bridges because it provides "a more detailed picture of the health of their bridges than the broad NBI condition."

NDOR inspectors fill out their "Field Inspection Form" for each bridge they inspect. It has general information about the bridge including the structure number, location, year built, year reconstructed and the geolocation. The Structure Inventory and Appraisal (SI&A) rating for the deck, superstructure, substructure, and culvert are recorded into the NBI database. Element level inspection data is also recorded in the form. For each element, a different type of deterioration is recorded. Each deterioration has four condition states. The inspector records the portion of each element in each condition state into the "Field Inspection Form." This information is then recorded into a database along with a picture of the bridge so that engineers are able to access and load rate a bridge.

NDOR load rate most of their bridges using the LFR, with the exception of the new ones that were designed using the LRFD philosophy. Rating these new bridges with

the LRFR is easier for the engineer because the LRFR goes parallel to the LRFD. Since October 2010, NDOR started designing bridges using the LRFD, therefore there are only a few bridges that need to be rated using the LRFR.

The deterioration of bridges designed by the LRFD is presently minimal because the use of the LRFD was adopted for design in 2010. A reasonable procedure for implementing the ϕ_c will be needed as these structures age in the future. The vague description for condition states necessary for the use of the ϕ_c has led NDOR to pursue this project to better understand the ϕ_c in the LRFR, and to calibrate it specifically to their bridges.

4.2 Bridge Surveying and Describing and Profiling the Deterioration

NDOR, following NBIS's guidelines, performs biannual inspections during which they also take pictures to record the current field condition of the bridge. Using those pictures and surveying a few bridges in the vicinity of Lincoln, NE, it was clear that corrosion was a major concern in steel girder bridges. Identification of corrosion pattern along the section and along the span in the field in bridges is necessary to calculate the capacity of the section. Out of many corrosion patterns seen in the field, two profiles of corrosion along the section are selected to be modeled in this study.

4.2.1 Deterioration Patterns

One of the predominant corrosion patterns for simple span bridges is corrosion in the bottom flange and the bottom 1/4th of the web. In Figure 4.1, deterioration of the entire web height can be seen near the support. In Figure 4.2, a couple of examples of deterioration in the bottom flange and the bottom portion of the web can be seen.

The second prevalent corrosion pattern was the entire girder section had deteriorated randomly along the span. In this type of corrosion, there was no common pattern along the span as the corrosion pattern was often seen below deck cracks. These cracks allowed the leakage of electrolytes (water and deicing salt), which accelerated the corrosion. Figures 4.3 and 4.4 have examples of this type of pattern.



Figure 4.1 Deterioration pattern at girder ends



Figure 4.2 Bottom flange deterioration along the girder



Figure 4.3 Deterioration pattern where entire section of girder is deteriorated



Figure 4.4 Entire girder section deteriorated below the cracked slab

4.2.2 Girder Deterioration Profile Models

Two deterioration profiles were selected for this research during as a result of studying multiple deterioration profiles in literature and considering the field condition of girder deterioration, two deterioration profiles were selected for this research.

Kayser and Nowak in “Reliability of Corroded Steel Girder Bridges” modeled deterioration pattern along the span as the entire web and the bottom flange corroded at the ends, and the bottom 1/4th of the web and the bottom flange is corroded elsewhere. In this deterioration profile, the height of the deteriorated web decreases until it reaches 1/4th of the web height at 1/10th of the length and the deteriorated web height remains constant throughout the rest of the span. This pattern was modeled assuming that the bottom flange accumulates water and deicing salt and accelerates the deterioration. The leakage through the joint at the support deteriorates the entire web. This type of profile was seen for the decks in Good condition without leakage. Figure 4.5 and Figure 4.6 shows the deterioration profile and section deterioration profile respectively. This type of deterioration will be referred to as “girder deterioration profile 1,” or “GP1,” in this report.

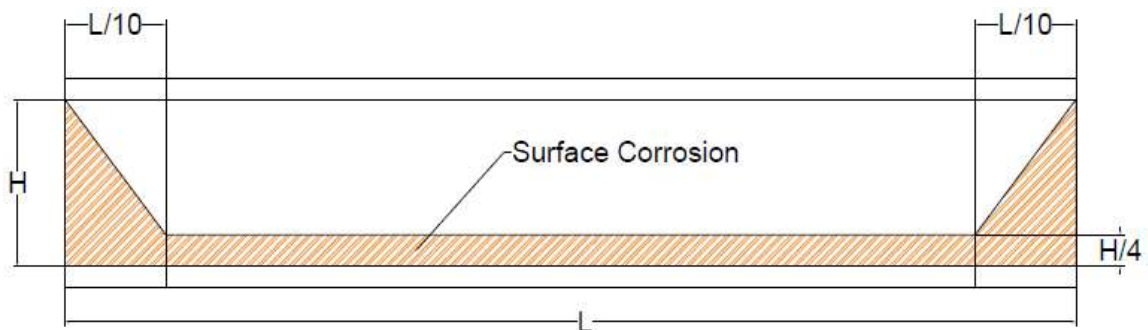


Figure 4.5 Deterioration profile “GP1”

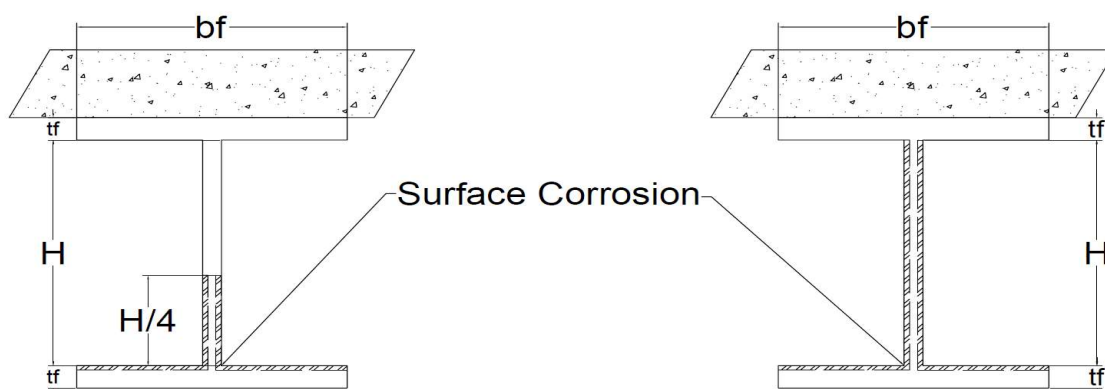


Figure 4.6 Section deterioration “GP 1”

The second predominant corrosion pattern exhibits corrosion along the full height of the section. In this deterioration profile, the entire girder including both the flanges and the web, is deteriorated, and the deterioration is present in random location along the span. This type of deterioration profile was caused by the leakage of deicing salt and water through the damaged or cracked deck. Figure 4.7 shows this type of deterioration profile and the section profile. This type of deterioration will be referred to as “girder deterioration profile 2,” or “GP2,” in this report.

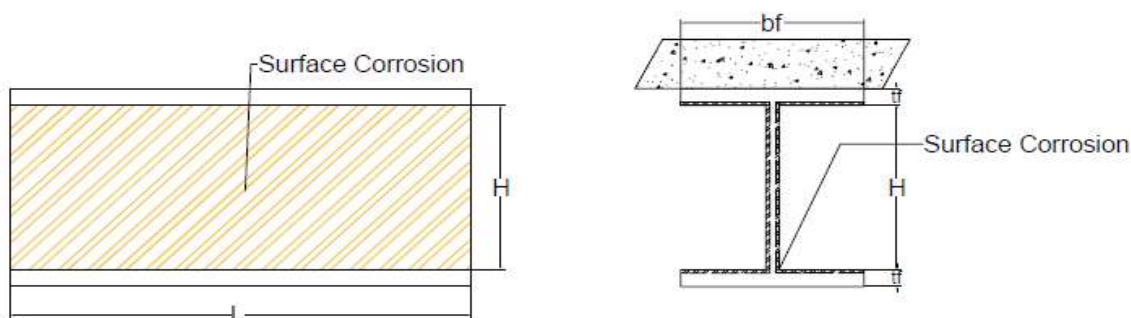


Figure 4.7 Entire web deteriorated along the span “GP 2”

4.3 Conclusion

Each condition state has a ϕ_c that needs to account for the increased uncertainty related to corrosion. The uncertainty in the remaining cross-section increases with the

increasing deterioration of the girder because of uneven corrosion along the section. Varying demand and capacity along the span brings uncertainty in the location of the critical load rating section. There is uncertainty as to the exact percentage loss because the percentage loss is binned together in each condition state. Depending on the corrosion pattern the uncertainty in capacity varies. Future loss due to corrosion is also accounted for in this study using Komp's corrosion model. All of these uncertainties are binned together and accounted for by the ϕ_c .

Chapter 5: Reliability Analysis

In the LRFR, the ϕ_c is present to provide consistent reliability across all bridges depending on the condition of the girder. All the uncertainty associated with the current condition of the girder is quantified and combined together to be accounted for by the ϕ_c . This study uses Rackwitz-Fiessler, a modified matrix procedure, to account for the uncertainties and to provide a consistent reliability among all bridges.

5.1 Rackwitz-Fiessler Reliability Analysis

The Rackwitz-Fiessler reliability analysis was performed to find the ϕ_c for each condition state. Rackwitz-Fiessler is used for this study because it can account for non-normal random variables. It uses the “equivalent normal” value for each non-normal random variable. The mean, standard deviation, and probability distribution of all the random parameters involved in the limit function are required. The mean and standard deviation of non-normally distributed random variables are converted to an equivalent normal mean and standard deviation. These equivalent values are used in the analysis on the failure bound described by $g=0$. The ratio between the mean moment capacity and the design point for the moment capacity is the ϕ_c , which provides a reliability index of 3.5.

Reliability analysis is performed on the load rating equation shown below in Eq. (11). This equation contains the capacity, dead-load from a wearing surface, dead-load from components, any other permanent loads and a live-load with impact. For this study, the loads wearing surface and permanent loads on the bridges are ignored. The dead-load includes the dead-load from the slab and the girder self-weight. The live-load in the analysis is HL 93 truck, which includes an HS 20 truck load and a lane-load of 0.64 kip/ft.

The process of performing reliability analysis starts with the rating equation, along with defining the variables and their parameters.

$$\text{Load Rating (LR)} = \frac{\phi\phi_s\phi_c R_n - \gamma_{DC}(DC) - \gamma_{DW}(DW) \pm \gamma_p(P)}{\gamma_{LL}(LL + IM)} \quad (11)$$

$$\text{Load Rating (LR)} * \gamma_{LL}(LL + IM) = \quad (12)$$

$$\phi\phi_s\phi_c R_n - \gamma_{DC}(DC) - \gamma_{DW}(DW) \pm \gamma_p(P)$$

Where,

ϕ , ϕ_s , and ϕ_c = Resistance factor

R_n = Capacity of the girder

γ_{DC} and γ_{DW} = Dead load factor for component dead load and wearing surface

DC and DW = Dead load from the component and wearing surface

γ_p = Load factor for permanent loads

P = Permanent loads

γ_{LL} = Live load factor

LL = Live load

IM = Impact factor

Some changes and assumption for parameters in Eq. (12) for this study are listed below:

- No permanent loads are considered ($P=0$)
- Wearing surface is ignored ($DW =0$)
- Dead load is considered a constant value to keep the load factor constant to the suggested value in the MBE (AASHTO, 2014). All the uncertainty in the dead-load is assumed to be accounted for by the load factor to keep the load

rating process the same as it is in the present for the practicality of implementation.

Some of the information that are provided from AASHTO include:

- $\phi = 1.0$ for flexure.
- $\phi_s = 1$ for multi-girder bridges.
- IM (impact factor) = 1.33
- LL is calculated for an HL 93 truck for Inventory rating with a COV of 0.18 (Moses, 2001).

Other modification to simplify the equations are:

- LR and γ_{LL} are combined together to Γ_{LL}
- $\phi * \phi_s * \phi_c$ is combined to Γ_{RN}

The modified governing equation for the failure surface is:

$$g = \Gamma_{RN} * R_n - [\Gamma_{LL}(LL + IM) + \gamma_{DC}(DC)] \quad (13)$$

Where,

$$\Gamma_{LL} = LR * \gamma_{LL}$$

$$\Gamma_{RN} = \phi \phi_s \phi_c$$

$R_n = \text{Plastic moment capacity of a girder}$

The capacity is the plastic moment capacity of the remaining sound section, and it is modeled as a normally distributed random variable. Dead load is the moment caused by an 8-inch slab and the self-weight of the girder, and it is modeled as a constant value because it was assumed that the variation in dead-load did not change with the decreasing condition of the girder (Kayser & Nowak, 1989b). All the uncertainty associated with

dead-load was accounted for during the calibration of ϕ and the load factors. Live load is the moment caused by the HL93 truck, and it has a lognormal distribution with a COV of 0.18 and a bias of 1.00, which is consistent with the AASHTO LRFD design specification (Moses, 2001).

The load rating and the ϕ_c are products of the reliability analysis. The design point of the moment capacity and the live-load shift during the reliability analysis to reach a target reliability. The ratio between the design point and the mean values used during the analysis are the LR and the ϕ_c . These multipliers provide consistent reliability across all bridges that are rated using the LRFR and the provided ϕ_c (AASHTO, 2014).

All the load parameters are specific to a bridge. The mean load on the bridge depends on the length and the configuration of the bridge. They are independent of the condition state of the girder. Live load, impact, and dead-load are constant for all condition states, as they are independent of the deterioration in the girder. Load factors and ϕ factors are calibrated in the LRFD to account for any changes in future loads. The live-load along the span is equal to the moment envelope generated by an HL93 truck. Girder line analysis uses the girder distribution factor to find the appropriate ratio of the live-load distributed to the girder. The dead-load along the span is the moment generated by a uniformly distributed load equal to the weight of the concrete slab and the girder.

Capacity is dependent on the remaining sound material of the girder, therefore, it changes with deterioration. The mean and standard deviation for each condition state is calculated by taking the mean and standard deviation of all the possible values within each condition state. The bias for capacity is taken as 1.00 because the mean capacity is used in the reliability analysis. The capacity of the girder is calculated using AASHTO's

LRFD design (see APPENDIX A). The flexural capacity of the girder is the plastic moment capacity because only composite steel girders are considered for this research. Local buckling is not possible as the compression flange is braced. All appropriate checks are done following the AASHTO design code to ensure the plastic moment capacity is reached.

LRFR is a rating procedure that provides uniform reliability for the load rating throughout all the bridges. There are two levels of target reliability: 3.5 for inventory and 2.5 for operating. Reliability of the inventory level rating is consistent with the LRFD design. Deterioration of the bridge decreases the capacity, which will decrease the load rating. As it would be an economical burden to post all bridges, AASHTO allows the rating to be done at operating level which decreases the reliability of the load rating, but it is justified because of regular inspection to ensure the bridge safety. The lower reliability index in the rating procedure is achieved by lowering the live-load factor. The live-load factor for inventory levels is 1.75 and 1.35 for the operating level.

The limit state function is represented by $g \geq 0$, where g is defined in Eq. (13).

The Rackwitz-Fiessler reliability procedure outlined below is followed.

1. An initial design point for capacity is set to the mean capacity of the girder.
2. The live-load can be calculated by solving the equation below.

$$LL = R_n - \gamma_{DC}(DC) \quad (14)$$

3. Equivalent normal parameters are determined for all non-normal parameters.

The live-load has a lognormal distribution with a COV of 0.18 and a bias of 1.00 (Moses, 2001) and the capacity, which is binned together for each condition state is modeled as normally distributed. This is an assumption

because not enough data is present to model the distribution of capacity within each condition state.

4. The mean and standard deviation of the normally distributed variables are used to find the column vector $\{G\}$, which is the partial derivatives of g with respect to the reduced variables, in this case, LL and Rn .

$$\{G\} = \begin{cases} -\frac{\partial g}{\partial Rn} \\ -\frac{\partial g}{\partial LL} \end{cases} \quad (15)$$

5. $\{\alpha\}$ the column vector is found.

$$\alpha = \frac{[\rho]\{G\}}{\sqrt{\{G\}^T[\rho]\{G\}}} \quad (16)$$

As the live-load and capacity are independent of each other; the coefficient of correlation $[\rho]$ is a 2 X 2 identity matrix.

6. A new design point in reduced variates for $n-1$ of variables is determined using:

$$z_{RN}^* = \alpha_{RN} \beta_{target} \quad (17)$$

7. The corresponding design point values (x_{RN}^*) in original coordinates for the $n-1$ values from the step 6 using the following equation:

$$x_{RN}^* = \mu_{X_{RN}}^e + z_{RN}^* \sigma_{X_{RN}}^e \quad (18)$$

8. Determine the values of the live-load using the equation $g=0$ and recalibrate the mean of capacity (μ_{x_i}) using the following equation.

$$\mu_{x_i} = \frac{x_{RN}^*}{1 + \alpha_{RN} \beta V_{x_{RN}}} \quad (19)$$

9. Repeat step 3 through 8 until $\{\alpha\}$ converges
10. Once convergence is achieved, calculate the design factors (γ_i) using

$$\gamma_i = \frac{x_i^*}{\mu_{x_i}} \quad (20)$$

To find RF (Rating Factor)

$$RF = \frac{Y_{LL}}{L L_f} \quad (21)$$

and ϕ_c

$$\Phi_C = \gamma_{RN} \quad (22)$$

This process is used multiple times to generate the ϕ_c in this study (Nowak S. & Collins R., 2013).

The Rackwitz- Fiessler reliability analysis was used for all the analysis performed in this research. There are four approaches for choosing the ϕ_c depending on the uncertainties associated with each approach. Within each approach, there are at least two sets of analysis for the two girder distribution profiles. All the uncertainties that are accounted for by the ϕ_c are discussed in detail in Chapter 6: Uncertainty Contributions to Condition Factors.

Chapter 6: Uncertainty Contributions to Condition Factors

The factor ϕ_c accounts for the uncertainties associated with the current condition of the girder. These uncertainties include the change in the variation of measurement within sections (section 6.1 Uncertainties in Section Deterioration), possible future corrosion (section 6.2 Future Corrosion), the exact measurement of the remaining section of the girder (section 6.3 Uncertainty due to Range of Section Loss in each Condition State) and the location of section loss along the span (section 6.4 Uncertainty in the Location of the Deterioration). As there are three condition states of the girder, and a range of the percentages loss are combined within each condition state, a new set of uncertainties associated with the exact percentage loss in the girder emerges. This uncertainty is also accounted for by the ϕ_c . As each approach has a different set of uncertainties associated with it, there are multiple sets of ϕ_c to account for the lack of details in the inspection report.

6.1 Uncertainties in Section Deterioration

One of the uncertainties accounted by ϕ_c is the increase in variation of thickness after corrosion occurs. The corrosion along the section is non-uniform and causes variation in thickness of the member which increases uncertainty in the capacity of the girder. A relationship between the percentage loss and the variation in the measurement needs to be identified and used in the reliability analysis for the ϕ_c to capture the increased uncertainty and provide uniform reliability in the load rating.

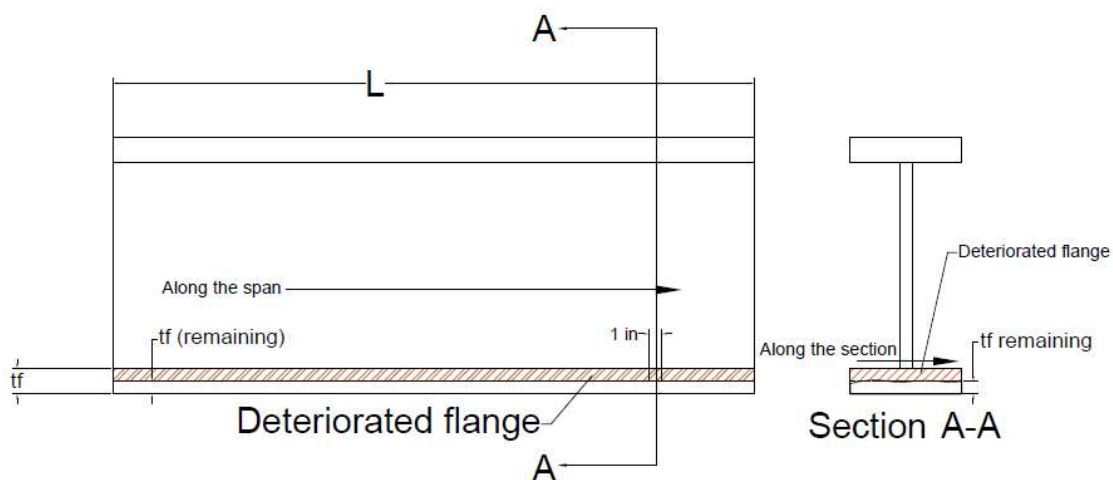


Figure 6.1 Section deterioration

There can be multiple deterioration profiles along the span due to non-uniform corrosion. Different profiles in girders with equal percentage loss will provide equal plastic moment capacity (see Appendix Figure D). Therefore, using an average percentage loss and the COV is justified for the study. As no prior study to measure the variation in section measurement for percentage loss in the section, measurements were taken in the field for various girders to quantify the uncertainty.

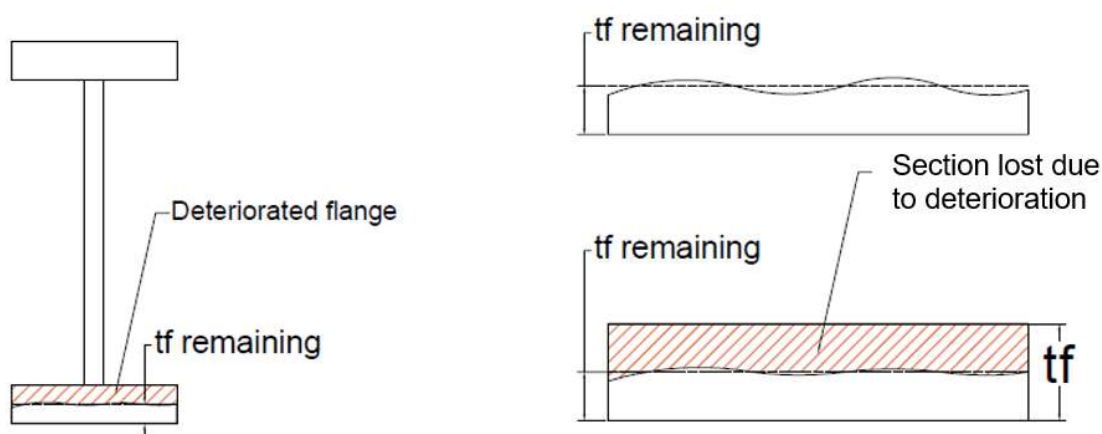


Figure 6.2 Variation of the flange thickness along the section

6.1.2 Measurement in the Field

NDOR provided a list of 60 steel girder bridges near Lincoln, Nebraska, along with their recent inspection report. The reports helped identify the worst condition state present in the girder. There was a diverse range of bridges with all four condition states present.

The bridges were categorized into four groups depending on the worst condition state present in the bridge. Out of the 60 bridges, 4 bridges had condition state 4 as their worst condition state in the inspection report, 28 bridges had condition state 3, 24 bridges had condition state 2, and 4 bridges had condition state 1. Out of these bridges, three bridges from each category were visited, but not all of them were accessible for measurement. The list of 9 bridges that were measured is shown in Table 6.1.

Table 6.1 List of bridges visited, their condition state and max % loss summary

Structure Number	Worst CS classification	Max % loss
S006 28494	CS 3	3 %
S033 01026	CS 3	3 %
S006 30574	CS 1	1 %
S006 28424	CS 3	3 %
S077 06205L	CS 1	1 %
S077 06205R	CS 3	1 %
S006 32007	CS 3	14 %
S136 14969	CS 3	8 %
S015 03097	CS 3	8 %

Each girder was measured in three different states along the bottom flange at one location along the span (see Figure 6.1). There were 10 sets of measurements of each state at a section along a side of the bottom flange. The three states of measurements are: deteriorated, brushed and grounded. The first state of measurement was taken of the deteriorated section; any debris was cleaned, and 10 sets of measurements along the section are taken, as seen in Figure 6.3. The location of the 10 measurements were at a

random location along the section (see Figure 6.3) but within a narrow 1-inch width along the span (see Figure 6.1). The second state at which the measurement was taken was after brushing; The measurements were taken after the girder was cleaned using a steel brush at the same section where the first set of measurements were taken. For the third state, which was the grounded state, the measurements were taken after grinding the girder with a mechanical grinder.

The same girder was also measured at an undeteriorated section along the span of the girder to get the measurement of the original section. Similarly, 10 sets of measurements along the span were taken for the undeteriorated section. These measurements provided information on the variation present in the undeteriorated girder along the section.

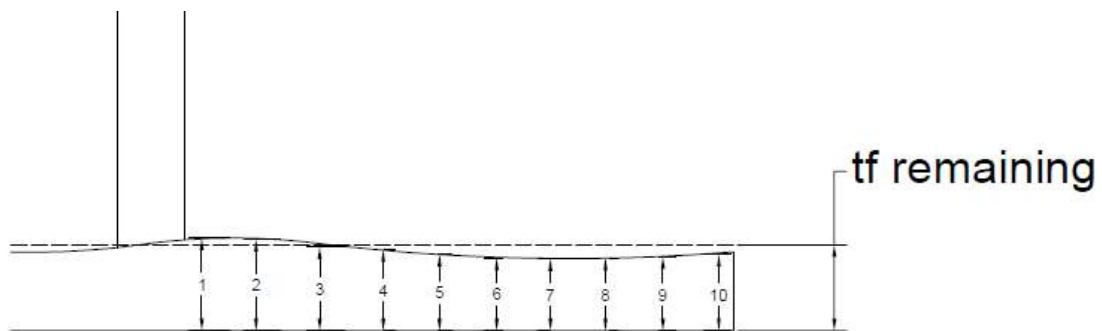


Figure 6.3 Sample location of measurement taken along the bottom flange

Using the measurements from the undeteriorated section and the three states of measurements along the sections, the mean percentage loss and the variation for that percentage were calculated.

During the field visit, it was observed that the steel brush did not remove all of the rust. Therefore, the girder needed to be grinded. The MBE suggests that a sound section is found after removing the rust with a steel brush, but because multiple measurements

needed to be taken, grinding was required (AASHTO, 2014). The ASTM G103 has mentioned the loss of material using mechanical grinding as a concern. Mechanical grinding was the only option for removing all of the rust from the steel because of other procedures, including chemical or electrolysis techniques, which were not feasible due to the lack of accessibility in the field. The grinding process was carefully performed to ensure no sound material was removed. A material that is softer than steel was used for grinding, and the grinding was stopped soon after sparks appeared. These precautions were taken to ensure the removal of corrosion without the loss of sound material.

One of the difficulties in capturing the variation in thickness due to deterioration is the lack of access. A micrometer with a deep throat was used to measure the section thickness which requires access to both faces. Only the bottom flange could be measured because of this. As the variation in the thickness of a deteriorated section is the interest of this study measuring only the bottom flange can be justified.



Figure 6.4 Wide mouth caliper used for measurement of the flange

All the measurements were taken using a deep mouth micrometer (see Figure 6.4) because of its accessibility and its high precision. These measurements along the section were taken to capture and quantify the variability in section deterioration due to corrosion. A deep mouth micrometer allowed measurements to be taken at a certain location along the section in the bottom flange (see Figure 6.3). The precision of the micrometer was important because it helped capture small differences between the measurements. All 10 measurements were taken along a 1-inch wide section as shown in Figure 6.1. These measurements were recorded on a data sheet similar to the one shown in Figure 6.5 which was also used to find the percentage loss and the variation in the measurement.

Excel was used to record and analyze all the measurements. This excel sheet recorded information including the structure number and location of the bridge, the length of each condition state, and the total length of the girders. See Figure 6.5 for an example of the measurement sheet. A set of ten measurements within each state was taken and recorded. The mean, standard deviation, COV, median, quartiles and outlier boundaries were calculated in the excel sheet. Any measurement that is beyond the outlier boundaries were highlighted to be given extra attention later during analysis. The COV and the mean loss are the two most important parameters, as they are used for reliability analysis to generate the ϕ_c .

The percentage loss is calculated using the mean values of the undeteriorated section and the grinded section. The difference between the two divided by the mean undeteriorated value is the percentage loss. The COV is the standard deviation divided by the mean value. The COV of the grinded measurement is then linked to the percentage

loss for measurement that is used for the reliability analysis. A list of all the percentage losses and the corresponding COVs are shown below in Table 6.2.

Structure Number		S006 28424			
Date of Inspection		7/20/2016			
Location		3N DORCHESTER at JOHNSON CREEK			
Total length [ft.]		450			
Condition State		CS 1	CS 2	CS 3	CS 4
Length [ft.]		440	0	10	0
	[mm]	[mm]	[mm]	[mm]	[mm]
Reading	No deterioration	After Brushing	After Grinding	After Brushing	After Grinding
1	38.68	37.08	38.8	38.39	37.04
2	38.46	36.24	37.91	37.92	37.27
3	38.84	36.67	37.71	38.50	37.33
4	38.74	36.98	37.81	38.57	37.64
5	38.51	37.68	37.43	38.30	37.70
6	38.62	37.64	37.09	38.41	38.01
7	38.49	37.95	37.41	38.25	38.11
8	38.82	37.8	37.46	37.87	37.92
9	38.8	38.01	36.87	37.73	37.76
10	38.59	38.00	36.88	37.64	37.61
Mean	38.66	37.41	37.54	38.16	37.64
Standard Deviation	0.142	0.6225	0.5724	0.3200	0.3237
% loss	0%	3%	3%	1%	3%
COV	0.0037	0.0166	0.0152	0.0084	0.0086
median	38.65	37.66	37.45	38.275	37.67
1st quartile	38.53	37.01	37.17	37.8825	37.40
3rd quartile	38.78	37.91	37.79	38.405	37.88
lower fence	38.15	35.64	36.25	37.09875	36.68
upper fence	39.17	39.27	38.71	39.18875	38.60

Figure 6.5 Example field measurement sheet along with the calculated loss and COV

The COVs and the percentage losses were then plotted to find a relationship between the percentage loss and the COV. No solid trend was found; a linear fitting had a R^2 of 0.65,

which is a poor correlation (see Figure 6.6). A step ladder approach to assign a COV to a percentage loss is used, where the larger COV between the COV for the considered section percentage loss and the COV that was assigned to a lower percentage section loss is selected. For example, the COV for a 4% loss is 0.028 and the COV for a 5% loss is 0.011; the COV used for a 5% loss is 0.028 because that is the maximum COV for all values less than or equal to a 5% loss. The solid line (red) in Figure 6.6 shows this approach. A summary of the percentage section loss and the corresponding COV is shown in Table 6.3. As there are no data point for values over 14% loss the maximum COV is used for all percentage losses above that threshold. This COV is added to the variation during the reliability analysis. (see section 7.1.1 Quantifying Uncertainty in Approach 1)

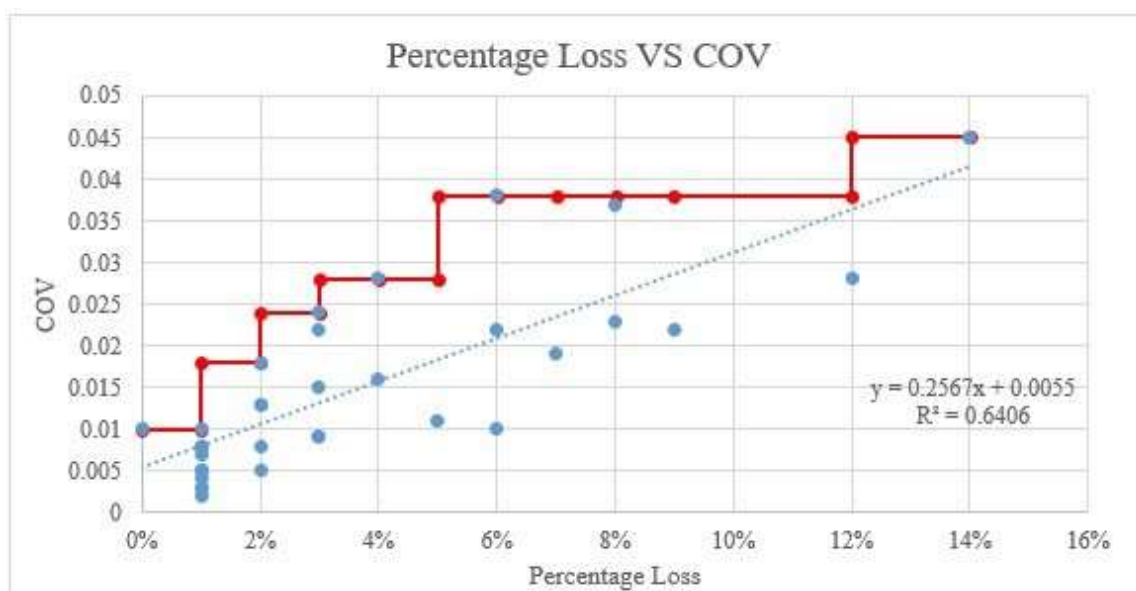


Figure 6.6 Percentage loss VS COV

Table 6.2 Summary of % loss and COV of bridges after being grinded

Structure number	% loss	COV
S077 06205R	0%	0.01
S006 28494	1%	0.005
S033 01026	1%	0.008
S136 14969	1%	0.003
S077 06205R	1%	0.008
S006 30574	1%	0.003
S006 28494	1%	0.002
S077 06205L	1%	0.007
S077 06205R	1%	0.010
S006 28424	1%	0.005
S077 06205R	1%	0.004
S006 28494	2%	0.008
S006 28494	2%	0.013
S033 01026	2%	0.013
S033 01026	2%	0.018
S006 28424	2%	0.005
S006 28424	3%	0.009
S136 14969	3%	0.024
S 015 03097	3%	0.022
S006 28424	3%	0.015
S033 01026	3%	0.009
S136 14969	4%	0.028
S 015 03097	4%	0.016
S 015 03097	5%	0.011
S 015 03097	6%	0.022
S136 14969	6%	0.038
S 015 03097	6%	0.010
S006 32008	7%	0.019
S 015 03097	8%	0.023
S136 14969	8%	0.037
S006 32007	9%	0.022
S006 32007	12%	0.028
S006 32007	14%	0.045

Table 6.3 Summary of max COV for all percentage loss

Percentage Loss	Max COV
0	0.010
1	0.010
2	0.018
3	0.024
4	0.028
5	0.028
6	0.038
7	0.038
8	0.038
9	0.038
12	0.038
≥14	0.045

6.2 Future Corrosion

Second uncertainty that is accounted for by the ϕ_c is the future possible deterioration until the next inspection. Corrosion is the focus deterioration of this study, and the uncertainty of the future corrosion is accounted in the Rackwitz-Fiessler reliability analysis as a bias (λ). Similar to NCHRP 301, Komp's corrosion model including modifications for the presence of deicing salts and sheltered condition, is used to account for future corrosion loss. This model makes prediction based on the material and the environment. There are three environments and two types of steel in the Komp's model which gives a total of six different predictions for future corrosion. Komp's corrosion model has also been used by Nowak and other researchers. Modification included in NCHRP 301 are by McCrum, Cosaboom and Zoccola, McKenzie, Larrabee, Sereda, Albrecht, and Naeemi (Moses & Verma, 1987). These modifications are used to account for the influence of the environment and other chemicals and to predict the corrosion rate of the bridges.

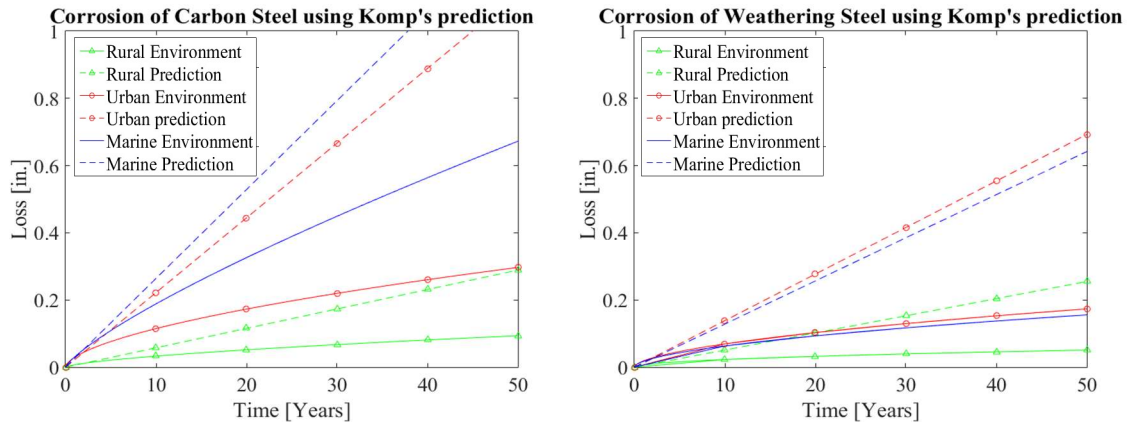


Figure 6.7 Prediction of future corrosion

Komp's model is an asymptotic function, therefore the rate of corrosion decreases in time, but to be conservative a secant rate of the initial 2 years is used for the study. The rate that is used for the study is shown in Figure 6.7. There are six different rates because there are three environments in which the carbon steel and weathering steel corrode in a different rate. As the estimation was already conservative using the secant rate, using one rate for all six cases would make this estimation overly conservative. As there are six different rates of corrosion, there will be six possibilities for future corrosion resulting in six different sets of ϕ_c . Instead of suggesting six sets of ϕ_c , multipliers have been suggested. Future corrosion is accounted for by using bias in the reliability analysis. The projected plastic moment capacity after corrosion is taken as the nominal value and the current mean is assumed to be mean. The ratio between the mean and the nominal is the bias (λ). Bias (λ) for this research is shown in Eq. (23). The suggested ϕ_c is calibrated for carbon steel in a rural environment because this was the most prevalent case in Nebraska. Other environments and type of steel are suggested as a multiplier to the ϕ_c .

$$\lambda = \frac{\mu}{d} = \frac{\mu_{RN}}{\mu_{RN,CR}} \quad (23)$$

Where,

$\mu = \text{Mean}$

$d = \text{Nominal}$

$\mu_{RN} = \text{Mean plastic moment capacity of the girder}$

$\mu_{RN,CR} = \text{Moment capacity after corrosion (carbon steel in rural environment)}$

This research uses multipliers for varying corrosion due to different types of steel and environment. In Eq. (24), the base ϕ_c that accounts for future deterioration of carbon steel in rural environment is calculated using the bias mentioned in Eq. (23). Similar ϕ_c for other types of steel and environments can be found and the equation is shown is Eq. (25) some algebra in Eq. (26) and Eq. (27) is performed to show that a ϕ_c in different environments can be calculated using the base ϕ_c and a multiplier (see Eq. (28)). The Eq. (21) shows that the multiplier is the ratio between the mean plastic moment capacity after corrosion of carbon steel in rural environment ($\mu_{RN,CR}$) and the mean plastic moment capacity after corrosion of any other type of steel in any environment ($\mu_{RN,F}$).

$$\phi_{C,CR} = \lambda \frac{R^*}{\mu_{RN}} = \frac{\mu_{RN}}{\mu_{RN,CR}} * \frac{R^*}{\mu_{RN}} = \frac{R^*}{\mu_{RN,CR}} \quad (24)$$

$$\text{Similarly, } \phi_{C,F} = \frac{R^*}{\mu_{RN,F}} \quad (25)$$

$$\phi_{C,F} = \frac{R^*}{\mu_{RN,F}} * \frac{\mu_{RN,CR}}{\mu_{RN,CR}} \quad (26)$$

$$\phi_{c,F} = \frac{R^*}{\mu_{RN,C}} * \frac{\mu_{RN,CR}}{\mu_{RN,F}} \quad (27)$$

$$\phi_{c,F} = \phi_{C,CR} * Multiplier \quad (28)$$

$$Multiplier = \frac{\mu_{RN,CR}}{\mu_{RN,F}} \quad (29)$$

Where,

R^* = design value from reliability analysis

μ_{RN} = Mean plastic moment capacity of the girder

$\mu_{RN,CR}$ = Moment capacity after corrosion (carbon steel in rural environment)

$\phi_{C,CR}$ = Condition factor future corrosion (carbon steel in rural environment)

$\phi_{c,F}$ = Condition factor future corrosion (any steel in any environment)

$\mu_{RN,F}$ = Average predicted moment capacity of the girder after corrosion

$\mu_{RN,N} = \mu_{RN,CR}$ for carbon steel girder in rural environment

A two-year estimation is used because inspections are performed every two years on all bridges. A conservative estimation of loss due to corrosion in two years can be used to estimate the maximum loss in section properties. This remaining section is used to calculate the capacity of the girder present until the next inspection cycle. Accounting for future loss ensures that the bridge will have that load rating until the next inspection cycle. The rate of corrosion is constant for all levels of losses but the change in capacity will vary depending on the remaining section.

A less conservative method of predicting the future corrosion based on the current corrosion was studied and is discussed further in Appendix B:ALTERNATIVE FUTURE CORROSION on page 136. This method is consistent with the decrease in the loss with Komp's inverse exponential function, which predicts a decrease in the rate of corrosion in time. This is contrary to the popular belief that the corrosion rate increases as the corrosion increases. The alternative method to predict the future corrosion did not seem viable, because according to this model, it would take over 100 years for steel to lose 50% of its section. Yet, field observations have documented localized through- thickness (100%) corrosion at girder ends, resulting in holes in webs and sometimes in flanges. Many researchers including McCrum used a linear prediction of the corrosion rate. They used the initial corrosion rate, which is also the maximum rate and interpolated it for all levels of corrosion. As the initial loss is the maximum possible rate of corrosion, the predicted value from this model is the maximum corrosion until the next inspection.

6.3 Uncertainty due to Range of Section Loss in each Condition State

A range of section loss needs to be defined for each condition state to quantify the uncertainties in the condition state. Defining a range of section loss brings consistency in the inspection process and provides an accurate translation of the current bridge condition to the load-rating engineer. A consistent inspection process also ensures that the quantification of uncertainty for each condition state is accurate. This study looks into the current inspection process and suggests a range of section loss for each condition states, and a range that would provide consistent reliability in load rating with the suggested set of ϕ_c in the MBE (AASHTO, 2014).

Setting a range of section loss for each condition state helps clarify the categorization of bridge deterioration into one of the condition states, but it also introduces a new level of uncertainty associated with the amount of section loss present in the girder. For example, a hypothetical element level inspection report for a bridge has 10% CS1, 20% CS2, and 70% CS3 (see Figure 6.8). As the exact loss within each condition state is unknown the uncertainty within each condition state increases. This uncertainty is accounted for by ϕ_c . A mean and standard deviation of all the percentages losses within each condition state is used in the reliability analysis. For example, if condition state 1's ranges from 0 to 5% section loss, after finding the moment capacity associated with that section for all percentages loss between 0% and 5%, a mean, standard deviation, and COV can be calculated and used in the reliability analysis.

The variation in percentage loss in each condition state is assumed to be normally distributed for simplicity in the analysis. For future research, detailed surveying and measurement within each condition state could provide more insight on the distribution within each condition state. A range for each condition state needs to be set to quantify the uncertainty within each condition state.



Figure 6.8 Bridge with multiple condition states

6.3.1 Determining Range of Section Loss within each Condition State

Condition state, a term used in AASHTO's Manual for Bridge Element Inspection (MBEI), categorizes defects into 4 levels of severity (see Table 6.4). Elements are inspected for multiple types of defects; each defect is categorized into one of the four condition states. The description for each condition state is vague and subjective.

The SI&A rating used in the NBI is used to describe the entire superstructure including all elements above the bearing of the bridge. This rating is used to determine the condition of the girder. NDOR's BRIM includes a range of percentages loss in their description for the superstructure condition rating (see Table 6.5). Using percentage section loss makes the rating procedure more objective and consistent among all bridges.

Table 6.4 Element #107 condition state definitions

Defect	Condition State			
	1	2	3	4
	Good	Fair	Poor	Severe
Corrosion	None	Freckled Rust. Corrosion of the steel has initiated	Section Loss is evident or pact rust is present but does not warrant structural review	The condition warrants a structural review to determine the effect on strength or serviceability of the element or bridge, OR a structural review has been completed and the defects impact strength or serviceability of the element or bridge.
Cracking	None	Cracks that has self-arrested or has been arrested with effective arrest holes, doubling plates, or similar.	Identified crack that is not arrested but does not warrant structural review.	
Connection	The connection is in place and functioning as intended.	Loose fasteners or pack rust without distortion is present but the connection is in place and functioning as intended	Missing bolts, rivets, or fasteners; broken welds; or pact rust with distortion but does not warrant a structural review.	
Distortion	None.	Distortion not requiring mitigation or mitigated distortion.	Distortion that requires mitigation that has not been addressed but does not warrant structural review.	
Damage	Not Applicable.	The element has impact damage. The specific damage caused by the impact has been captured in Condition State 2 under the appropriate material defect entry.	The element has impact damage. The specific damage caused by the impact has been captured in Condition State 3 under the appropriate material defect entry.	

Table 6.5 Table C6A.4.2.3-1- from MBE: description of member condition

Code	Condition	Description
N	NOT APPLICABLE	For example, a culvert.
9	EXCELLENT CONDITION	No noticeable or noteworthy deficiencies that affect the condition of the structure.
8	VERY GOOD CONDITION	Bent steel or slight misalignment, not requiring repairs.
7	GOOD CONDITION	Heavy rust in localized areas without any section loss.
6	SATISFACTORY CONDITION	Initial section loss (heavy rust) in localized areas of structural steel members in non-critical stress areas
5	FAIR CONDITION	Substantial but not critical collision damage to structural support elements, steel girders, trusses, etc. Initial section loss (heavy rust) in localized areas of structural steel members in critical stress areas.
4	POOR CONDITION	Critical collision damage sustained to structural support elements. Precautionary measures such as traffic restrictions or temporary shoring may be needed. Significant section loss (heavy rust) of structural steel girder in critical stress areas. (More than 30% section loss).
3	SERIOUS CONDITION	Disintegration of or damage condition of a structural member which requires traffic restriction or shoring. Severe section loss (heavy rust) or structural steel member in critical stress areas requiring immediate repairs. (More than 50% loss of section).
2*	CRITICAL CONDITION	The need for repair or rehabilitation is urgent. Facility must be closed until the indicated repair is complete.
1*	IMMINENT FAILURE CONDITION	Facility is closed. Study should determine the feasibility for repair.
0*	FAILED CONDITION	Facility is closed and is beyond repair.

The description with percentage loss from the SI&A rating and the corresponding equivalent condition state (see Table 4.2) are used to determine a range for each condition state. Condition state 1 corresponds to “Good or Satisfactory” in the structural condition of a member, which has a superstructure condition rating of 6 or higher; similarly, condition state 2 is “Fair” with a condition rating 5. Condition state 3 is “Poor”

with a condition rating of 4, and condition state 4 is “Severe”, which is assigned a condition rating of 3 or lower. This equivalent condition state and the SI&A rating are compared to NDOR’s description of condition ratings, which can be seen in a tabular form in Table 6.6.

Table 6.6 Condition state and its equivalent condition rating and its description

Condition State	Condition of Member	Condition Rating	NDOR’s Description
1	Good	6 or higher	Initial section loss in localized areas of structural steel members in non-critical stress areas.
2	Fair	5	Initial section loss (heavy rust) in localized areas of structural steel members in critical stress areas.
3	Poor	4	Significant section loss (heavy rust) of structural steel girder in critical stress areas. (More than 30% section loss).
4	Severe	3 or lower	Severe section loss (heavy rust) or structural steel member in critical stress areas requiring immediate repairs. (More than 50% loss of section).

NDOR’s description for condition rating (see Table 6.5) has a Poor condition with more than 30% section loss, the similarly Severe condition is defined as having more than 50% loss of section, which can limit condition state 3’s section losses between 30% to 50%. The Fair condition does not have any descriptive percentages. A lower limit for the Fair condition was set to be 10% to keep the range of section loss equal to condition state 3. Condition state 2 ranges from 10% to 30%. Condition state 1 ranges between 0 to 10%. Although having a 10% section loss is contrary to the description in the MBEI, it is closer to the Good condition description rating because the Good condition can have “initial section loss in localized areas of structural steel members in non-critical stress areas.” This 10% is an upper limit and a conservative assumption; it has a lower range of

section loss compared to other condition states. For condition state 4, the MBE does not have a condition rating associated with it. An upper limit of 80% was arbitrarily set as having more than an 80% loss in member, which would be getting too close to the complete loss of section. The range of section loss for each condition state is shown in Table 6.7.

Table 6.7 Condition state and a range of section loss in each condition state

Condition State	Range of section loss
1	<10%
2	10-30%
3	30-50%
4	50-80%

Reliability analysis was performed to find the ϕ_c for this range of section loss. The ϕ_c for condition state 1 would be around 0.96; the ϕ_c for condition state 2 would be around 0.82, and the ϕ_c for condition state 3 would be around 0.68. These penalties seem too large and following this recommendation would require a new girder to be rated at 96% of its capacity. This is partly due to the fact that future corrosion is being considered but the main reason seems to be the mean value used for rating is 5% loss in the section for condition state 1. In addition to the severe penalty, it was not consistent with the inspection procedure followed by NDOR inspectors as they were not using SI&A rating for classifying the condition state. A new range consistent with Element Level Inspection was determined.

6.3.2 Range Consistent with NDOR's Current Inspection Procedure

A range based on NDOR's current element inspection description for condition states using the description in Table 6.4 Element #107 condition state definitions, is suggested in this section. Condition state 1 has no rust, setting the max percentage loss

for condition state 1 as 0%. Condition state 2 is described as having some freckled rust with no measurable section loss, and a maximum loss of 1% was selected. Condition state 3 is defined as having evident section loss. An arbitrary range between 1% to 50% section loss is categorized into condition state 3. Condition state 4 is defined as a section that would require structural review by an engineer. The lower limit of 50% was set for condition state 4 because the SI&A rating of 3 (serious condition) has a limit of 50% section loss (see Figure 6.5). The final range is shown in Table 6.8.

Table 6.8 Range of condition state consistent with Element Inspection

Condition State	Range of Section Loss
1	0%
2	0-1%
3	1-50%

After running a reliability analysis, it was found that NDOR's Element Inspection description for each condition state would not provide consistent reliability in the load rating using the suggested ϕ_c values. For example, a girder with freckled rust is categorized as condition state 2 and the suggested penalization of 5% ($\phi_c = 0.95$) to the girder capacity; this 5% penalization is very high penalty for non-measurable section loss. All girders with measurable section loss is categorized as condition state 3, the massive range in condition state 3 is getting penalized by 15% ($\phi_c = 0.85$); this penalty cannot account for all the uncertainties present in that range of section loss. Preliminary analysis for the ϕ_c showed that the ϕ_c for the suggested range need to be 1.00 for CS1, 1.00 for CS2, and 0.40 for CS3 to provide consistent reliability in the load rating. Table 6.9 has the preliminary ϕ_c s for the two girder deterioration profiles (GP).

Table 6.9 ϕ_c for two deterioration profiles using the range consistent with NDOR

	CS1	CS2	CS3
GP1	1.00	1.00	0.70
GP2	1.00	1.00	0.40

The suggested range for the ϕ_c is extremely penalizing for the condition state 3. Recalibration of the range of section loss to match the ϕ_c values suggested in MBE seemed to be a more logical process for load rating. Redefining the range would require a modification to the inspection process, but it would be a more accurate and reliable load rating for the bridge.

6.3.3 Calibrating the Range of Condition State to MBE Values

A range of section loss for each condition state, that provides consistent reliability among all bridges rated using the ϕ_c in the MBE, is determined in this section. The ϕ_c would account for future section loss due to corrosion, uncertainty associated with the exact section loss present in the girder, and the variation in depth along the section.

A range of section loss for each condition state, that would provide a consistent reliability in load rating a bridge using the ϕ_c suggested by the MBE, was determined by the trial and error method. Multiple ranges of section loss for each of the condition state were analyzed to find the ϕ_c . For simplicity, the entire girder was set to be in one condition state. The mean and the standard deviation of the plastic moment capacity for the range of section loss in each condition state were used in the analysis. The uncertainty associated with the variation along the section is included in the standard deviation by adding the standard deviation using the square root of the sum of the squares (SRSS), and the possible future corrosion is accounted for as the bias in the Rackwitz-Fiessler reliability analysis.

Table 6.10 Range of section loss for condition state and their corresponding ϕ_c

GP 1							
Length	Shape	CS 1	CS 2	CS 3	ϕ_c 1	ϕ_c 2	ϕ_c 3
50	W30X99	1%	7%	31%	0.99	0.94	0.85
60	W33X118	1%	7%	32%	0.99	0.94	0.85
70	W36X135	1%	7%	35%	0.99	0.94	0.85
80	W40X167	1%	7%	35%	0.99	0.94	0.85
90	W36X194	1%	7%	36%	0.99	0.95	0.85
100	W40X215	1%	7%	35%	0.99	0.95	0.85
110	W44X230	1%	7%	35%	0.99	0.95	0.85
120	W44X262	1%	7%	35%	0.99	0.95	0.85
Final Range		1%	7%	31%			
GP 2							
Length	Shape	CS 1	CS 2	CS 3	ϕ_c 1	ϕ_c 2	ϕ_c 3
50	W30X99	0%	5%	20%	0.98	0.95	0.84
60	W30X116	0%	5%	20%	0.98	0.95	0.85
70	W33X130	0%	5%	20%	0.98	0.95	0.85
80	W36X150	0%	5%	21%	0.98	0.95	0.85
90	W36X182	0%	7%	25%	0.99	0.95	0.85
100	W33X201	0%	7%	25%	0.99	0.95	0.85
110	W40X211	0%	5%	22%	0.99	0.95	0.85
120	W40X249	0%	10%	30%	0.99	0.95	0.85
Final range		0%	5%	20%			

As there are two deterioration profiles being considered for this research, the ranges of section loss for each condition state were found for both. For GP1, a range of section loss between 0 - 1% would require a ϕ_c of 0.99 to provide consistent reliability across all load rating. Similarly, for GP2, a max loss of 0% in condition state 1 would require a ϕ_c of 0.98. Similar ranges for condition state 2 and 3 were found for multiple girder lengths and girder sizes. In Table 6.10 some of the limits for condition states and their corresponding ϕ_c s are shown. The shortest range is taken as the finalized range.

For condition state 2 the lower end of the range is the upper limit of condition state 1. Both girder deterioration profiles (GP1 and GP2) have different ranges because

the location of corrosion is different for the two profiles. Similarly, the lower range of condition state 3 was the maximum of the condition state 2.

The range for each condition state for both GP1 and GP2 are shown in Table 6.11.

This is the final range set for each condition state and will be used for the research.

Table 6.11 Range of section loss for condition states

Condition state		Range of section loss
GP 1	1	0-1%
	2	1-7%
	3	7-31%
	4	31-80%
GP 2	1	0%
	2	0-5%
	3	5-20%
	4	20-80%

6.4 Uncertainty in the Location of the Deterioration

6.4.1 Introduction

Load rating is a function of the structural demand induced by the load, which varies along the span. The critical load rating section for a new girder is at the mid-span because the flexural demand by the load is maximum at the mid-span, and the capacity of an undeteriorated girder is uniform throughout the span. Varying levels of section loss along the span results in non-uniform capacity, which could shift in the critical load rating location. For example, a hypothetical girder with a span length of 50 ft. has a section loss along the span as shown in Figure 6.9. The section loss of 50% at 12.5 ft. is the maximum loss present in the girder. Section loss of 20% at the mid-span is the least amount of loss in the girder. Load rating of the 50 ft. W 30 X 99 girder for an HL 93 truck is plotted in Figure 6.10. The load rating at the mid-span is 1.041, and the load rating at the location of maximum deterioration is 1.034. The critical load rating value of

0.9568, is located at 18.5 ft. along the span. Similar scenarios of section loss in the field can cause a shift in the load rating away from the mid-span. Typically, the load rating is only performed at either the mid-span or at the location of the maximum section loss. The distribution of corrosion along the span is vital for determining an accurate load rating of the girder.

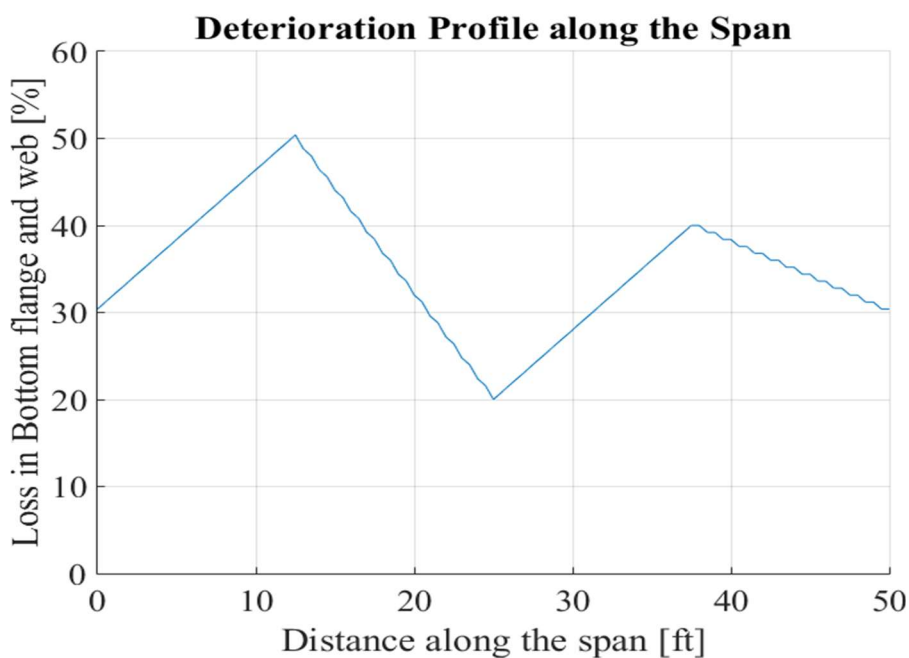


Figure 6.9 Example section loss profile along the span

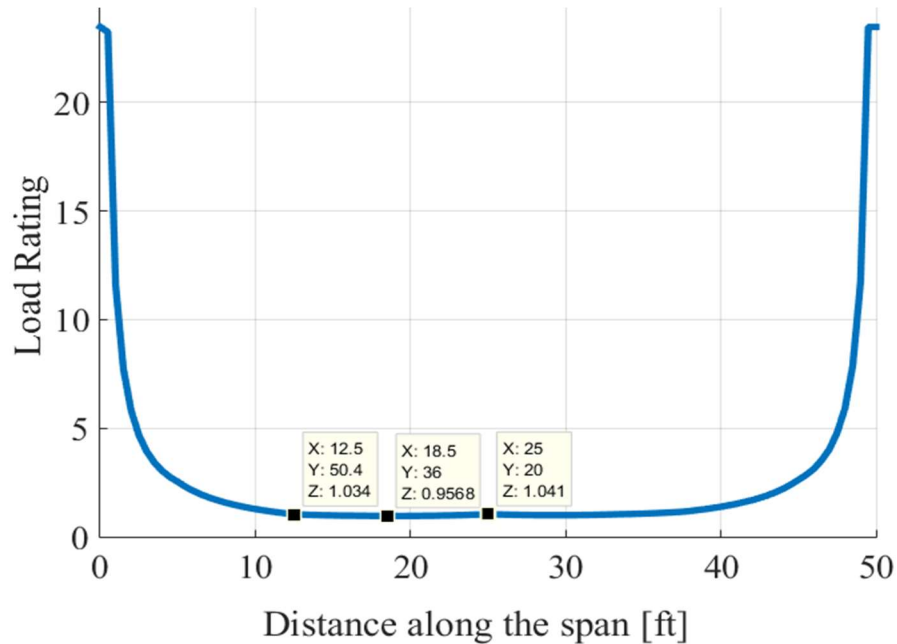


Figure 6.10 Load rating along the span for the section loss shown in Figure 6.9

Inspection details provide valuable information about the section loss along the span. The amount of information about the corrosion varies with the detail in inspection data. As discussed earlier in “Chapter 4: Overview of Methodology” on page 36, four approaches were suggested. The approaches are:

- only the worst condition state in the girder is known (Approach 1),
- all condition states present in the girder and the corresponding total length of girder segments classified in each condition state are known (Approach 2),
- all condition states present in the girder and the corresponding length of girder segments classified in each condition state along with the location is known (Approach 3), and
- deterioration profile along the span is known (Special Approach).

6.4.2 Stratification of ϕc Depending on the Survey Information

The four approaches have different uncertainties associated with them because of the amount of information known about the amount and location of section loss.

Uncertainties for each approach have been quantified and are included in the reliability analysis. A set of ϕc s are suggested for each approach to account for the quantified uncertainty.

In Approach 1, the only information known is the worst condition state in the girder. The uncertainties in this approach include the amount of each condition state, the location of the condition state, the actual section loss within each condition state, the variation of loss along the section, and the loss due to corrosion until the next inspection.

In Approach 2, all the condition states and their corresponding length in the girder are known. The uncertainties in this approach include the location of each condition state, the actual section loss within each condition state, the variation of the loss along the section and the loss due to corrosion until the next inspection cycle.

In Approach 3, all the condition states present in the girder, its corresponding length, and the location of each condition state are known. The uncertainties in this approach include actual deterioration within each condition state, the variation of loss along the section and loss due to corrosion until the next inspection.

The three common uncertainties on all of the approaches are actual deterioration within each condition state, the variation of loss along the section and the loss due to corrosion until the next inspection. The uncertainty due to the range of loss percentages in each condition state is accounted for by using the mean value and standard deviation of all the percentage loss in that condition state. For example, CS2 has a range between 1%

and 5% loss; the mean and standard deviation within that range is calculated using Eqn. (48) and (49) respectively. The calculated mean and standard deviation of the plastic moment capacities are used in the reliability analysis as a normally distributed random variable to account for the variation. The variation of deterioration along the section is accounted for using the COV as an additional standard deviation, as discussed in section 6.1 Uncertainties in Section Deterioration on page 53, which is added using square root of the sum of the squares (SRSS). The uncertainty due to possible future corrosion is discussed in section 6.2 Future Corrosion on page 62.

$$Average = \frac{\sum_{i=1}^n x_i}{n}, \quad (30)$$

$$standard\ deviation = \sqrt{\frac{\sum((x - Average)^2)}{n - 1}} \quad (31)$$

Where,

x_i is plastic moment capacity with i^{th} percentage loss in each condition state

n is number of capacities in each condition state.

See Chapter 7: Condition Factor Calculation and Implementation for more detail.

A simulation of all the possible spread and distributions of section loss within the girder is performed to quantify the lack of knowledge of the location and the distribution of the section loss. This simulation is done for a 5% girder length increment; each of the 5% section can be any one of the three condition states. If all the possible scenarios are simulated, then we can account for them in the analysis to correctly calculate the variation and to quantify it for finding the ϕ_c . There are 231 possible scenarios of the spread with a 5% girder length increment. As seen in Figure 6.11, the girder length is segmented into 20 sections and each section can have one of the three condition states.

“1” represents condition state 1 and is green, “2” represents condition state 2 and is yellow, and “3” represents condition state 3 and is red.

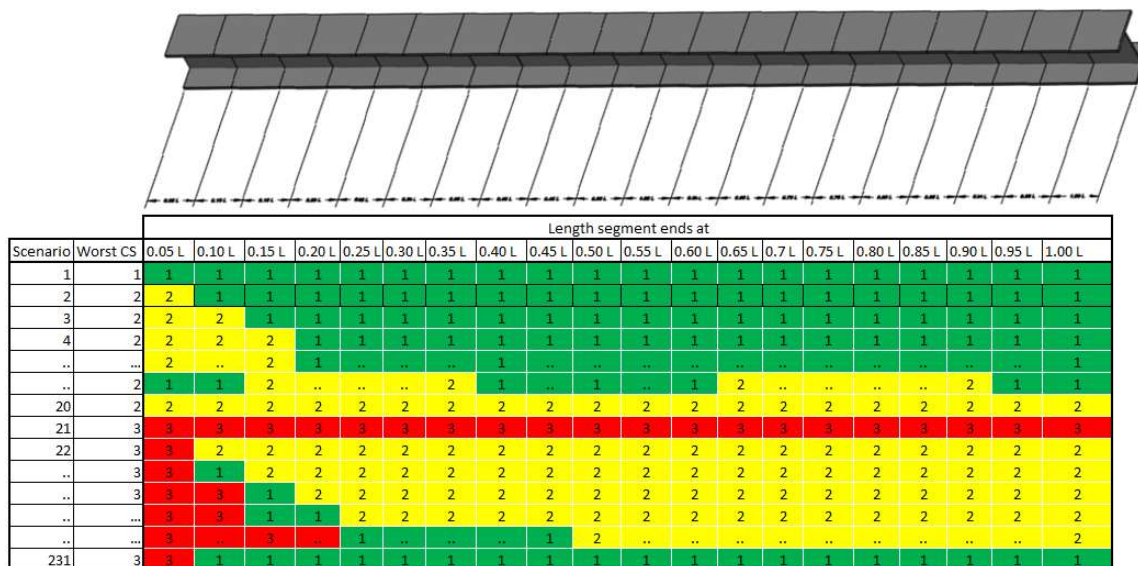


Figure 6.11 Example scenarios for various levels of section loss along the span

In Approach 1, the worst condition state is known. Simulation of the worst condition state ranges between 5% to 100% of the girder. Within each scenario of the distribution, the location of the conditions are further simulated to provide all possible locations of that condition state. For example, scenario 2 in Figure 6.13 has 20 possible variations with the condition state 2 and could be anywhere in the span. (see Figure 6.13) As only the worst condition state is known all the scenarios with that worst condition are further combined into a category CS. There are 3 CS groups: CS 3 groups includes all the scenarios with condition state 3, CS 2 group has all the scenarios with condition state 2 but no condition state 3, and CS 1 group has the scenario where the entire girder is in condition state 1. A flow chart of the process of categorizing the scenarios into one of the three condition states is shown in Figure 6.12. These simulations are done to reduce the over penalization in the load rating that would occur if the worst condition state was

assumed to be at the mid-span. The simulation accounts for the worst case along with its probability.

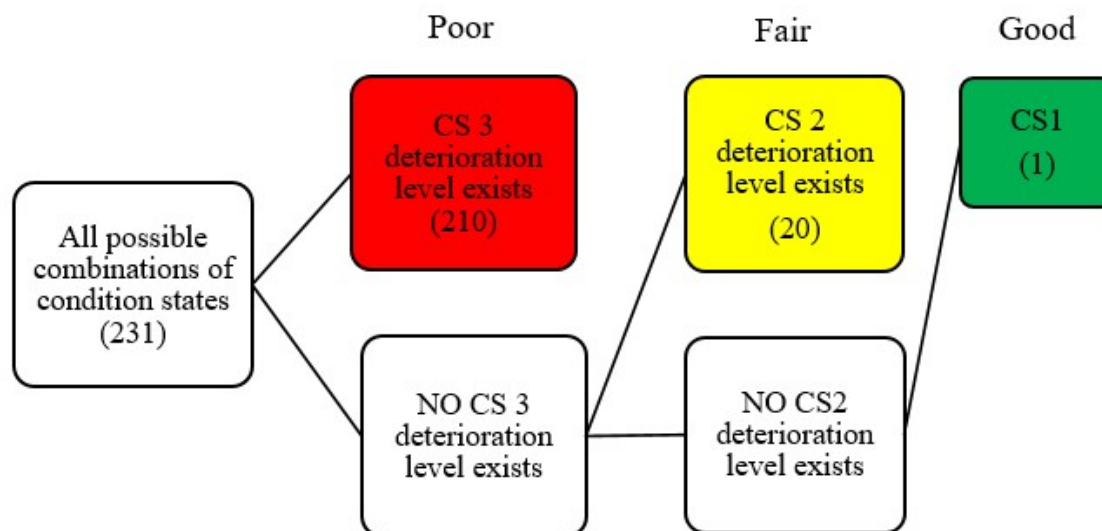


Figure 6.12 Flowchart to categorize CS's

Similarly, in Approach 2 the portion of the girder of each condition state is known, which means that the proportion of girder length corresponding to each condition state in the girder is one of the 231 scenarios that has been simulated in Figure 6.11. Finally, for Approach 3, the location of the condition state and its corresponding length is known. Therefore, there are no uncertainties associated with the location of the condition state.

having an equal length $1/20^{\text{th}}$ of the total span. For example, a girder can have 100% CS 1 or 100% CS2 or 100% CS 3, it can also have 30% CS 1, 30% CS2 and 40% CS 3. These 231 scenarios are due to an increment size of 5% of the girder in each condition state. For purpose of discussion, the list of all scenarios with a courser 25% increment in each condition state is shown in Table 6.13. The use of 25% increment reduces the total number of scenarios from 231 (at 5% length increments, which is used for ϕ c calibration in the succeeding chapter) to 15, all of which is shown in Table 6.12.

Table 6.12 Categorization of possible condition state into CS's

CS	Condition State 1 %	Condition State 2%	Condition State 3%
3	0%	0%	100%
3	0%	25%	75%
3	0%	50%	50%
3	0%	75%	25%
2	0%	100%	0%
3	25%	0%	75%
3	25%	25%	50%
3	25%	50%	25%
2	25%	75%	0%
3	50%	0%	50%
3	50%	25%	25%
2	50%	50%	0%
3	75%	0%	25%
2	75%	25%	0%
1	100%	0%	0%

Further categorization of these scenarios on the basis of the worst condition state present in the scenario was required for Approach 1. This categorization ensured that all possible scenarios for the grouped condition state were combined along with their uncertainty and probability. For example, if a scenario has some condition state 2 were grouped into CS2. Out of the 20 scenarios shown in Table 6.13, all of them are

categorized into one of the three CS's and the categorization can be seen in the first row of the table. Using the theory of probability and statistics, all the variations in each category are calculated and accounted for in the reliability analysis.

Each possible scenario in Table 6.12 is a case for Approach 2. For example, NDOR inspection reports a girder with a length of 200 ft. that has 50 ft. of CS 3, 50ft. of CS2, and 100 ft. of CS1. This corresponds to 25% CS 3, 25% CS 2 and 50% CS 1; it is highlighted in Table 6.13. Within that one scenario, there can be hundreds of possible variations for the location of the condition state. For example, the CS 3 can be in the middle, at the ends, or distributed randomly anywhere along the span, and CS 2 and CS 1 could similarly be distributed anywhere along the span. Using the concept of expected value from the probability theory, a mean and standard deviation accounting for all possible distributions was calculated; this value was used in the reliability analysis to find the ϕ_c .

Table 6.13 Sample scenarios of condition states distribution in percentage

Condition State 1 %	Condition State 2 %	Condition State 3 %
0%	0%	100%
0%	25%	75%
0%	50%	50%
0%	75%	25%
0%	100%	0%
25%	0%	75%
25%	25%	50%
25%	50%	25%
25%	75%	0%
50%	0%	50%
50%	25%	25%
50%	50%	0%
75%	0%	25%
75%	25%	0%
100%	0%	0%

6.5 Conclusion

All the uncertainty discussed in this chapter is associated with the condition of the girder and needs to be accounted for by the ϕ_c . The condition state of the girder that is observed and reported by the inspector, helps with the load rate of a bridge. An accurate definition of the condition of the girder and its location along the span produces an accurate load rating, and any diversion or misinterpretation of the condition state causes the load rating to be inaccurate. An objective definition with a range of section loss for each condition state is defined in order to provide the correct translation of the observed condition of the girder to the load-rating engineer. As there can be a varying amount of detail provided through the inspection, multiple approaches have been defined in this chapter to produce a load rating that provides a reliability consistent with the LRFR.

Chapter 7: Condition Factor Calculation and Implementation

Evaluation of condition factors should be consistent with the details available from inspections. The four approaches have different uncertainty associated because of varying amount of information about the amount and location of section loss associated with each Approach. The procedure to use the four approaches previously mentioned in Chapter 4: Overview of Methodology, along with the associated uncertainty, will be further discussed in detail in this chapter. Uncertainties for each Approach have been quantified and is included in the reliability analysis. Reliability analysis for known loads and capacity can be performed along the span of the girder to generate a ϕ_c in order to provide consistent reliability. This ϕ_c would account for the section loss due to corrosion and the variation of loss along the section. As a range of section loss is binned together for each condition state, an uncertainty due to the lack of exact percentage loss present in the girder along the span emerges, which is also accounted for by ϕ_c .

7.1 Approach 1

Load rating engineers can use Approach 1 when the worst condition state in the girder is known. In this approach, simulation of all the possible scenarios i.e. portion and location of the condition state are further categorized into one of the three condition state (CS) groups as mentioned on page 78. For example, with courser scenarios of 25% increment shown in Table 6.12 are categorized into one of the three CS groups. Scenarios with condition state 3 are grouped into CS 3 group, whereas those without condition state 3 but with 1 or 2 are grouped into CS 2 group, and finally scenario with only condition state 1 are group to CS 1 group. Color coding is also shown in Table 6.12 for CS 1, CS 2 and CS 3 groups as green, yellow and red, respectively. Similarly, for 5% increment

results in 231 possible scenarios out of which 210 have condition state 3 (CS 3 group), twenty have condition state 2 (CS 2 group) and remaining scenario has condition state 1 (CS 1 group). Consequently, categorizing into CS 1, CS 2 and CS 3 groups leads to uncertainty of actual condition state distribution in the field.

7.1.1 Quantifying Uncertainty in Approach 1

In Approach 1, the ϕ_c needs to account for the uncertainties due to variation in the amount of corrosion within a section, lack of exact percentage loss within a condition state, unknown location of deterioration and lack of knowledge of the portion of girder in each condition state. The uncertainty due to variation in the amount of corrosion within a section is accounted through COV associated with each percentage loss (see section 6.1 Uncertainties in Section Deterioration). Lack of exact percentage loss uncertainty is accounted by standard deviation of all capacities within each condition state (see section 6.3 Uncertainty due to Range of Section Loss in each Condition State). The uncertainty due to unknown location of deterioration is accounted by finding standard deviation of the moment capacities of possible condition states within each scenarios (see section 6.4 Uncertainty in the Location of the Deterioration). Lastly, lack of knowledge of the portion of girder in each condition state is accounted by using the average standard deviation of the moment capacities of possible condition states of all the scenarios within each of the condition state groups (CS 1, CS 2 and CS 3 groups), refer to section 6.4 Uncertainty in the Location of the Deterioration

Consequently, the combined uncertainty due to variation in the amount of corrosion, lack of exact percentage loss, unknown deterioration location and lack of knowledge of the portion of girder in each condition state, can be evaluated using

Eq.(34), Eq. (37), and Eq. (40) respectively, for CS 1, CS 2 and CS 3 groups. In Eq. (34) and Eq. (35), the expected capacity ($E(CS1)$) is calculated using Eq. (32) i.e. by taking arithmetic average of plastic moment capacities of all condition states within CS 1 group. Whereas, in Eq. (35) and Eq. (38), the expected capacities $E(CS2)$ and $E(CS3)$ respectively, are calculated using weighted average of plastic moment capacities based on percentage areas corresponding to the condition states 1, 2 and 3. These expected capacities are then used in Eq. (36) and Eq. (39) respectively, to calculate average standard deviation from weighted variances using percentage condition state areas as weights. The calculated average standard deviation is then further combined to the variation in section deterioration using SRSS method as shown in Eq. (37) and (40). By implementing these calculations, an equivalent probabilistic distribution is generated for each condition state group (CS 1, CS 2 and CS3) accounting for combined uncertainties in Approach 1.

For CS 1

$$E(CS1) = \frac{\sum_{i=1}^n x_i}{n} \quad (32)$$

$$SD(1) = \sqrt{\left(\frac{\sum_{i=1}^m ((x_i - E(CS1))^2)}{m - 1} \right)} \quad (33)$$

$$SD(CS 1) = \sqrt{(SD(1)^2 + (E(CS1) * COV_{\max_1})^2)} \quad (34)$$

Where,

$E(CS1)$ = Expected plastic moment capacity of the girder in CS 1 group

$SD(CS1)$ = Standard deviation of plastic moment capacities in CS 1 group

x_i = Plastic moment capacity for i^{th} percentage loss within condition state 1

m = Number of plastic moment capacity values within condition state 1

COV_{max_1} = COV corresponding to the maximum percentage loss in condition state 1

For CS2

$$E(CS2) = \sum_{s=1}^{20} \frac{\sum_{i=1}^m a_s * x_{i,1}/m + \sum_{j=1}^n b_s * x_{j,2}/n}{20} \quad (35)$$

$SD(2)$

$$= \sum_{s=1}^{20} \left(\frac{\sqrt{\frac{\sum_{i=1}^m a_s * (x_{i,1} - E(CS2))^2 + \sum_{j=1}^n b_s * (x_{j,2} - E(CS2))^2}{m+n-1}}}{20} \right) \quad (36)$$

$$SD(CS2) = \sqrt{(SD(2))^2 + (E(CS2) * COV_{max_2})^2} \quad (37)$$

$E(CS2)$ = Expected plastic moment capacity of the girder in CS 2 group

$SD(CS2)$ = Standard deviation of plastic moment capacities in CS 2 group

$x_{i,1}$ = Plastic moment capacity for i^{th} percentage loss within condition state 1

$x_{j,2}$ = Plastic moment capacity for j^{th} percentage loss within condition state 2

m = Number of plastic moment capacity values within condition state 1

n = Number of plastic moment capacity values within condition state 2

a_s and b_s = % area of girder in condition state 1 and 2 respectively for s^{th} scenario

s = number of scenarios in CS 2 group = 20

COV_{max_2} = COV corresponding to the maximum percentage loss in condition state 2

For CS3

$$E(CS3) = \frac{\sum_{s=1}^{210} \sum_{i=1}^m a_s * x_{i,1}/m + \sum_{j=1}^n b_s * x_{j,2}/n + \sum_{k=1}^o c_s * x_{k,3}/o}{210} \quad (38)$$

$$SD(3) = \sum_{s=1}^{210} \left(\frac{\sqrt{\left(\frac{\sum_{i=1}^m a * (x_{i,1} - E(CS3))^2 + \sum_{j=1}^n b * (x_{k,2} - E(CS3))^2 + \sum_{k=1}^o c * (x_{k,3} - E(CS3))^2}{m + n + o - 1} \right)}}{210} \right) \quad (39)$$

$$SD(CS 3) = \sqrt{(SD(3)^2 + (E(CS3) * COV_{\max_3})^2)} \quad (40)$$

$E(CS3)$ = Expected plastic moment capacity of the girder in CS 3 group

$SD(CS3)$ = Standard deviation of plastic moment capacities in CS 3 group

$x_{i,1}$ = Plastic moment capacity for i^{th} percentage loss within condition state 1

$x_{j,2}$ = Plastic moment capacity for j^{th} percentage loss within condition state 2

$x_{k,3}$ = Plastic moment capacity for k^{th} percentage loss within condition state 3

m = Number of plastic moment capacity values within condition state 1

n = Number of plastic moment capacity values within condition state 2

o = Number of plastic moment capacity values within condition state 3

a_s, b_s and c_s

= % area of girder in condition state 1, 2 and 3 respectively for s^{th} scenario

s = number of scenarios in CS 3 group = 210

COV_{\max_3} = COV corresponding to the maximum percentage loss in condition state 3

7.1.2 Procedure to Find ϕ_c for Approach 1

The values for m, n and o are the number of plastic moment capacities in condition states 1, 2 and 3 respectively. Plastic moment capacities within each condition states are calculated for 1% increment loss. As there are three different ranges for condition states the number of values in each range varies. A summary of the values of m, n and o are summarized in Table 7.1.

Table 7.1 Summary of values of m, n and o used in Eq. (24) through (32)

		m	n	o
NDOR Distribution Range	GP 1 & GP 2	1	1	49
Range Consistent with MBE	GP 1	2	6	24
	GP 2	1	5	15

The value for COV_{max} is the COV corresponding to maximum percentage section loss in each scenario. For CS 1 group, the maximum percentage section loss is the upper limit in condition state 1. Similarly, CS 2 and CS 3 group's maximum percentage loss are the upper limit of condition state 2 and 3 respectively. Using the COV associated with the maximum loss in each condition state ensure that the variation is maximum. The COV_{max} values are shown in Table 7.2. It was found using Table 6.3, Table 6.8 and Table 6.11, which has the COV for each percentage loss and the range of percentage loss of section for NDOR's range and range consistent with MBE.

Table 7.2 Summary of values of COV_{max} used in Eq. (34), (37) and (40)

		COV_{max_1}	COV_{max_2}	COV_{max_3}
NDOR Distribution Range	GP 1 & GP 2	0.01	0.01	0.045
Range Consistent with MBE	GP 1	0.01	0.038	0.045
	GP 2	0.01	0.028	0.045

The expected value for the CS groups is a function of plastic moment capacity of the girder. Using Eq. (32) and Eq. (34), the mean and standard deviation of the plastic moment capacities for CS 1 group was found. Similarly, Eq. (35) and Eq. (38) were used to find the mean plastic moment capacities for CS 2 and CS 3 group respectively. For the standard deviation for CS 2 and CS 3 group, Eq. (37) and Eq. (40) respectively were used. For example, a sample mean and standard deviation of the plastic moment capacity of a “W30 X 99” girder with deterioration profile of GP1 and GP2 is summarized in Table 7.3. These values were used in the reliability analysis to find the ϕ_c for each CS's.

Table 7.3 Sample mean and standard deviation for CS's with GP1 and GP2

'W30X99'	GP 1		GP 2	
	Mean	Std. Dev.	Mean	Std. Dev.
CS 1	1806.33	18.06	1775.58	17.76
CS 2	1801.12	68.54	1767.25	67.40
CS 3	1709.80	150.49	1613.38	225.21

The span length and girder spacing was changed to account for the effect of girder size and load effect in the reliability analysis. The various span lengths considered for the study was between 50ft. and 120 ft. with an increment of 10 ft. The girder spacing varied from 3.5 to 7 ft. and the increment was 0.5 ft. The change in length and girder spacing directly affects the Girder Distribution Factor (GDF), which was found using AASHTO LRFD Design Manual equation. These variations resulted in a total of (8 * 8 =) 64 cases; these cases had different load effects from the HL 93 truck and the dead-load and/ or girder sizes. The load effect from the live-load varied with varying GDF and span length, and the load effect from the dead-load varied with the girder spacing and the span length. The plastic moment capacity changed with changing span length. These values were used in the reliability analysis to find a ϕ_c .

ϕ_c was found through reliability analysis using the mean and standard deviation values of the capacity and the load effects. There are 64 cases with varying capacity and load effects, and each case has three CS groups. A total of $64 \times 3 = 192$ runs of reliability analysis is performed to get ϕ_{cs} . A beta target of 3.5 was used in the reliability analysis. The details on the reliability analysis and how ϕ_c is explained in section 5.1 Rackwitz-Fiessler Reliability Analysis. Uncertainty due to possible future corrosion was accounted using the bias as mentioned in 6.2 Future Corrosion. A sets of average ϕ_c accounting for future corrosion of carbon steel in rural environment is given in Table 7.4. The five sets multipliers are found following the recommendation suggested in “6.2 Future Corrosion” are summarized in Table 7.5 and Table 7.6 for carbon steel and weathering steel in the various environment respectively. These multipliers are the average values of the set of 64 values found for each variation in span length and girder spacing.

As there are four different girder deterioration profiles, the process is repeated four times using the same method mentioned above. The parameters that changed are the range in each condition state and the section where the corrosion occurs (see sections 6.3.2 Range Consistent with NDOR’s Current Inspection Procedure, 6.3.3 Calibrating the Range of Condition State to MBE Values and 4.2.2 Girder Deterioration Profile Models for more details).

Engineers need an equivalent plastic moment capacity of the girder to load rate a bridge. If engineers only know the worst condition state, they need to use the same mean plastic moment capacity in each CS group used in this research to ensure accuracy in the load rating procedure. This information is presented in the form of percentage loss for simplicity and is summarized for all four girder deterioration profiles in Table 7.7.

7.1.3 ϕ_c for Approach 1

Table 7.4 ϕ_c for carbon steel when the worst CS is known in a rural environment

Carbon Steel in Rural Environment		CS 1	CS 2	CS 3
NDOR Distribution Range	GP 1	0.99	0.94	0.69
	GP 2	0.98	0.94	0.42
Range Consistent with MBE	GP 1	0.99	0.93	0.80
	GP 2	0.98	0.92	0.75

Table 7.5 Multiplier for ϕ_c for carbon steel in urban and marine environment

Multiplier for		Carbon Steel					
		Urban Environment			Marine Environment		
		$\phi_c 1$	$\phi_c 2$	$\phi_c 3$	$\phi_c 1$	$\phi_c 2$	$\phi_c 3$
NDOR Distribution Range	GP 1	0.98	0.98	0.97	0.97	0.97	0.96
	GP 2	0.96	0.96	0.93	0.95	0.95	0.91
Range Consistent with MBE	GP 1	0.98	0.98	0.97	0.97	0.97	0.96
	GP 2	0.96	0.96	0.95	0.95	0.95	0.94

Table 7.6 Multiplier for ϕ_c for weathering steel in the three environments

Multiplier for		Weathering Steel								
		Rural Environment			Urban Environment			Marine Environment		
		$\phi_c 1$	$\phi_c 2$	$\phi_c 3$	$\phi_c 1$	$\phi_c 2$	$\phi_c 3$	$\phi_c 1$	$\phi_c 2$	$\phi_c 3$
NDOR Range	GP 1	1.00	1.00	1.00	0.99	0.99	0.99	0.99	0.99	0.99
	GP 2	1.00	1.00	1.00	0.98	0.98	0.96	0.98	0.98	0.97
Consistent with MBE	GP 1	1.00	1.00	1.00	0.99	0.99	0.99	0.99	0.99	0.99
	GP 2	1.00	1.00	1.00	0.98	0.98	0.98	0.98	0.98	0.98

Table 7.7 Percentage loss for condition states in Approach 1

Distribution Profile	Condition State	Percentage Loss to use for Load Rating
GP 1	1	0.5%
	2	2.3%
	3	8.4%
GP 2	1	0%
	2	1.3%
	3	7.2%
NDOR's Range (Both Profiles)	1	0 %
	2	0.26%
	3	9.5%

7.2 Approach 2

Load rating engineers can use Approach 2 when portions of the girder in each condition state is known but not its location. The 231 possible scenarios generated using the 5% length increment have multiple variations of distribution of the condition states within the girder as explained in section 6.4.2 Stratification of ϕ_c Depending on the Survey Information. For example, Figure 7.1 shows one of the scenarios with a certain amount of condition state 1, 2 and 3 shown in green, yellow and red respectively distributed randomly along the span. This scenario has multiple variation in the spread of condition state and some of the variation can be seen in the figure. Depending on the condition state present in the critical load location (near mid-span for simply supported girder) the moment capacity of the girder varies. In this approach all the possible moment capacities are accounted for by using the expected value and the standard deviation.

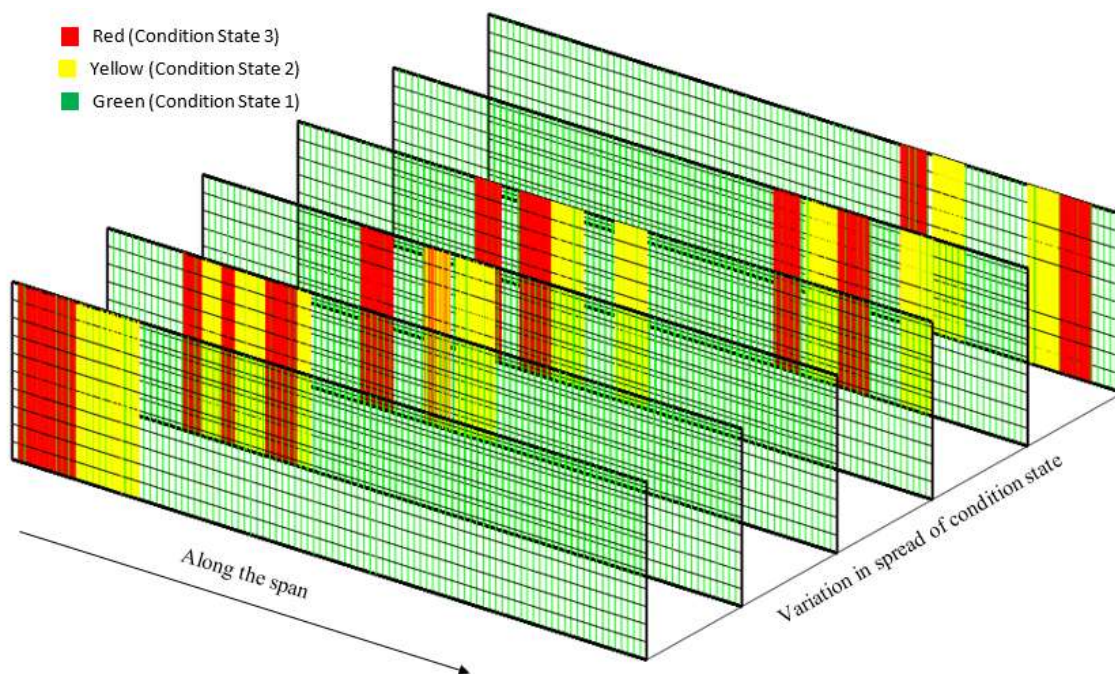


Figure 7.1 Sample of possible distribution for one of the scenarios

7.2.1 Quantifying uncertainty in Approach 2

In Approach 2, the ϕ_c needs to account for the uncertainties due to variation in the amount of corrosion within a section, the lack of exact percentage loss within a condition state and unknown location of deterioration. These uncertainties are accounted using similar process as mentioned in Section 7.1.1 Quantifying Uncertainty in Approach 1.

Consequently, the combined uncertainty due to variation in the amount of corrosion within a section, the lack of exact percentage loss within a condition state and unknown location of deterioration can be evaluated using Eq. (43). The expected capacity for each scenario is calculated using Eq. (41), which is weighted average of plastic moment capacities based on percentage areas corresponding to the condition states 1, 2 and 3. The expected capacity is used in Eq. (42) to calculate the standard deviation from weighted variances using percentage condition state areas as weights. Finally, the standard deviation for the scenario is calculated by using the SRSS of the value in Eq. (42) and the standard deviation from the variation in the amount of corrosion associated with the maximum percentage loss (see section 6.1 Uncertainties in Section Deterioration).

$$E(capacity) = \sum_{j=1}^3 p_j * \mu_{cs_j} \quad (41)$$

$$SD = \sqrt{\frac{\sum_{j=1}^3 \sum_{i=1}^{m_j} p_j (x_{i,j} - E(capacity))^2}{(\sum_{j=1}^3 m_j) - 1}} \quad (42)$$

$$SD(capacity) = \sqrt{SD^2 + (E(Capacity) * COV_{max_j})^2} \quad (43)$$

Where,

$E(\text{capacity}) = \text{Expected plastic moment capacity of a scenario}$

$SD(\text{capacity}) = \text{Standard deviation of expected moment capacities of a scenario}$

$j = 1, 2 \text{ or } 3 \text{ for condition state } 1, 2 \text{ or } 3 \text{ respectively}$

$p_j = \text{percentage of girder in } j^{\text{th}} \text{ condition state}$

$m_j = \text{number of plastic moment capacity in } j^{\text{th}} \text{ condition state.}$

$\mu_{cs_j} = \text{expected plastic moment capacity within } j^{\text{th}} \text{ condition state}$

$x_{i,j} = \text{moment capacities with } i^{\text{th}} \text{ percentage loss within } j^{\text{th}} \text{ condition state}$

$COV_{\max_j} = \text{COV associated with the max percentage loss in } j^{\text{th}} \text{ condition state}$

Eq. (41), Eq. (42) and Eq. (43) are the simpler concise form of the equations in Approach 1. These equations are simpler than the ones in the Approach 1 because only one scenario is considered. $E(\text{capacity})$ is the expected weighted capacity for a scenario calculated using Eq. (41). These parameters in the equations p_j represents a_s , b_s and c_s ; m_j represents m , n and o ; COV_{\max_j} represents CO_{\max_1} , COV_{\max_2} and COV_{\max_3} in from the equation in Approach 1. The values given in Table 7.2 can be used here.

Using Eq. (41) and Eq. (43), a mean and standard deviation of the plastic moment capacity can be found. These values are found for the coarser 25% increment and the reliability analysis is performed to generate ϕ_c and is summarized in Table 7.8. This process with the finer 5% increment was performed for this research, which resulted in ϕ_c for each of the 231 scenarios.

Table 7.8 ϕ_c and distribution variable for combinations shown in Table 7.3

Condition State 1 %	Condition State 2 %	Condition State 3 %	Mean	Standard deviation	ϕ_c
0%	0%	100%	1347.13	96.27	0.83
0%	25%	75%	1392.84	88.55	0.86
0%	50%	50%	1438.54	90.34	0.86
0%	75%	25%	1484.24	84.77	0.88
0%	100%	0%	1529.94	67.99	0.92
25%	0%	75%	1408.96	96.98	0.84
25%	25%	50%	1454.66	87.19	0.87
25%	50%	25%	1500.37	79.87	0.89
25%	75%	0%	1546.07	54.78	0.95
50%	0%	50%	1470.79	108.21	0.82
50%	25%	25%	1516.49	80.61	0.90
50%	50%	0%	1562.20	45.14	0.96
75%	0%	25%	1532.62	102.27	0.85
75%	25%	0%	1578.32	35.15	0.98
100%	0%	0%	1594.45	15.94	1.00

The effects of varying span length and girder spacing to the ϕ_c is studied following the procedure in Approach 1. There are 231 scenarios for a specific span length and girder spacing. As there are 64 variations, a ϕ_c is generated for each variation. A database of over 14784 (64*231) scenarios along with the percentage of condition states and the average plastic moment capacities is generated to suggest a ϕ_c to the load-rating engineer.

A hypothesis that there is a function between the moment capacity and the ϕ_c was tested. The ϕ_c VS the expected moment capacity was plotted and is shown in Figure 7.2, but no trend between them was apparent. Therefore, the hypothesis was proven wrong and a function between the percentage of condition states and a ϕ_c needed to be explored.

As there are three independent variables (percentages of condition state 1, condition state 2 and condition state 3) and a dependent variable (ϕ_c), finding the

equations to relate becomes complicated. A linear function was explored, but the prediction for the ϕ_c was not accurate. A non-linear function needed to be explored, and Artificial Neural Networks (ANNs) was used to find a non-linear function to predict the ϕ_c values using the percentage of girder in each condition state.

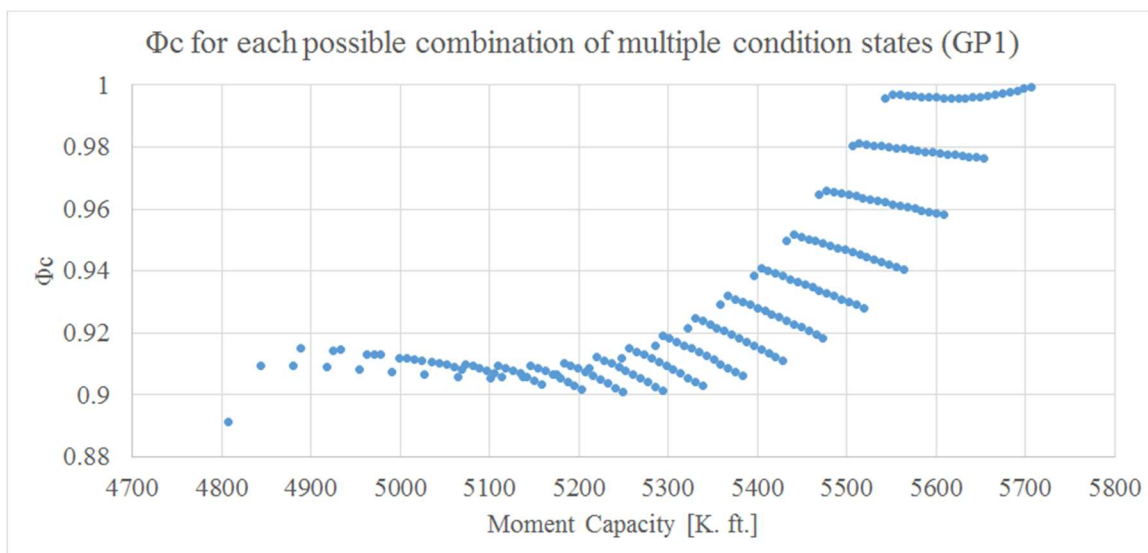


Figure 7.2 Moment capacity VS ϕ_c for the 231 combinations

7.2.2 Artificial Neural Networks (ANNs)

Artificial Neural Networks (ANNs) are a biologically inspired computer program designed to simulate the way the human brain processes the information to detect patterns and relationships in data and learn through experience (Agatonovic-Kustrin & Beresford, 2000). ANNs are trained until the error predictions are minimized and the network reaches a specified level of accuracy. Once the network is trained and tested, it can be given new input information to predict the output.

ANNs are used in this study to predict the ϕ_c values. Training of the ANNs was done using the percentage in each condition state as the input and the ϕ_c values from the Rackwitz-Fiessler as the output. There were over 14700 inputs for training, validation,

and testing for ANNs Neural network toolbox in MATLAB. The particular ANN created for the prediction of ϕ_c uses ten hidden networks and an output layer to give output. Figure 7.3 shows the network with inputs of condition state percentages, each condition state percentage goes through ten hidden networks, each with a weight and a bias. The results from the ten hidden networks further go through the output layer with a set of 10 weights and a bias. The result from the output layer is the prediction for ϕ_c . The weights and bias of the hidden layers (Layer 1) and the output layer (Layer 2) for GP1, GP2 are shown in Table 7.10, and Table 7.11 respectively. Similarly, the weights and bias from the prediction of ϕ_c for the deterioration range consistent with NDOR's current policy with section deterioration profile GP1 and GP2, are shown in Table 7.12 and Table 7.13 respectively. These weights, biases, and levels can be overwhelming to use, therefore an excel sheet with inputs for the percentage of each condition state is created to predict a ϕ_c .

Engineers, in order to load rate a bridge knowing the portion of each condition state in the girder, need to find the capacity of the bridge with the mean percentage loss used during reliability analysis. The percentage loss to be used is found by multiplying the portion of girder in each condition state to the corresponding percentage loss shown in Table 7.9. The percentage loss that is used for calculating the plastic moment capacity is found by using the same formula that is used for the expected capacity of the girder for each CS's in the reliability analysis, which would mean the mean value is used for load rating eliminating the need for bias.

$$\begin{aligned} \% \text{ loss} = & Portion_{CS} * \% Loss_{CS1} + Portion_{CS2} * \% Loss_{CS2} \\ & + Portion_{CS3} * \% Loss_{CS3} \end{aligned} \quad (44)$$

7.2.3 ϕ_c for Approach 2

Table 7.9 Percentage loss for each condition state for Approach 2

Distribution Profile	Condition State	Percentage Loss for Load Rating
GP 1	1	0.5%
	2	4%
	3	19%
GP 2	1	0
	2	2.5%
	3	12.5%
NDOR's Range (Both Profiles)	1	0 %
	2	0.5%
	3	25.5%

Table 7.10 ANN multiplier for GP1 deterioration profile

GP1 with range consistent with MBE						
Layer 1				Layer 2		
	CS_1 %	CS_2 %	CS_3%	Bias	Weights	Bias
W_1	1.93	-1.92	0.82	-3.06	0.19	-0.12
W_2	1.79	1.61	-1.17	-2.97	0.05	
W_3	-1.59	1.90	1.49	1.77	-0.05	
W_4	2.01	-0.01	2.42	-1.23	-0.83	
W_5	0.60	1.92	2.47	-0.38	-0.83	
W_6	-2.09	-1.92	0.51	0.63	-0.95	
W_7	-1.12	-1.33	2.07	-1.13	0.17	
W_8	0.38	2.86	-0.61	1.52	0.01	
W_9	1.82	2.03	1.48	1.85	1.54	
W_10	1.54	1.75	-0.81	2.99	-0.59	

Table 7.11 ANN multiplier for GP2 deterioration profile

GP2 with range consistent with MBE						
Layer 1				Layer 2		
	CS_1 %	CS_2 %	CS_3%	Bias	Weights	Bias
W_1	-0.98	-1.40	0.46	0.87	3.28	0.437
W_2	-2.10	3.35	-1.94	3.78	3.23	
W_3	-0.58	-0.35	-2.17	-2.41	4.22	
W_4	4.62	-2.94	3.30	-5.35	3.15	
W_5	1.07	-2.23	-2.24	1.00	-1.05	
W_6	4.26	-0.80	1.66	-1.65	0.04	

W_7	2.30	-1.46	-1.44	1.83	0.37	
W_8	-3.99	2.29	-3.88	2.16	-1.39	
W_9	-2.56	0.27	0.33	-3.31	-1.84	
W_10	1.15	-1.05	3.84	-3.93	-0.30	

Table 7.12 ANN multiplier for GP 1 deterioration profile with NDOR Range

GP1 with range consistent with NDOR's current policy						
Layer 1					Layer 2	
	CS_1 %	CS_2 %	CS_3%	Bias	Weights	Bias
W_1	1.04	1.09	-1.67	-3.8819	-0.13	0.024
W_2	1.04	0.99	-2.09	-2.4450	1.03	
W_3	-0.40	2.84	0.01	1.8869	0.30	
W_4	1.85	-1.82	1.35	-0.6974	0.21	
W_5	1.05	0.96	-0.95	-0.2376	0.46	
W_6	2.35	-2.01	0.25	0.3942	-0.02	
W_7	-0.42	-2.34	0.20	-1.4051	0.09	
W_8	-2.92	1.12	0.74	-1.8546	0.02	
W_9	0.85	0.02	-1.03	2.5113	1.03	
W_10	0.87	1.71	-1.78	3.4655	-0.08	

Table 7.13 ANN multiplier for GP2 deterioration profile with NDOR Range

GP2 with range consistent with NDOR's current policy						
Layer 1					Layer 2	
	CS_1 %	CS_2 %	CS_3%	Bias	Weights	Bias
W_1	-0.18	1.21	2.13	3.19	-0.02	0.261
W_2	0.68	-1.17	-2.38	-2.11	0.03	
W_3	2.02	-2.23	2.31	-3.64	-0.24	
W_4	0.93	1.27	2.78	-1.32	-0.71	
W_5	1.90	1.91	1.51	-0.64	-0.59	
W_6	0.47	2.59	2.61	-0.42	-1.07	
W_7	-1.97	1.15	1.25	-2.04	0.25	
W_8	-2.28	-2.30	-0.77	-0.99	-0.66	
W_9	-1.66	-1.75	-1.65	-2.49	-1.12	
W_10	-0.13	-0.20	-3.18	-4.33	3.12	

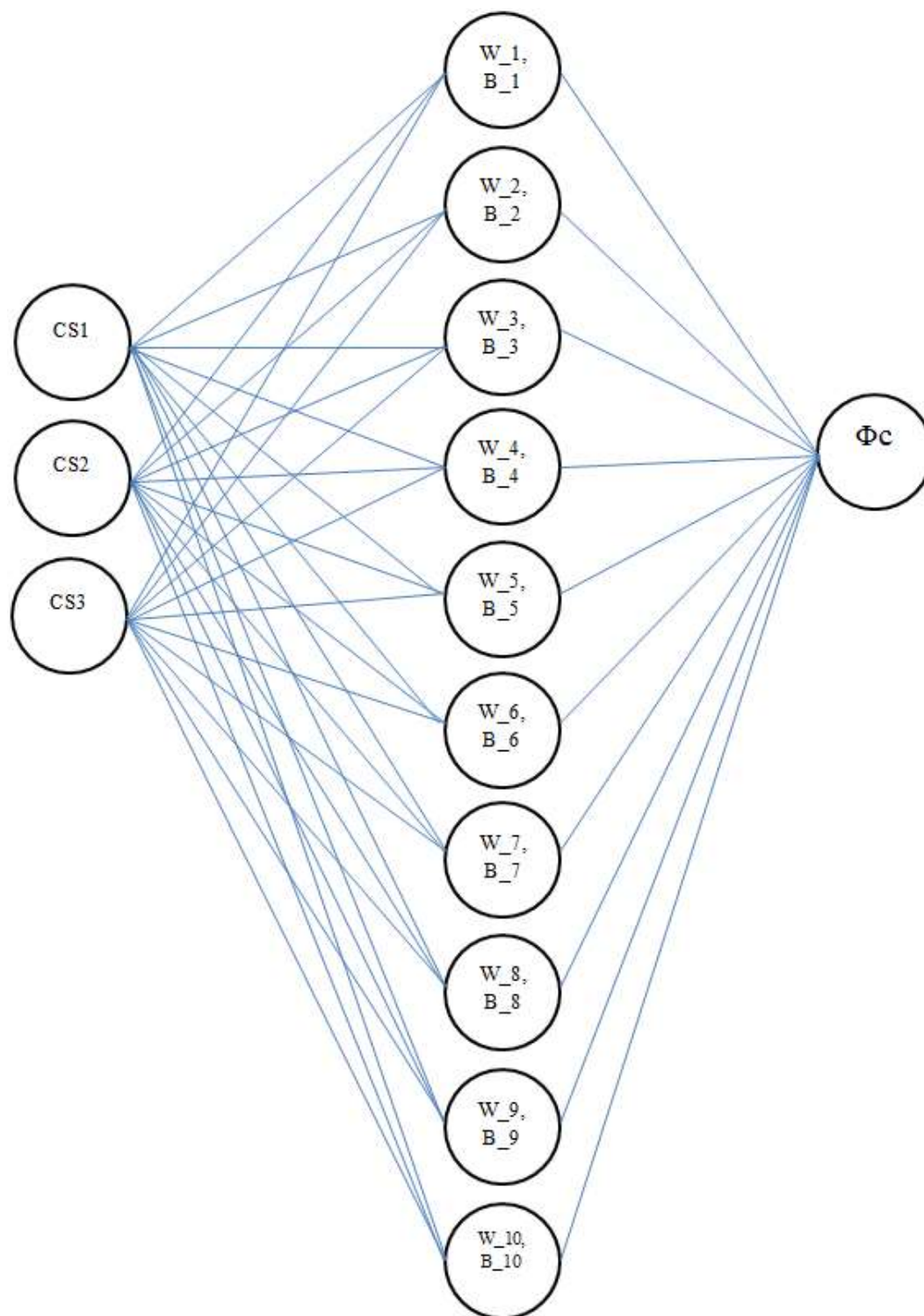


Figure 7.3 ANN's neural networks layers

Predictions of ϕ_c from ANN were compared to the values found from analysis to verify the accuracy of the predictions. Figure 7.4 and Figure 7.5 have plots of ANN predicted values and values from reliability analysis to check the accuracy of the prediction.

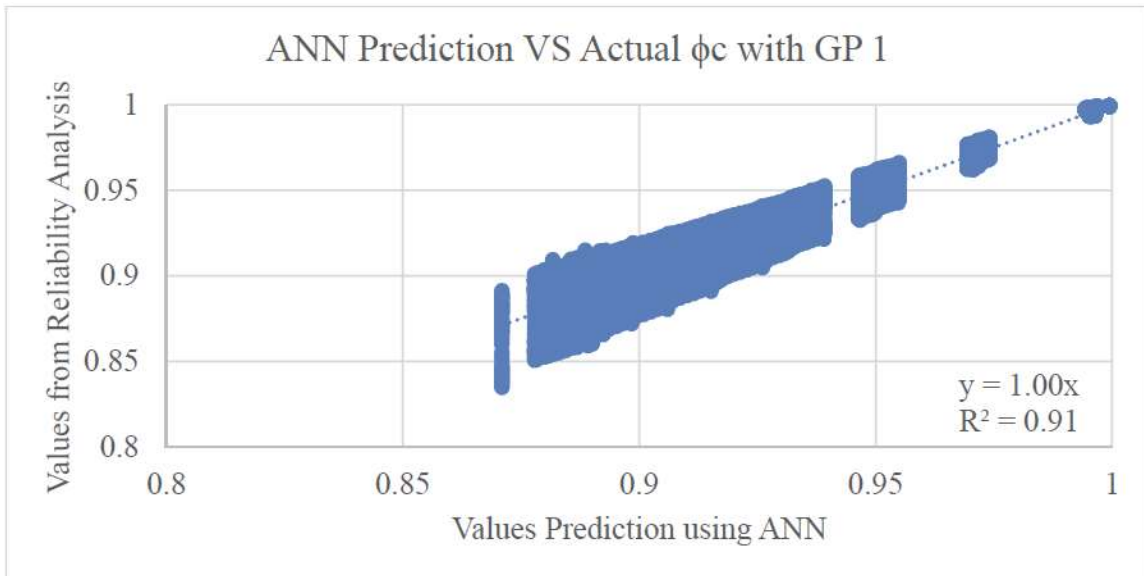


Figure 7.4 ϕ_c predicted using ANN VS actual ϕ_c for girder with GP1

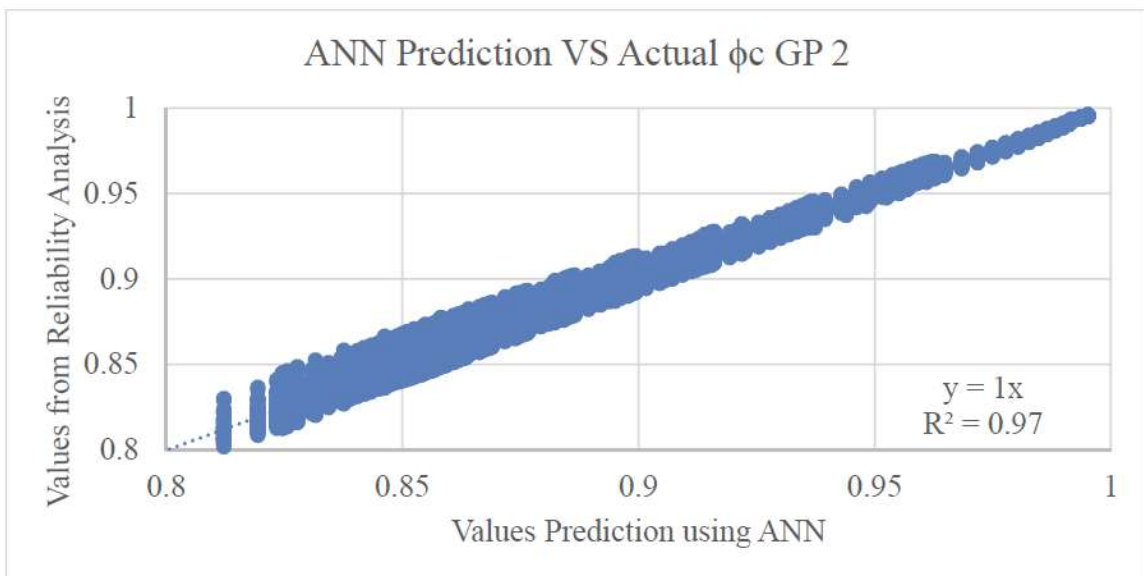


Figure 7.5 ϕ_c predicted using ANN VS actual ϕ_c for girder with GP2

The prediction for GP1 using ANN has a very good R^2 value of 0.97. Further examination of the differences in prediction shows that the maximum difference between ANN predicted ϕ_c and ϕ_c from the analysis is 0.036116, minimum difference is -0.02775, and the average difference is -0.00016. These predictions are accurate and are usually conservative because the mean value is negative and close to zero.

The prediction for GP2 using ANN has a good R^2 value of 0.91. Further examination of the differences in prediction shows that maximum difference between ANN predicted ϕ_c and ϕ_c from the analysis is 0.0124, minimum difference is -0.0211, and the average is $-2.017 \text{ E } -05$. These predictions are accurate and are usually conservative because the mean value is negative and close to zero.

Predictions of ϕ_c from ANN for the deterioration range consistent with NDOR's policy (see Table 6.8) were compared to the values found from analysis to verify the accuracy of the predictions. Figure 7.6 and Figure 7.7 have plots of ANN predicted values and values from reliability analysis to check the accuracy of the prediction for the section deterioration range GP1 and GP2 respectively.

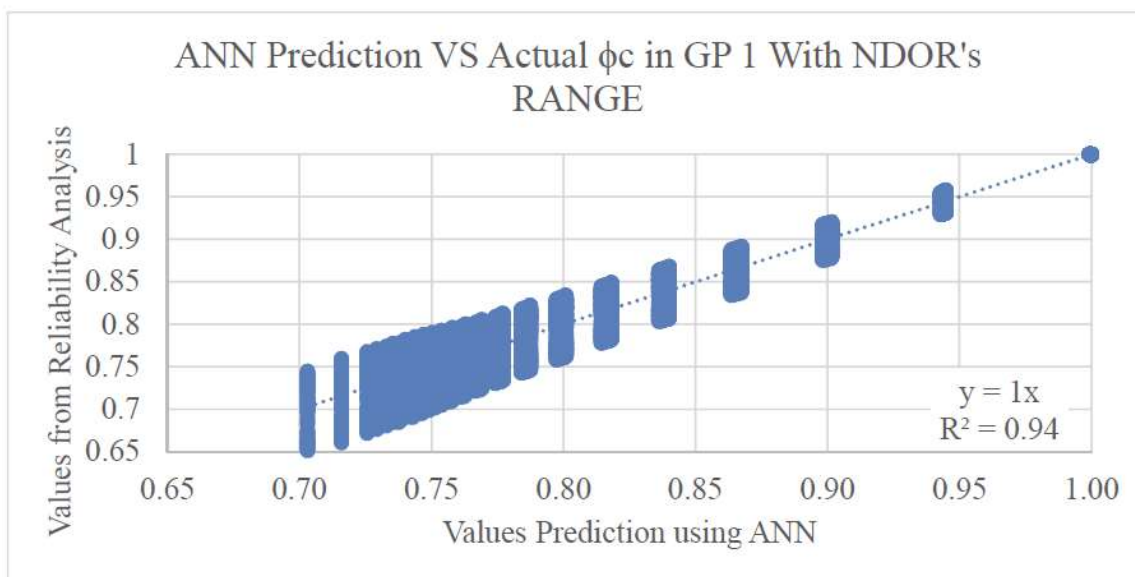


Figure 7.6 ϕ_c predicted using ANN VS actual ϕ_c with GP1 and NDOR's Range

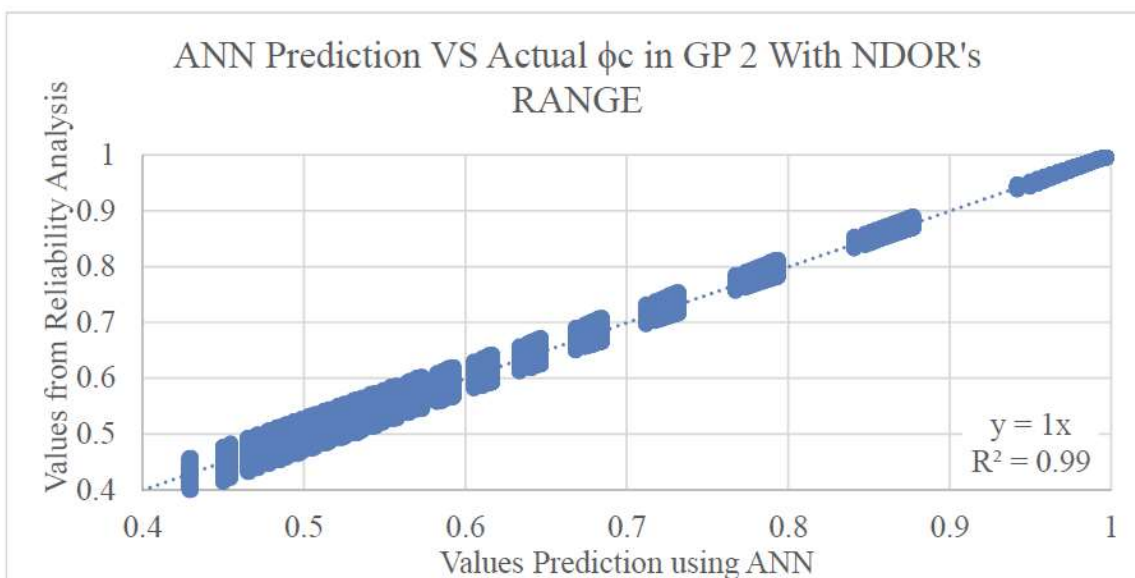


Figure 7.7 ϕ_c predicted using ANN VS actual ϕ_c with GP2 and NDOR's Range

The prediction for GP1 using ANN has a good R^2 value of 0.94. Further examination of the differences in prediction shows that the maximum difference between ANN predicted ϕ_c and ϕ_c from the analysis is 0.06, minimum difference is -0.04, and the

average is 0.0005. These predictions are accurate and are usually lenient because the mean value is positive and close to zero.

The prediction for GP2 using ANN has an excellent R^2 value of 0.99. Further examination of the difference in prediction shows that the maximum difference between ANN Predicted ϕ_c and ϕ_c from the analysis is 0.0406, minimum difference is -0.03251, and the average is 4.09424 E -05. These predictions are accurate and is usually lenient because the mean value is positive and close to zero.

7.3 Approach 3

Load rating engineers can use Approach 3 when the location and the portion of all condition state present in the girder is known. In this approach, engineers need to model the equivalent condition state percentage loss at the location of as seen in the field. An example of the distribution of condition states in a girder is shown in Figure 7.8. This hypothetical girder with a length of 50 ft. has condition state 2 in the first 5ft. (10%), the next 13 ft. (26%) is in condition state 1, the next 10ft. (20%) is in condition state 3, the next 17ft. (34%) is in condition state 1, and the last 5ft. (10%) in condition state 2. As mentioned above in 6.4 Uncertainty in the Location of the Deterioration, the load rating is a function of the load effect that varies along the span. Therefore, a detailed modeling and load rating at every location along the section helps identify the critical load rating section.

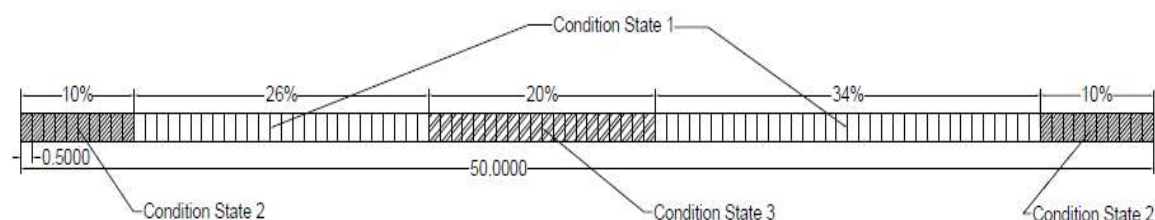


Figure 7.8 Modeled condition state in a girder

7.3.1 Quantifying Uncertainty in Approach 3

In Approach 3, the ϕ_c needs to account for the uncertainties due to variation in the amount of corrosion within a section and the lack of exact percentage loss within a condition state. These uncertainties are accounted using similar process as mentioned in Section 7.1.1 Quantifying Uncertainty in Approach 1.

Consequently, the combined uncertainty due to variation in the amount of corrosion, and lack of exact percentage loss can be evaluated using Eq.(50) for the three condition states. In Eq.(49) and Eq. (50) the expected capacity ($E(C S j)$) is calculated using Eq. (48) i.e. by taking arithmetic average of plastic moment capacities of each condition states. The variation due to lack of exact percentage loss is calculated using Eq.(49), which is added using SRSS to the standard deviation to account for uncertainty due variation in the amount of corrosion as shown in Eq. (50).

$$E(C S j) = \frac{\sum_{i=1}^n x_{i,j}}{m_j} \quad (45)$$

$$SD = \sqrt{\left(\frac{\sum_{i=1}^{m_j} \left((x_{i,j} - E(C S j))^2 \right)}{m_j - 1} \right)} \quad (46)$$

$$SD(C S j) = \sqrt{(SD^2 + (E(C S j) * COV_{\max_j})^2)} \quad (47)$$

Where,

$j = 1, 2$ or 3 for condition state $1, 2$ or 3 respectively

$x_{i,j}$ = percentage of girder with i^{th} percentage loss in j^{th} condition state

$E(C S j)$ = Expected plastic moment capacity of condition state j

$SD(C S j)$ = Standard deviation of the j^{th} condition state

$m_j =$ number of plastic moment capacity in j^{th} condition state.

$COV_{max_j} =$ COV associated with the max percentage loss in j^{th} condition state

Similar analysis to Approach 1 and Approach 2 using the mean and standard deviation of each condition state is performed to find ϕ_c for each condition states. The set of ϕ_c for the range of percentage section loss with GP1, GP2, NDOR range with GP1 deterioration profile and NDOR range with GP2 deterioration profile are shown in Table 7.15. The ϕ_c suggested for GP1 and GP2 are the values in the MBE because the range of percentage losses in each condition state was calibrated for that ϕ_c .

All of the ϕ_c suggested in Table 7.15 are calibrated for carbon steel in a rural environment. The multiplier for ϕ_c for each condition state is a function of the environment and the type of steel. Multipliers for any bridge that is made of carbon steel and is in the urban or marine environment are given in Table 7.16. Similarly, use the multiplier in Table 7.17 for bridges made with weathering steel in the rural, urban or marine environment.

Engineers can load rate a bridge knowing the location and portion of each condition state in the girder by finding the capacity of the bridge with the percentage of section loss in Table 7.14. The percentage of section loss corresponding to each condition state needs to be modeled as it is present in situ and load rated with the corresponding ϕ_c suggested in Table 7.15. Similar to Approach 1 and 2, bias is 1.0. The least value of load rating is the critical value.

7.3.2 ϕ_c for Approach 3

Table 7.14 Percentage loss for each condition state in Approach 3

Distribution Profile	Condition State	Percentage Loss to use for Load Rating
GP 1	1	0.5%
	2	4%
	3	19%
GP 2	1	0%
	2	2.5%
	3	12.5%
NDOR's Range (Both Profiles)	1	0 %
	2	0.5%
	3	25.5%

Table 7.15 ϕ_c for each condition state and the range of percentage loss

	Condition State 1 range	Condition State 2 range	Condition State 3 range	ϕ_c for Condition State 1	ϕ_c for Condition State 2	ϕ_c for Condition State 3
NDOR Range with GP1 deterioration	0%	0-1%	1-50%	1.00	1.00	0.70
NDOR Range with GP2 deterioration	0%	0-1%	1-50%	1.00	1.00	0.40
GP 1	0-1%	1-7%	7-35%	1.00	0.95	0.87
GP 2	0%	0-10%	10-30%	1.00	0.94	0.85

Table 7.16 Multiplier for ϕ_c for carbon steel in urban and marine environment

		Carbon Steel					
		Urban Environment			Marine Environment		
Multiplier for		ϕ_c 1	ϕ_c 2	ϕ_c 3	ϕ_c 1	ϕ_c 2	ϕ_c 3
NDOR Distribution Range	GP 1	0.98	0.98	0.97	0.97	0.97	0.96
	GP2	0.96	0.96	0.93	0.95	0.95	0.91
Range Consistent with MBE	GP 1	0.98	0.98	0.97	0.97	0.97	0.96
	GP2	0.96	0.96	0.95	0.95	0.95	0.94

Table 7.17 Multiplier for ϕ_c for weathering steel in the three environments

		Weathering Steel								
		Rural Environment			Urban Environment			Marine Environment		
Multiplier for		$\phi_c 1$	$\phi_c 2$	$\phi_c 3$	$\phi_c 1$	$\phi_c 2$	$\phi_c 3$	$\phi_c 1$	$\phi_c 2$	$\phi_c 3$
NDOR Range	GP 1	1.00	1.00	1.00	0.99	0.99	0.99	0.99	0.99	0.99
	GP2	1.00	1.00	1.00	0.98	0.98	0.96	0.98	0.98	0.97
Consistent with MBE	GP 1	1.00	1.00	1.00	0.99	0.99	0.99	0.99	0.99	0.99
	GP2	1.00	1.00	1.00	0.98	0.98	0.98	0.98	0.98	0.98

7.4 Special Approach

The concept of ϕ_c was introduced in NCHRP 301 to account for future corrosion and increased variability in section properties for the deteriorated member. The lack of measurement from the field and the concept of condition state as a range of section loss combined together increased the uncertainty in the load rating procedure. If the measurements are taken in the field, there would be no uncertainty associated with the exact remaining section in the bridge.

Knowing the percentage of section loss can be used to determine the remaining moment capacity, and ϕ_c associated with that percentage loss can be used to provide consistent reliability across all bridges. The only uncertainties that would need to be accounted for by ϕ_c are increased variability remaining and possible section loss due to corrosion between inspections. They have been discussed in detail in “6.1 Uncertainties in Section Deterioration” and “6.2 Future Corrosion” respectively. Using the COV for section variability and the bias for future corrosion in the reliability analysis was performed for all percentage loss from 0 to 50%. The ϕ_c values for all percentage loss are given in Table 7.18, the percentage loss in the section have been combined for ϕ_c values of an increment of 0.05 for the ease of use. The multiplier for carbon steel in the urban

and marine environment, and for weathering steel in the rural, urban and marine environment are given in Table 7.18.

Table 7.18 ϕ_c and multiplier for different range of deterioration

Percentage loss	Carbon Steel			Weathering Steel		
	Rural	Urban	Marine	Rural	Urban	Marine
Up to 3.0%	1.00	*1.00	*1.00	*1.00	*1.00	*1.00
Up to 8.0%	0.95	*1.00	*1.00	*1.00	*1.00	*1.00
Up to 28.0%	0.90	*0.95	*0.95	*1.00	*1.00	*1.00
Up to 45.0%	0.85	*0.95	*0.95	*1.00	*1.00	*1.00
Up to 50.0%	0.80	*0.95	*0.95	*1.00	*1.00	*1.00

7.5 Selection of ϕ_c for Load Rating

Four approaches can make the selection of the right set of ϕ_c complicated. In this chapter, a process is laid out to simplify the selection of the correct set of ϕ_c s depending on the information provided by the inspection. The first step is to find the type of steel the bridge has and the environment where the bridge is located. This process is shown in Figure 7.9. This information should be available through bridge drawings or old records and the location of the bridge. Once the material and the type of environment are known, the second step is to determine the type of deterioration profile present in the girder. If this information is unknown, GP2 can be assumed and moved to the next step. The type of steel, environment and the type of deterioration profile present in the girder are the information required for determining the type of approach to use. This information is used in Figure 7.10 to find the type of approach to use for the information that has been provided to the load-rating engineer. The Special Approach is not suggested through Figure 7.10 because it requires a special inspection to provide engineers with the measurements of the remaining section along the girder. If the information for the Special Approach is present, Figure 7.14 can be used for the process.

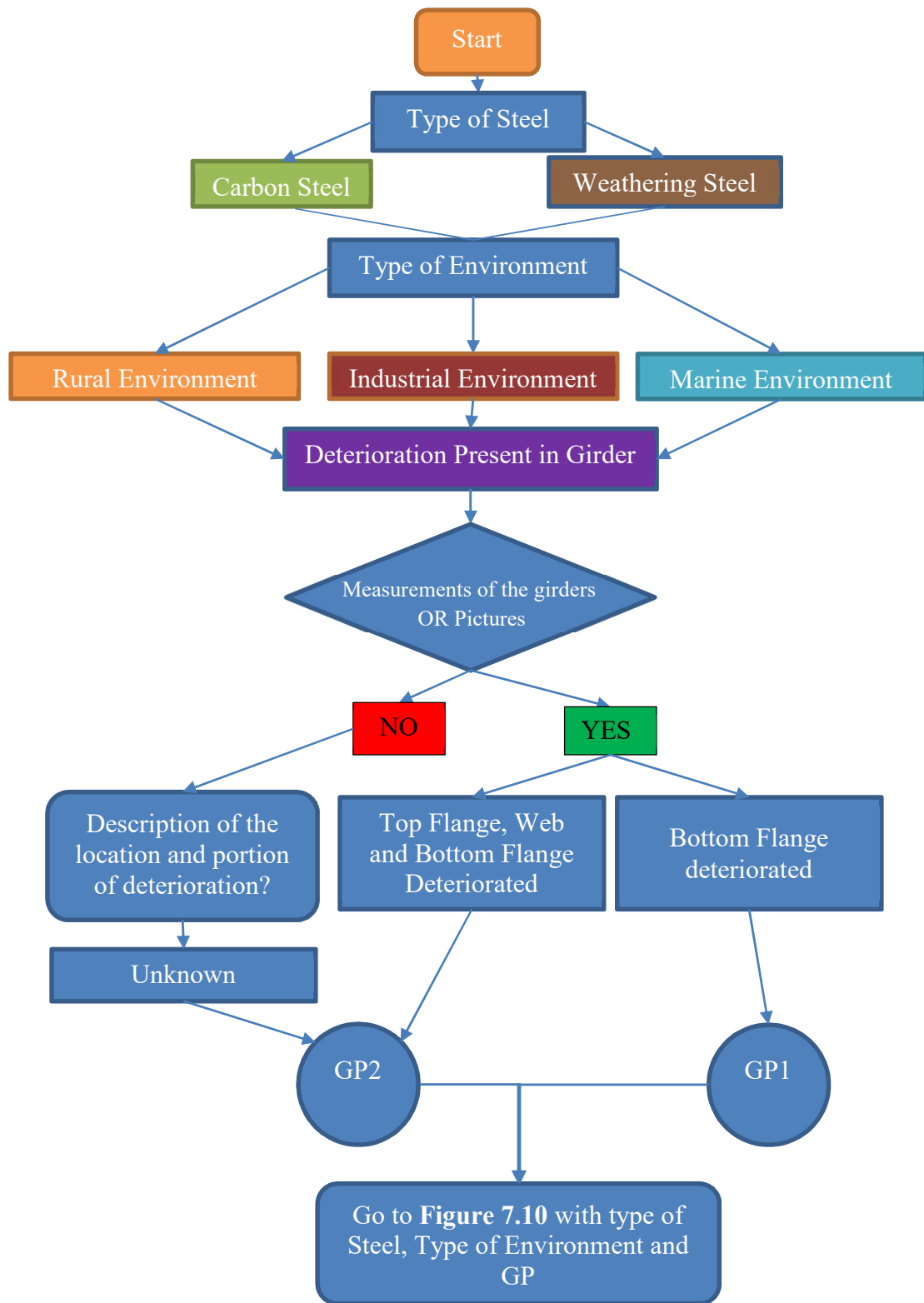


Figure 7.9 Flowchart to start the rating procedure

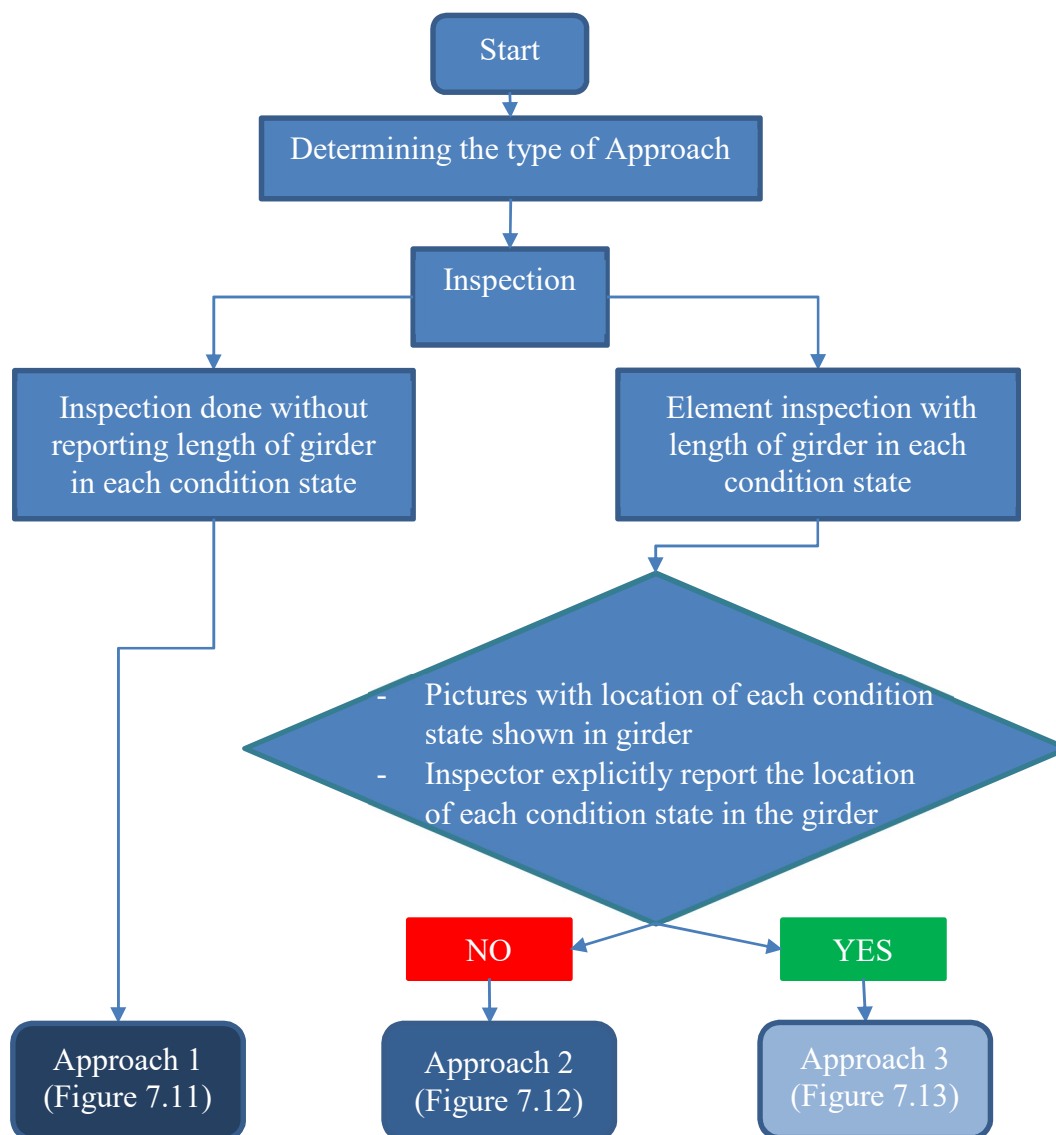


Figure 7.10 Flowchart to determine the approach needed to be used

The three approaches have their own procedure that has been shown in their respective flow chart. The process of load rating with Approach 1 is shown in Figure 7.11. Approach 1 is the simplest approach and depending on the worst condition state seen from the inspection report, a ϕ_c is suggested. ϕ_c is shown in Table 7.4 for girders that have weathering steel and/or are in the urban or marine environment. A multiplier in

Table 7.5 or Table 7.6 is used on the base value to find the ϕ_c . Depending on the condition state, an estimated percentage loss that needs to be modeled for each CS's is given in Table 7.9. The percentage loss depends on the type of deterioration profile and the condition state.

Similarly, the load rating process for Approach 2 is shown in Figure 7.12.

Approach 2 is a complicated approach because there are no tables to use for the values of ϕ_c . An excel sheet for each GP and NDOR's inspection process is set up to determine the percentage loss and the ϕ_c . The excel sheet utilizes the ANN weights and biases to determine the ϕ_c after the percentage of girder in each condition state is inputted. A percentage loss that needs to be modeled for the entire girder is also shown in the same excel sheet.

Finally, the load rating procedure and selection of ϕ_c for Approach 3 is shown in Figure 7.13. Approach 3 requires the load-rating engineers to model the percentage section loss corresponding to each condition state at the location along the span as in situ. The corresponding percentage section loss to each condition state is given in Table 7.14, and it depends on the type of deterioration profile (GP1 and GP 2) and NDOR's range. The values of ϕ_c are given in Table 7.15.

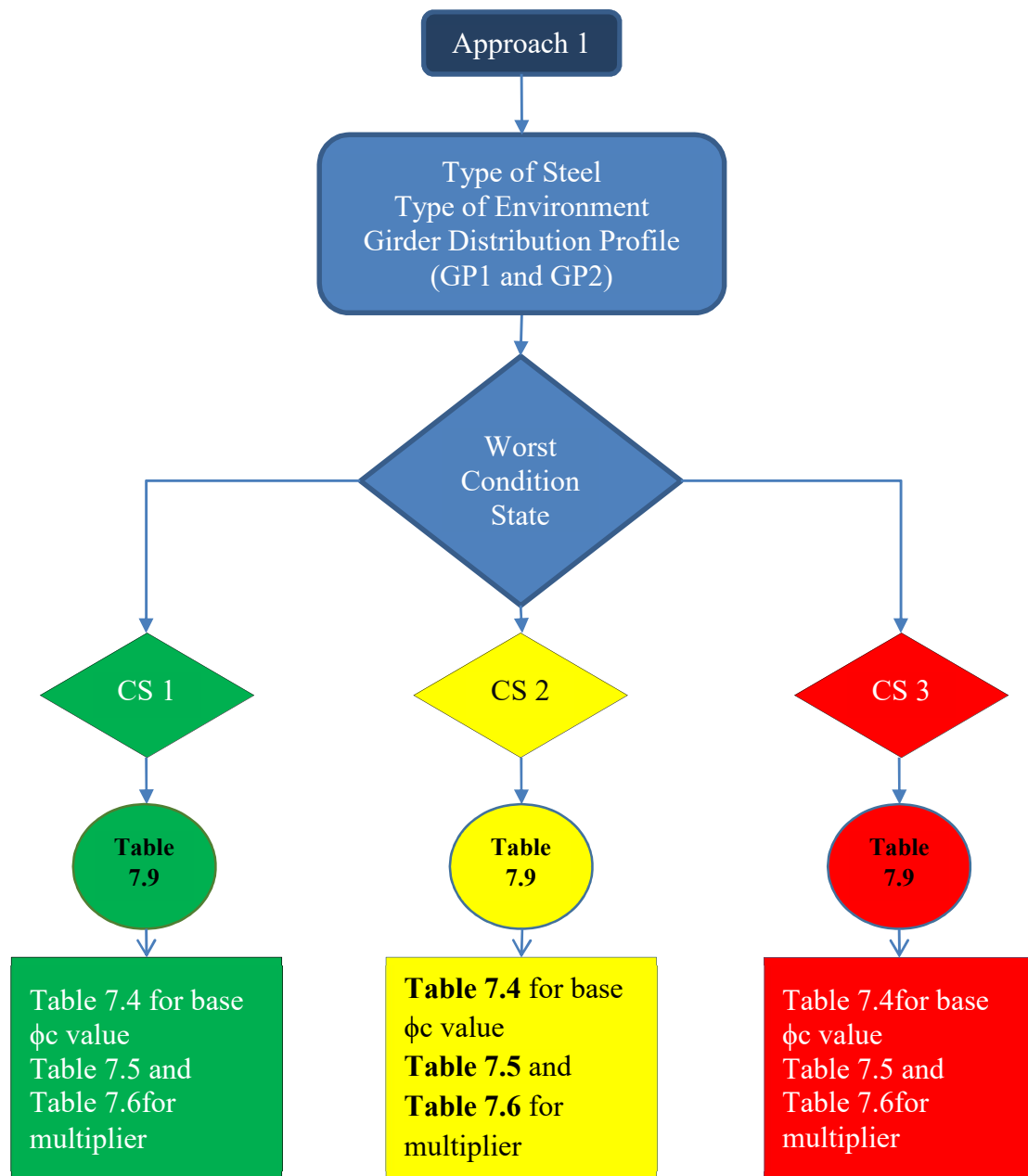


Figure 7.11 Flowchart to determine the ϕ for Approach 1

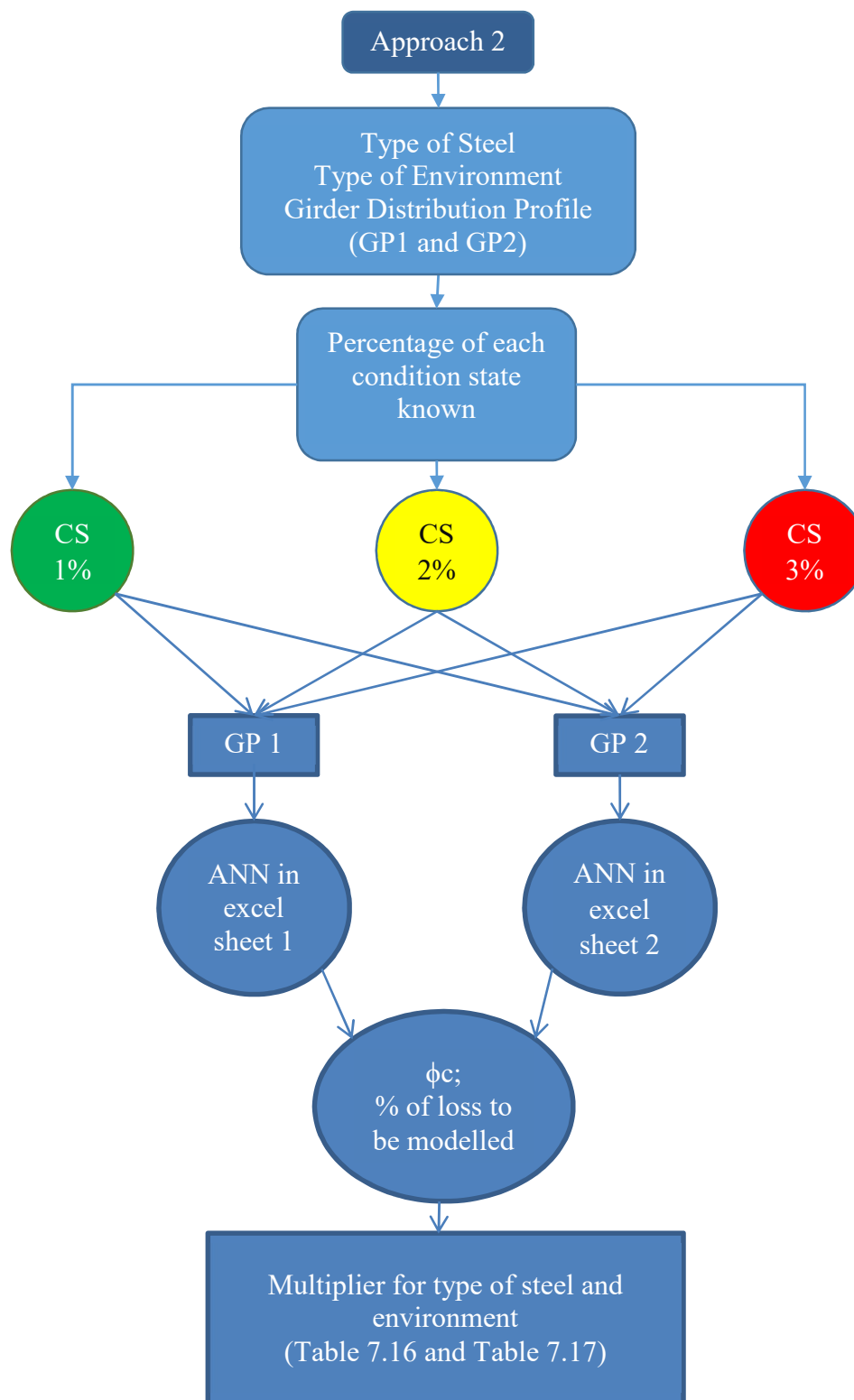


Figure 7.12 Flowchart to determine the ϕ_c for Approach 2

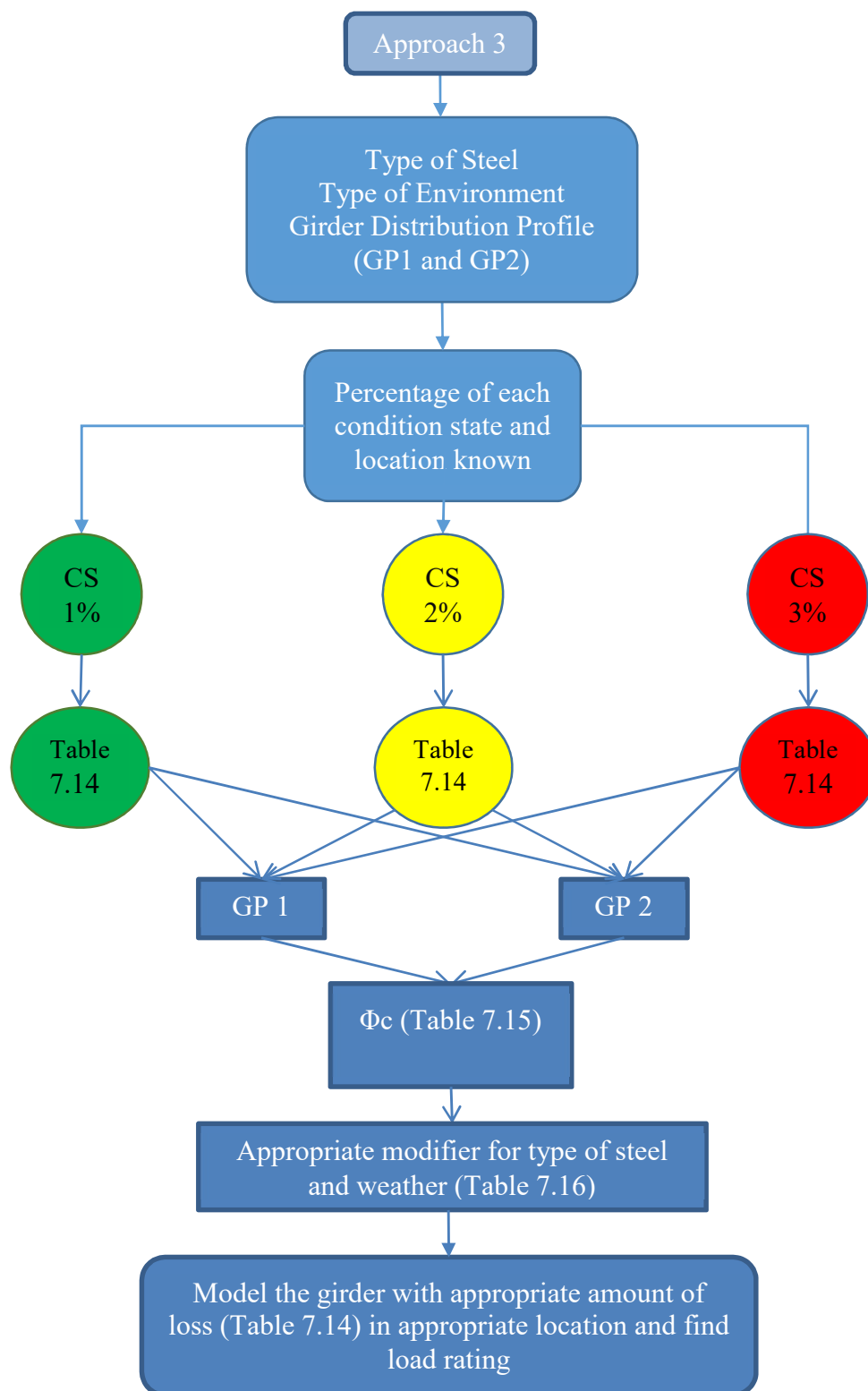


Figure 7.13 Flowchart to determine the ϕ_c for Approach 3

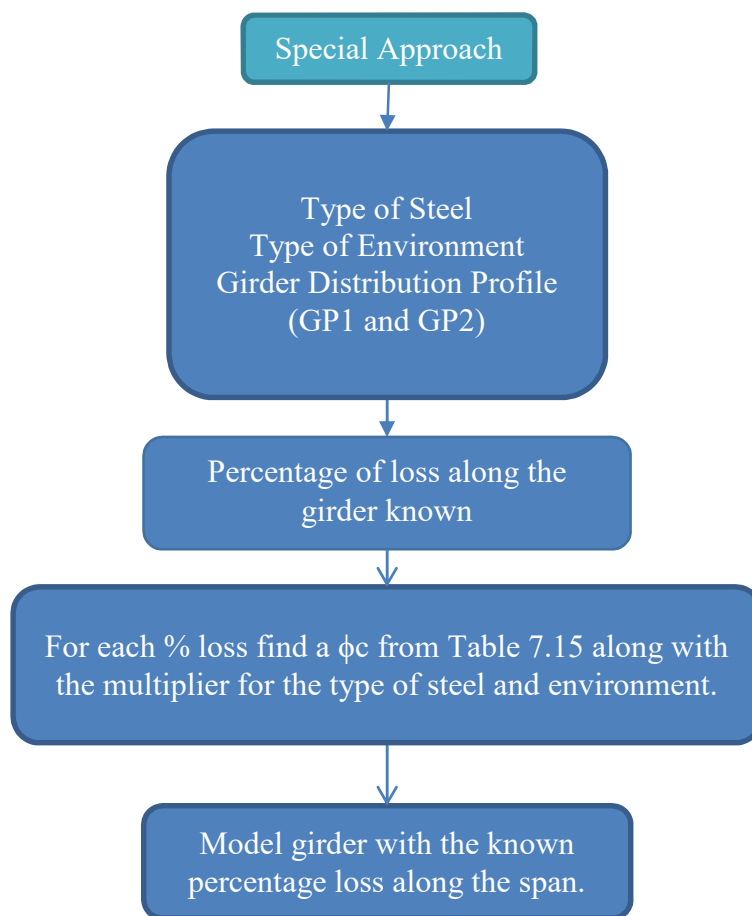


Figure 7.14 Flowchart to determine the ϕ_c for Special Approach

7.6 Conclusion

Using ϕ_c in load rating ensures consistent reliability for bridges in their current condition determined through inspection. Four approaches were suggested because of the inconsistency in the inspection procedure and the reporting. The process of selecting the right set of ϕ_c that varies from approach to approach can be confusing. A consistent inspection and rating procedure for a department can make this process clearer, as only one type of approach will be appropriate for the specific inspection performed.

Approach 1 was intended to be the most conservative approach with only knowing the worst condition state. This is the least amount of information required to perform the load rating using LRF as suggested by this research. As a less conservative approach was used by calibrating the ϕ_c for the population of bridges (which includes all possible scenarios as mentioned in section 6.4 Uncertainty in the Location of the Deterioration). After performing some preliminary load rating for extreme cases, the use of Approach 1 is not recommended unless the load-rating engineer is 100% sure the worst deterioration is not at or near the mid-span of the bridge for safety purposes. For example, a bridge with condition state 3 (following the NDOR's range definition) at the mid-span. The load rating using Approach 1 resulted in a higher value compared to Approach 3, because Approach 1 would use a ϕ_c of 0.69 and the capacity would be calculated with a section loss of 9.5%, whereas using in Approach 3, the critical load rating would be at the mid-span using a ϕ_c of 0.70 and the capacity would be calculated with a section loss of 25%. The load rating value from Approach 1 was higher than the more accurate load rating value calculated using Approach 3. This suggests that a detailed inspection is the most important factor in the load rating procedure.

An inspection procedure that requires inspectors to report the location of the condition state would remove the need for Approach 1 and Approach 2. It is crucial to know the location of the section loss because without knowing the location, the theory of probability needs to be used which includes capturing uncertainty due to unknown location of the deterioration (see section 6.4 Uncertainty in the Location of the Deterioration). As shown above by the condition state 3 example, this added uncertainty is not necessarily conservative because simulating all possible variations includes less

conservative scenarios. Although the outcome is likely to be over-conservative for most bridges, the surest way to guarantee that each individual bridge will possess at least the target reliability is to use Approach 3 with the assumption that the entire girder is in the worst condition state. This technique can be used when the location of the section loss is not provided in the inspection report. Approach 3 and Special Approach are the two approaches performed knowing the location of the condition state or the section loss present in the bridge.

Current inspection methods can be easily modified for Approach 3, but a more detailed inspection procedure is required for the Special Approach. For Approach 3, NDOR can use the pictures of the bridge taken during inspection making it fairly easy to locate of the condition states mentioned in the report. Information on the location and proportion of girder length corresponding to each condition state increases the accuracy in the load rating procedure. Using the Special Approach requires categorization of measured section loss into one of the five groups, each with a corresponding ϕ_c . This approach would be most accurate as there is no uncertainty associated with the nominal percentage of section loss present in the girder, as it is measured in the field. A detailed measurement to find the exact section thickness of the girder is needed, which can be labor intensive. The Special Approach requires more time-consuming inspections, so use of this approach can be limited to bridges that are crucial for the transportation system.

Chapter 8: Summary and Conclusion

Bounded ranges of section loss with corresponding calibrated ϕ_c values have been suggested by this study for the three condition states: Good, Fair, and Poor. The calibrated ϕ_c values account for increased uncertainty in the resistance of deteriorated members and the likely future deterioration of these members between inspection cycles. Ranges of section loss were estimated based on inference from the descriptions of the three condition states in the MBEI. These estimated ranges were referred to as NDOR's ranges, because NDOR (as well as other agencies) are currently using the subjective MBEI descriptions for inspection records. This thesis presents a new set of ϕ_c s, different from those provided by the MBE, in part to address the uncertainty in the suggested range. Additionally, two sets of percentage section loss ranges are suggested for the ϕ_c provided in the MBE to account for two girder deterioration profiles.

The lack of procedural guidance and of clear, objective definitions for condition states is a drawback that has made condition factors (ϕ_c) optional in the LRFR procedure. This research is an advancement towards an objective use of ϕ_c . This would improve the load rating and the inspection procedure by providing objective descriptions of girder conditions and condition states. Consistency in the description of girder conditions will significantly improve the LRFR procedure.

The increased uncertainty in the resistance of the deteriorated members accounted for by ϕ_c is caused by uncertainty due to non-uniform girder deterioration across a section, lack of knowledge of the location of the deterioration, and likelihood of further deterioration over the next inspection cycle. The ϕ_c is crucial for keeping structural reliability in load rating consistent among all bridges, which is the intent of the LRFR.

The ϕ_c values proposed in this thesis capture these uncertainties for all steel girder bridges regardless of the amount of girder deterioration observed during inspection, using the LRFR procedure. It is crucial to know the condition of the member to correctly load rate a girder, and this information is obtained through inspections.

Inspections provide vital information about the level of deterioration present in the girder, but due to varying detail in the information provided to the load-rating engineer, the uncertainty in the capacity varies, resulting in unintended and unaccounted for fluctuations in rating reliability. Multiple sets of ϕ_c are suggested to account for various scenarios in this study, because using only one value of ϕ_c for general categories of Good, Fair, or Poor is unlikely to consistently produce the intended margin of safety. Four approaches for varying levels of inspection information are suggested to account for any scenario of the inspection detail provided to the load-rating engineer. Three approaches are based on the current condition state description model, which categorizes the deterioration of the girder into one of the four condition states. The fourth approach deviated from the traditional condition state model to a more detailed rating procedure based on the section loss percentage present in the girder.

The location of the section loss along the span of the girder is the single most important information required for an accurate load rating. The unknown location of deterioration contributes additional uncertainty as described in Approaches 1 and 2, lowering the ϕ_c . The uncertainty in deterioration location can be mitigated with minimum effort during the inspection process by referring to pictures taken during inspections. Approach 3 and the Special Approach can be performed when the locations of the condition states are known. In Approach 3, the description in the notes section for the

portion(s) and location(s) of corrosion increases the accuracy of the load rating. The Special Approach requires measured values of section loss corresponding to positions along the girder lengths, resulting in the most accurate load rating.

One of the struggles is the interpretation of the description about the amount of deterioration by the load-rating engineer, as described in the inspection report. Currently, the condition state is used to describe the deterioration. This research suggests objective ranges of the percentage section loss due to corrosion for condition states, which brings uniformity in the inspection process and ensures reliable and consistent transfer of the information to the load-rating engineer. Uncertainties in a range of section loss can be quantified and accounted for, which improves the reliability in the load rating. The Special Approach does not use the traditional condition state descriptions, removing this aspect of uncertainty from the ϕ_c values provided for that Approach. This research paves the way for other improvements in the MBEI / MBE load rating procedure, as similar objective descriptions for other types of defects in other elements can improve inspection and rating consistency.

Future research is required to address the effects of other defects present in various types of bridges. Other defects, such as cracking, have characteristic condition states that need to be objectively characterized to improve the reliability of the load rating. Condition states ought to be well defined for all element types and associated defects in the MBEI, as has been described in this research for steel girder corrosion for. Inspection records based on clear, objective definitions for condition states will facilitate consistency among ratings with respect to reliability.

In conclusion, this research is a step towards improving the LRFR load rating procedure for structures containing appreciable deterioration. If a bridge with deterioration is carefully modeled with all its defects during load rating, the rating procedure should produce a capacity consistent with the reliability intended in LRFR. The ϕ_c in LRFR is the only factor that accounts for the increased uncertainties in the capacity of the girder due to deterioration, therefore, the use of ϕ_c is vital for consistently reliable load rating. The uncertainties associated with ϕ_c can be decreased with comprehensive inspection, which would consequently decrease the penalty by ϕ_c to achieve the target reliability in LRFR or increase the estimation of the nominal capacity. The four approaches show that penalty by ϕ_c decreases with increasing level of inspection detail. Moving forward inspection detail should be standardized and more types of defects in different elements, other than corrosion in steel girders, should be studied to extend the use of ϕ_c .

References

- AASHTO. (2014). *Manual for bridge evaluation, 2nd edition, with 2011, 2013, and 2014 Interim revisions* (2nd edition ed.). Washington, D.C.: AASHTO.
- Agatonovic-Kustrin, S., & Beresford, R. (2000). Basic concepts of artificial neural network (ANN) modeling and its application in pharmaceutical research. *Journal of Pharmaceutical and Biomedical Analysis*, 22(5), 717-727.
- Albrecht, P., & Naeemi, A. H. (1984). Performance of weathering steel in bridges. *NCHRP Report*, (272)
- Ambler, H., & Bain, A. (1955). Corrosion of metals in the tropics. *Journal of Applied Chemistry*, 5(9), 437-467.
- ASTM International. (2011). *ASTM G103(2011) standard practice for preparing, cleaning, and evaluating corrosion test specimens*. West Conshohocken, PA: ASTM International.
- ASTM International. (2015). *ASTM G5010(2015) standard practice for conducting atmospheric corrosion tests on metals*. West Conshohocken, PA: ASTM International.
- Baboian, R. R. B. (2005). *Corrosion tests and standards: Application and interpretation*
- Czarnecki, A. A., & Nowak, A. S. (2008). Time-variant reliability profiles for steel girder bridges. *Structural Safety*, 30(1), 49-64.

Dean, S. W. (1990). Corrosion testing of metals under natural atmospheric conditions.

Corrosion testing and evaluation: Silver anniversary volume () ASTM International.

Federal Highway Administration. (2010). ***Federal-aid policy guide***. Washington, D.C.:

U.S. Department of Transportation.

Federal Highway Administration. (2012). *Bridge inspector's reference manual*.

Washington, D.C.: U.S. Department of Transportation.

Kayser, J. R., & Nowak, A. S. (1987). Evaluation of corroded steel bridges. *Bridges and*

Transmission Line Structures, 35-46.

Kayser, J. R., & Nowak, A. S. (1989a). Capacity loss due to corrosion in steel-girder

bridges. *Journal of Structural Engineering*, 115(6), 1525-1537.

Kayser, J. R., & Nowak, A. S. (1989b). Reliability of corroded steel girder bridges.

Structural Safety, 6(1), 53-63.

Komp, M. (1987). Atmospheric corrosion ratings of weathering steels—calculation and

significance. *Materials Performance*, 26(7), 42-44.

Kulicki, J., Prucz, Z., Sorgenfrei, D., Mertz, D., & Young, W. (1990). *Guidelines for*

evaluating corrosion effects in existing steel bridges

McCrum, R., Arnold, C. J., & Dexter, R. (1985). Current status report: Effects of

corrosion on unpainted weathering steel bridges. *Current Status Report: Effects of*

Corrosion on Unpainted Weathering Steel Bridges,

Moses, F., & Verma, D. (1987). In Transportation Research Board (Ed.), *NCHRP report 301: Load capacity evaluation of existing bridges*. Washington, DC:

Moses, F. (2001). *NCHRP 454: Calibration of load factors for LRFr bridge evaluation*. Washington, D.C.: Transportation Research Board.

Nebraska Department of Roads: Bridge Division. (2015). Bridge inspection program manual.

Nowak S., A., & Collins R., K. (2013). *Reliability of structures* (second ed.). Boca Raton, FL: Taylor & Francis Group.

Patras, W. (2016). *Personal communication*

Wang, N. (2010). *Reliability-Based Condition Assessment of Existing Highway Bridges*,

Weseman, W. (1995). Recording and coding guide for the structure inventory and appraisal of the nation's bridges. *United States Department of Transportation (Ed.), Federal Highway Administration, USA*,

Yunovich, M., Thompson, N., Balvanyos, T., & Lave, L. (2001). Corrosion cost and preventive strategies in the united States—Appendix d—highway bridges. *Federal Highway Administration, FHWA-RD-01-157*,

Zmetra, K., Zaghi, A. E., & Wille, K. (2015). Rehabilitation of steel bridge girders with corroded ends using ultra-high performance concrete. *Structures Congress 2015*,

APPENDIX A: PLASTIC MOMENT CAPACITY USING LRFD

The plastic moment capacity of a composite compact girder is calculated using AASHTO 6.10.6 (Strength Limit State). C 6.4.4 in AASHTO has a flow chart for the LRFD Article 6.10.6 which is shown in Appendix Figure A.

For the composite section in flexure, a compact check is performed. AASHTO in section 6.10.6.2.2-1 has the following requirement for a straight bridge with a steel girder to be considered compact:

$$F_y \leq 70 \text{ ksi},$$

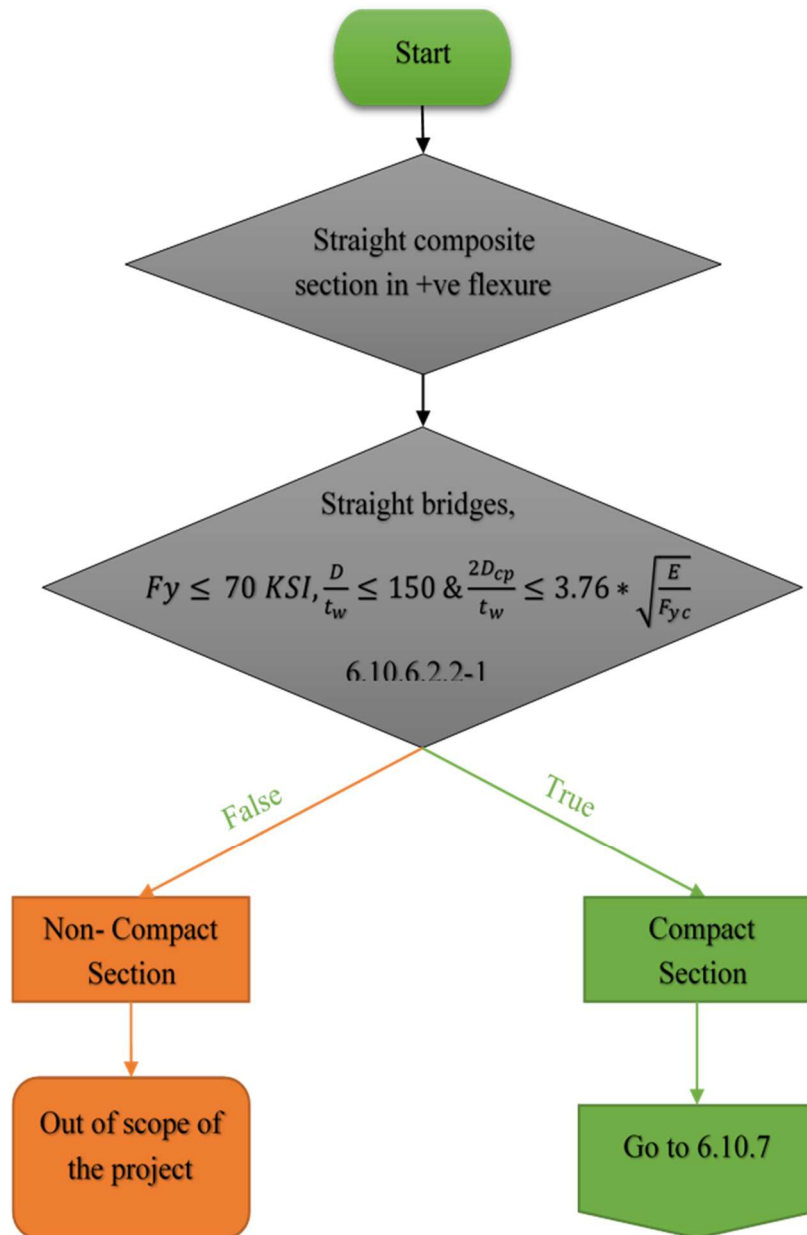
$$\frac{D}{t_w} \leq 150, \text{ and}$$

$$2 * \frac{D_{cp}}{t_w} \leq 3.76 * \sqrt{\frac{E}{F_y}}$$

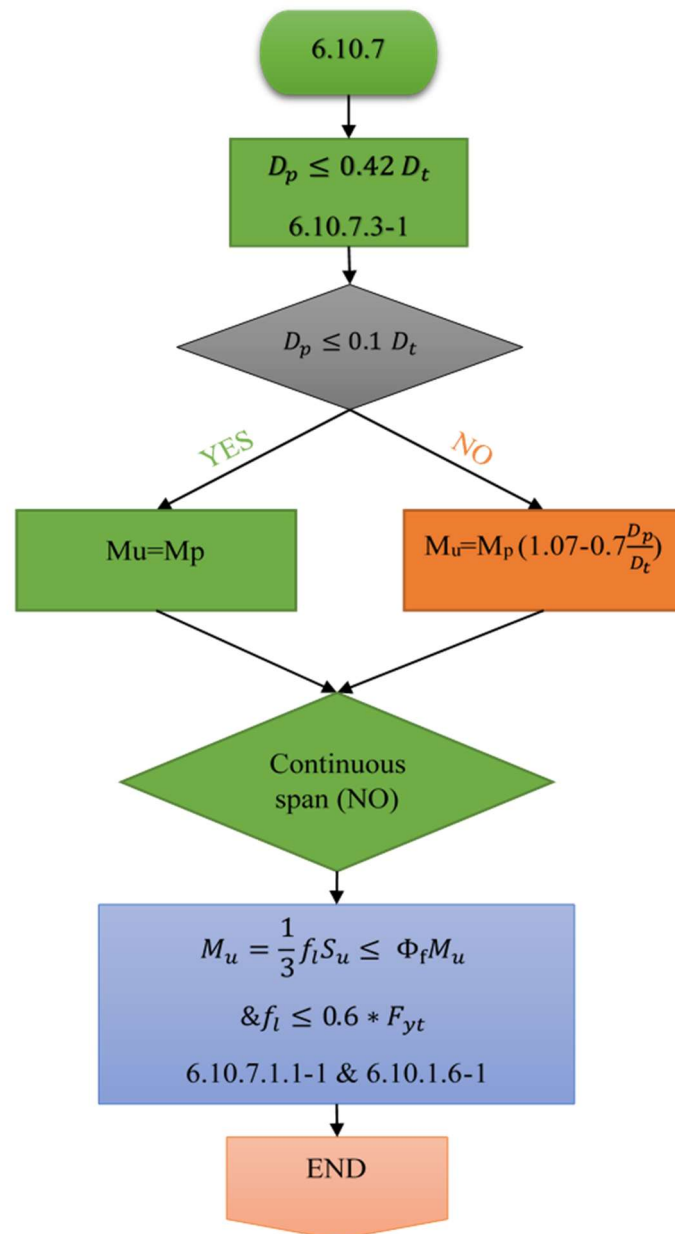
Where, F_y is the yield strength, D is the depth of the web, t_w is thickness of the web, D_{cp} is depth of the web in compression at the plastic moment determined as specified in Article D6.3.2 (in.),

$$D_{cp} = \frac{D}{2} \left(\frac{F_{yt}A_t - F_{yc}A_c - 0.85f'_cA_s - F_{yrs}A_{rs}}{F_{yw}A_w} + 1 \right) \text{ for positive flexure ,}$$

and E is the modulus of elasticity.



Appendix Figure A Flowchart for LRFD Article 6.10.6- strength limit state



Appendix Figure B Flowchart for Article 6.10.7- composite sections in positive flexure

Article 6.10.7 requires a ductility check $D_p \leq 0.42 D_t$ (AASHTO 6.10.7.3-1), where D_p is the distance from the top of the concrete deck to the neutral axis of the composite section at the plastic moment (in.), D_t is the total depth of the composite section (in.)

After checking the ductility and compactness of the section

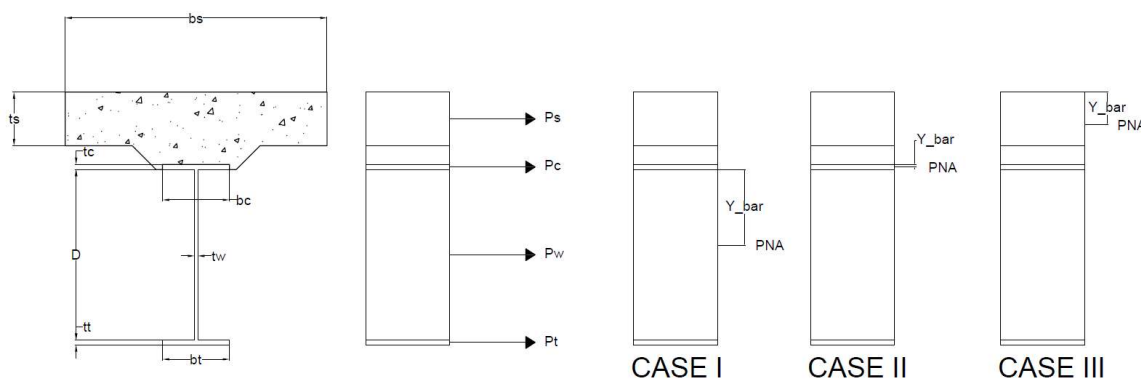
$$M_n = M_p, \text{ if } D_p \leq 0.1 D_t, \text{ Else}$$

$$M_n = M_p \left(1.07 - 0.07 * \left(\frac{D_p}{D_t} \right) \right) \quad (48)$$

Table D6.1-1 in AASHTO can be used.

Appendix Table A Equation for plastic moment capacity of composite girder

Case	PNA	Condition	Ybar and Mp
I	In Web	$P_t + P_w \geq P_s + P_c$	$\bar{Y} = \left(\frac{D}{2} \right) \left[\frac{P_t - P_c - P_s}{P_w} + 1 \right]$ $M_p = \frac{P_w}{2D} [\bar{Y}^2 + (D - \bar{Y})^2] + [P_s d_s + P_c d_c + P_t d_t]$
II	In Top Flange	$P_t + P_w + P_c \geq P_s$	$\bar{Y} = \left(\frac{t_c}{2} \right) \left[\frac{P_w + P_t - P_s}{P_c} + 1 \right]$ $M_p = \frac{P_c}{2t_c} [\bar{Y}^2 + (t_c - \bar{Y})^2] + [P_s d_s + P_w d_w + P_t d_t]$
III	Concrete	$P_t + P_w + P_c < P_s$	$\bar{Y} = (t_s) \left[\frac{P_c + P_w + P_t}{P_s} + 1 \right]$ $M_p = \frac{\bar{Y}^2 P_s}{2t_s} + [P_c d_c + P_w d_w + P_t d_t]$

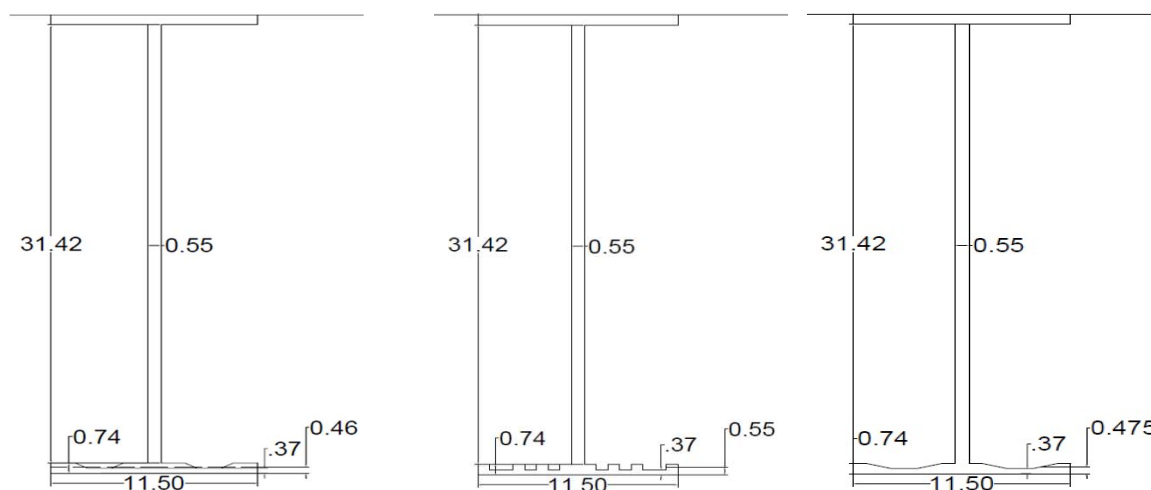


Appendix Figure C Location of Ybar and PNA to calculate moment capacity

APPENDIX B: USING MEAN SECTION FOR MOMENT CALCULATION

Use of Average thickness for calculation of Moment Capacity

Section loss due to corrosion along the section is uneven in the field. The mean thickness along the section dictates the moment capacity of the girder.



Appendix Figure D Different pattern of bottom flange corrosion

Appendix Figure D shows section diagram of a girder with a same cross section for the top flange, web but a varying deteriorated profile for the bottom flange. The patterns were developed such that all three bottom flange would have the same cross-sectional area and center of gravity in the y-axis. Although these bottom flanges look different and have a different minimum thickness, they would all have the same capacity because the plastic moment capacity of a girder is calculated using the yield strength of the material and the plastic section modulus. As all three girder flanges have equal cross-sectional area and the center of gravity resulting in them having equal plastic section modulus which is a function of area and the lever arm to the plastic neutral axis (PNA).

Plastic moment capacity of girder with holes can be calculated with the remaining section and the center of gravity. This remaining area with the corresponding center of

gravity can be transformed into a plate with the width of the original un-deteriorated section and thickness that would give the same cross-sectional area of the deteriorated section. All the flange with a same loss in area % is transformed into a plate with original width and corresponding thickness.

$$A_{deteriorated} = A_{remaining} = B_{original} * t_{deteriorated}$$

$$\% \text{ loss} = \left(1 - \frac{A_{remaining}}{A_{original}} \right) * 100\%$$

$$\% \text{ loss} = \left(1 - \frac{B_{original} * t_{deteriorated}}{B_{original} * t_{original}} \right) * 100\% = \left(1 - \frac{t_{deteriorated}}{t_{original}} \right) * 100\%$$

$$\% \text{ remaining section} = 1 - \left(1 - \frac{t_{deteriorated}}{t_{original}} \right) * 100\% = \left(\frac{t_{deteriorated}}{t_{original}} \right) * 100\%$$

As seen in the above equations, the remaining section is a function of the equivalent thickness of the deteriorated section. All the percentage loss discussed before can be converted to equivalent deteriorated thickness. This also means that any section with a hole does not necessarily mean that it has lost 100% of its section it still has some remaining area.

APPENDIX C: ALTERNATIVE FUTURE CORROSION CALCULATION

In NCHRP 301, condition factor accounted for the possible future deterioration of the girder. This research tried to modify the NCHRP 301 by using the current loss and projecting the maximum future deterioration in the next 2 years when the next inspection would occur. This research uses the same modifications and models used in NCHRP 301 to predict the future corrosion. Komp's corrosion equation is shown below.

$$C = At^b \quad (49)$$

Where C is the average corrosion penetration in microns

A and b are parameters

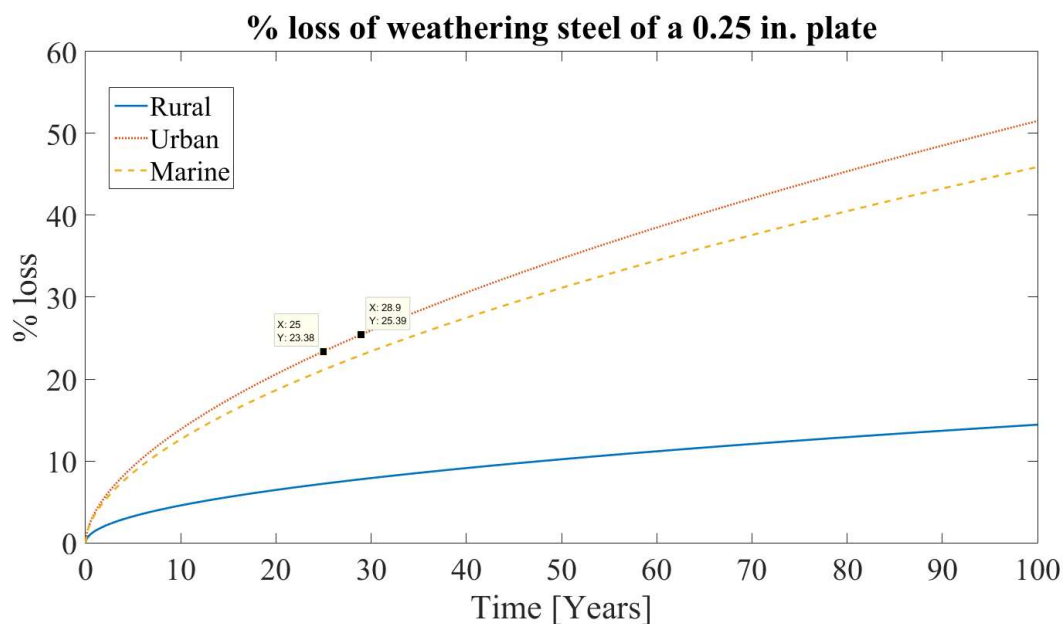
t is the number of years

Eq. (49) calculates surface loss due to corrosion in microns for a different type of steel and exposure environments by utilizing different parameters. These parameters are listed in Table 2.1. Komp's corrosion equation is a function of time so it can be modified to calculate the time if the amount of corrosion is lost. The modified equation is shown below.

$$t = \left(\frac{C}{A}\right)^{\frac{1}{b}} \quad (50)$$

Eq. (50) is used to calculate the time required for the section loss in the field. Two years are added to the resulting time and the maximum future deterioration is calculated using the equation shown above. For example, a girder with a flange thickness of $\frac{1}{4}$ inches has a 25% loss in thickness. This equates to a loss of 1/16th-inch loss, using the above Eq. (38) it would take 23.38 years for carbon steel exposed in a rural environment accounting for sheltered condition and deicing salts. Two years are added to the

calculated time and the new percentage loss is found, for this particular case, it would be 28.9% loss in 25.38 years. As Komp's model is asymptotic, the loss decreases in time, therefore the shorter the time the larger the apparent rate of future deterioration (i.e. secant rate). See Appendix Figure E for example of how the prediction is done. The marker shows the time required for the plate to lose 25% of its thickness



Appendix Figure F Loss of thickness predicted using Komp's corrosion model

APPENDIX D: CATEGORIZING THE ENVIRONMENT

ASTM uses three broadly classified qualitative categories: Rural, Industrial, and Marine. These classifications are based on the corrosive environment. Rural environment implies the least corrosive environment and Marine environment implies the most corrosive environment. (Ambler & Bain, 1955; Baboian, 2005; Dean, 1990)

Rural

Rural atmospheres are typically the most benign because rural environment does not contain a high level of chemical contaminants. There are exceptions if the location is close to a farm operation because the byproducts made of various waste materials can be extremely corrosive to most construction materials.

A location can be considered as a rural environment if it's away from factories, cities, and away from a farm location.

Industrial

Industrial atmospheres have aggressive corrosive environment because industrial environment contains sulfur compounds such as sulfur dioxide (SO₂) and nitrogen oxides (NO_x). Sulfur dioxide (SO₂) from burning fossil fuels combined with the moisture on dust particles makes sulfurous acid, which settles in microscopic droplets and fall as acid rain on exposed surfaces. The result is that contaminants in an industrial atmosphere produce a highly corrosive, wet, acid film on exposed surfaces.

A location is considered as an industrial environment if it's located within a city limit, downwind from a factory, and downstream and downwind from a farm that uses insecticides and pesticides. Most of Nebraska's bridges can be considered in this category.

Marine

Marine atmospheres have the most consistently severe corrosive environment because of high concentration of chloride ions and high humidity in the environment. Sea mist carried by the wind have salt crystals, which settles on the exposed surface which increases the rate of corrosion significantly. Other factors that increase the corrosion rate are time-of-wetness (TOW), wind direction and distance from the breaking surf.

A location is considered as a marine environment if it's located on or near an ocean. As the wind can carry the salt particle to long distances, any environment gets the ocean breeze can be considered in a marine environment.